escola superior de tecnologia e gestão
instituto politécnico de leiria

# *Comparative Study on Mechanical Strength of Acrylonitrile Butadiene Styrene [ABS] and Acryonitrile Styrene Acrylite [ASA] extruded filaments*

Master degree in Product Design Engineering

**YADUKUMAR**

Leiria, November 2020

*Comparative Study on Mechanical Strength of Acrylonitrile Butadiene Styrene [ABS] and Acryonitrile Styrene Acrylite [ASA] extruded filaments*

Master degree in Product Design Engineering

**YADUKUMAR**

Internship Report under the supervision of Doctor João Manuel Matias, Professor at School of Technology and Management of the Polytechnic Institute of Leiria.

Leiria, November 2020

# Originality and Copyright

# Dedication

Dedicated to all the students who lost their valuable lives due to the ongoing Covid-19 pandemic.

# Acknowledgments

I am graciously pleased to enthusiastically embrace this ideal opportunity to succinctly express my heartfelt gratitude to Dr. João Matias for his moral encouragement, active assistance, and valuable advice which were imperative for me to keep up with the project.

My heartfelt thanks to my best mates, Vrushaba Sachidanand Pattanshetty and Pramol Jain, who have always stood up for me, helped, and staunchly supported me at all times. I would also like to thank my friend Akhil Subramaniam for supporting me through the project.

I would also like to sincerely thank Mr. António Gonçalves and Ms. Sónia Silva from Controlo Qualidade Em Moldes [CQI], Rua de Pero Neto, Marinha Grande, along with Center for Rapid and Sustainable Product Development [CDRSP], Rua de Portugal, Zona Industrial, Marinha Grande, for opening up their spaces to let me perform all the various tests during this challenging time of Novel Corona Virus Pandemic, along with providing me with the material to work through.

I am equally pleased to adequately express my sincere gratitude to my friends from CQI, Luis Miguel Cruz, and Dario Rebecho Mateus for their willingness to assist me any time I needed help and assistance. I would also like to express my thanks to the CDRSP staff who involved in aiding me to perform the experiments.

Last but not least, to my dear Mother and my beloved Younger Brother, for all the generous sacrifices, necessary encouragement, and motivation.

# Resumo

O efeito dos principais parâmetros de fabricação de impressão 3D [padrão de enchimento e orientação de construção] na influência da resistência mecânica de dois filamentos termoplásticos usados no método de modelagem por deposição fundida [FDM] ou fabricação de filamento fundido [FFF]. I e. Acrilonitrila butadieno estireno [ABS] e acrilonitrila estéreo acrilato [ASA], que é apontado como um potencial sucessor do ABS, foram inspecionados neste trabalho acadêmico. A partir de achados experimentais, sugeriu provisoriamente que a resistência à tração, flexão e compressão dos espécimes de ABS é consistentemente mais alta do que a do espécime ASA. Os resultados empíricos do ABS supostamente mostram uma variação menor e confiabilidade ideal do que no caso do ASA. Os testes de tensão indicam que as resistências finais para os espécimes de ABS orientados em Y são marginalmente mais altas. As variações menores na resistência à tração final são relevantes para todas as correlações de pares para diferentes orientações dos espécimes ASA. Os achados dos testes de flexão e compressão estão bem correlacionados com os resultados dos testes de tração, novamente sinalizando que as habilidades de flexão e compressão são relativamente altas para o ABS orientado em Y e o modelo ABS vertical, respectivamente. Outra observação imperativa que foi feita voluntariamente durante a impressão do ASA é que ele estava mais sujeito a empenamento quando comparado ao ABS, pois uma tendência mais ampla, a orientação Y e o Preenchimento Retilíneo ofereceram maior resistência às partes expostas investigadas em ambos os materiais. Essas descobertas experimentais indicam ainda que os parâmetros de processamento, como Orientação de Construção e Padrão de Infill dos corpos de prova FDM, contribuem diretamente para impactar a resistência mecânica dos materiais testados.

**Palavras-chave:** “Modelagem por Deposição Fundida [FDM]”, “Fabricação de Filamento Fundido [FFF]”, “Acrilonitrila Butadieno Estireno [ABS]”, “Acrilonitrila Estéreo Acrilita [ASA]”, “Orientação de construção”, “Retilíneo”

# Abstract

The effect of the key 3D printing manufacturing parameters [Infill pattern and Build orientation] on the influence of mechanical strength of two thermoplastic filaments used in Fused Deposition Modelling [FDM] or Fused Filament Fabrication [FFF] method. I e. Acrylonitrile Butadiene Styrene [ABS] and Acrylonitrile Styrene Acrylate [ASA], which is touted as a potential successor to ABS were inspected in this academic work. From experimental findings, it tentatively suggested that the tensile, flexural, and compressive strength of the ABS specimens is consistently higher than that of the ASA specimen. The empirical findings of ABS purportedly show a lower variance and optimum reliability than in the case of ASA. Tension tests indicate the ultimate strengths for Y oriented ABS specimens are marginally highest. The minor variations in ultimate tensile strengths are relevant for all pairwise correlations for different orientations of the ASA specimens. The findings of the flexural and compressive tests are well correlated with the results of the tension tests, again signaling that the flexural and compressive abilities are relatively high for Y oriented ABS and Vertical ABS model, respectively. Another imperative observation that was voluntarily made while printing ASA is, it was more prone to warping when compared with ABS, as a broader trend, Y orientation, and Rectilinear Infill offered greater strength to the exposed parts investigated on both the materials. These experimental findings further indicate that the processing parameters, such as Build Orientation and Infill Pattern of the FDM specimens, directly contribute to impacting the mechanical strength of the tested materials.

**Keywords:** “ Fused Deposition Modelling [FDM]”, “Fused Filament Fabrication [FFF]”,“ Acrylonitrile Butadiene Styrene [ABS]”, “Acryonitrile Styrene Acrylite [ASA]”, “Build Orientation”, “Infill” .

# Contents

# List of Figures

# List of Tables

# List of Abbreviations and Acronyms

| | |
|---|---|
| ESTG | Escola Superior de Tecnologia e Gestão |
| CDRSP | Centro para o Desenvolvimento Rápido e Sustentavel do Produto |
| CQI | Chartered Quality Institute |
| CAD | Computer Aided Design |
| AM | Additive Manufacturing |
| RP | Rapid Prototyping |
| SLA | Stereolithography Apparatus |
| STL | Standard Triangulation Language |
| FFF | Fused Filament Fabrication |
| FDM | Fused Deposition Modeling |
| ASA | Acrylonitrile Styrene Acrylate |
| ABS | Acrylonitrile Butadiene Styrene |
| ASTM | American Society for Testing Materials |
| DSC | Differential Scanning Calorimetry |
| TGA | Thermogravimetric Analysis |
| CMM | Coordinate Measuring Machine |
| UTS | Ultimate Tensile Strength |
| CCD | Charge Coupled Device |
| SEM | Scanning Electron Microscopy |

# 1. Introduction

The insistence on reduction of product development duration does have a seminal influence on manufacturing practices and has culminated in the creation of a new generation production process which create part directly from the CAD (computer aided design) model on a layer by layer deposition concept without tools, die, fixtures and human interfearance this profound layered deposition processes is known as Rapid Prototyping, also referred as Additive Manufacturing, which facilitates a swift and simple changeover from concept generation in the form of computer images to the manufacturing of physical models. While RP is an inexpensive, versatile and easy way to pssroduce test parts before manufacturing, the availability of materials has historically restricted the technology from broad use[1][2].

Additive manufacturing (AM) technology using Fused Deposition Modeling ( FDM) or Fused Filament Manufacturing (FFF) is one of the most popular techniques and is extensively used for functional prototyping and production applications. That being said, the quality of the parts produced with FDM can be influenced by the various process parameters used. In this technique, the part can be built with various process parameters, such as build orientation and infill patterns, and these process parameters play a key role in the mechanical strength of the samples or the final part. This paper presents a comparative study of the variation in mechanical strength of specimens due to the influence of two types of printing parameters[Build Orientation and Infill Pattern] using the Fused Filament Manufacturing (FFF) 3D printing technique with respect to the two forms of thermoplastic material filaments I, e Acrylonitrile Butadiene Styrene (ABS) and Acryonitrile Styrene Acrylite (ASA).

ABS is the most common material used as it boasts good mechanical properties and high name recognition. A decade ago, when you wanted to print anything on a 3D printer, you had pretty much only one option: I,e. ABS. It wasn't exactly easy to get everything right. Soon, new materials started to appear, however, ABS remained among some of the most frequently purchased materials along with PLA and PETG due to their wide sprung availability. Acrylonitrile-Styrene-Acrylate is a relatively new form of thermoplastic filament used for 3D printing using the FFF or FDM processes[3]. ABS may be more recognizable than ASA because of its popularity in mass production. Because the number of available polymer forms is restricted, the number of applications that can gain from FFF is also limited. ASA is a thermoplastic, poised to replace ABS in the near future, but still has not yet landed in mainstream 3D printing recurrence. In order to design end-use parts with FFF, it is important to understand how the process parameters influence the final part [4][5].

## 1.1. Engineering Context and Objectives

Almost all engineering design initiatives commence with a few fundamental steps, no matter the application. After the birth of the initial concept, pivotal planning must be carried out to ensure that the engineer follows the steadiest possible course of action. Having this selection right for the first time by choosing the optimum design combination secures immense benefits for the development of any engineering service. 3D printing has been a potential technology that has been applied to an extensive range of disciplines. With a 3D printer, everyone could produce and build their own designs that could reduce the cost of the supply chain. In actuality, the consistency or strength of a 3D component depends on a number of factors, from the modeling stage to the printing stage, which can in turn affect the mechanical strength of the final part. However, it is not easy to monitor the physical properties of the printed component, and their consistency can vary. As a result, many parameters need to be considered when designing a product, like the size, the filament used, the build orientation, the style of the infill pattern selected, or potential deterioration when printing, etc.[6]. This confined study discusses the relation between the mechanical properties and the printing parameters of the obtained component.

The principal objective of the work is to gain an understanding of the potential impact of printing parameters, such as print orientation and infill pattern, on the strength of the FDM / FFF parts and to resolutely determine whether these parts can merely preserve their integrity when in-service loading. The academic study builds on the insights offered by previous researchers and further explores the profound impact of build orientation and infill pattern on the mechanical strength of ABS and ASA components obtained by FFF 3D printing. Based on the researchers' reviews of previous work in this area, there is no comprehensive published work assessing the influence of print parameters solely focusing on the mechanical strength of thermoplastic filament parts made by ASA at the miniature stage. The practical purpose of this paper is, therefore, to objectively evaluate and compare the mechanical strength of ASA, which is believed to be a possible substitute for ABS, and to compare its mechanical strength with the latter, along with an evaluation of the effect of the different printing orientations and the infill density on the mechanical strength of these thermoplastic materials.

## 1.2. Structure of the Work.

This internship/project is divided into seven chapters according to the brief description that follows.

A brief introduction to the theme is outlined in the first chapter, as well as the apparent motive for this work and the proposed objectives for its growth.

The second chapter and the third chapter are devoted to the state-of-the-art study of Additive manufacturing and Fused Filament manufacturing methods.

In the fourth chapter, a brief state of the art relevant to the process parameters in FDM / FFF, along with a literature analysis of the proposed parameters I.e. Build orientation and Infill pattern is done

Conceptual interpretation of this work is described in the fifth chapter, which illustrates the classification of the printed specimens and the experimental procedures intended while also discussing all works which were undertaken in order to be relevant to the experimental tests is presented.

The sixth chapter is reserved for the description and discussion of the results obtained from the experimental tests.

Ultimately, the seventh chapter lays out the overall findings of the study, and the potential structure for future work on the studied subje ct along with the forthcoming work is discussed.

# 2. Additive Manufacturing, an overview

Additive manufacturing (AM) technology (also referred to as Direct Digital Manufacturing) is defined by the American Society for Testing and Materials (ASTM) as the process of combining materials to create objects from 3D model data, typically layer by layer, as contrasted to subtractive manufacturing processes, such as conventional machining[7]. One of several distinctive characteristics of additive manufacturing has been its layer-wise manufacturing process which allows almost any geometrically complex shape to be developed [8]. That is completely contrast when compared with the subtractive processes, where traditional subtractive manufacturing is inherently sluggish, costly, and has limitations on design . Additive manufacturing process paves the way for quick, low-cost processes but does not substitute all of the conventional production methods[9]. 3D printing or additive manufacturing is a crucial enabler for developing and innovating, as well as providing capacity to complement existing processes [10].

The first ever 3D printed part was created in 1983 by Charles W. Hull as shown in Figure 1 where he sought a copyright in 1984 for his creation stereolithography through which he printed the first ever 3D printed part. Hull was the first individual to digitally 3D print the data. in 1986 3D Systems was co-founded by Chuck Hull and becomes the first ever 3D printing company in the world. The first commercially patented 3D printer emerged in the year 1987 which was based on Streolithography (SLA) technique [11]. Additive manufacturing is a innovative technique that has the potential to revolutionize the global production sector [12].

**Figure 1 Chuck Hull. The first person to record the digital information** [11]

3D printing has been affordable for a vast variety of businesses and economically viable**.** For this rationale, 3D printing or additive manufacturing is one of the most important enabling technologies in the fourth industrial revolution. According to recent research report by 3D hubs which compiled the data of all the leading buisness forecasting agencies, the projected worldwide increase in growth rate for additive manufacturing (also known as 3D Printing), is expected to surge from 4 billion dollars in 2014 to 34.9 billion dollars in 2024 [13] as depicted in figure 2. Forbes says that additive manufacturing (AM) industry consisting of all AM products and services worldwide, grew 21.2 percent to $11.867 billion in 2019 [14].

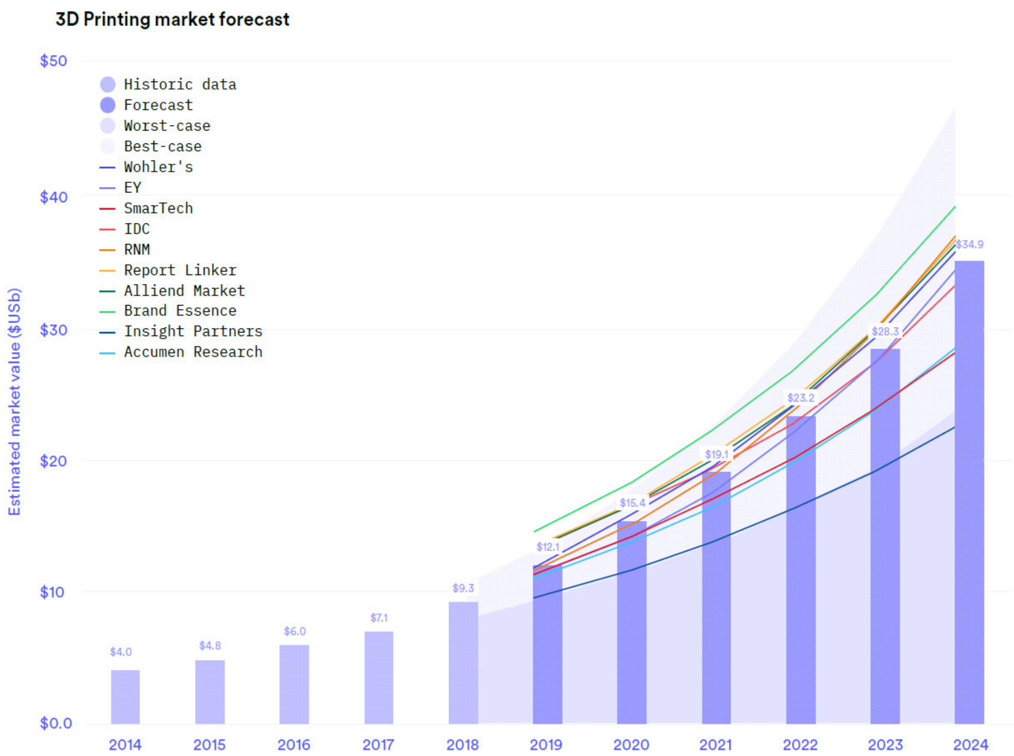


**Figure 2 Market Forecast, adapted from 3D hubs which integrates data reported by ten credible market analysts who have assessed the market segments of additive manufacturing.** [13]

## 2.1. Process Description

3D printing technologies, processes embraces a number of steps which pass from the virtual CAD definition to the resulting physical object. AM may be involved in different areas and to differing degrees of specific goods. Small, comparatively basic products may only use additive manufacturing for simulation models, whereas larger, highly advanced products with greater technological intrications may require additive manufacturing during the design, development or production phases across multiple stages and iterations[15]. But to summarize, the 3D printing method consists of three major stages. First, you'll need to obtain a printable 3D model or entity. You will then ready it for printing and the final stage will be the to print the job itself [16].

The first step is to have an entity in 3D which is normally an STL format. Nearly every 3D printing technology makes use of the STL file format. The word STL was originated from STereoLithograhy, the first industrial additive manufacturing advancements from

3DSystems in late 1990s. Considered a de facto norm, STL is a easy way to define a CAD model by itself in terms of its geometry. It functions by eliminating all construction details, modeling history, etc., and approximating the model's surfaces with a series of triangular facets[17]. Each triangular facet, the simpliest definition of a plane, contains the information about the coordinates of the three points and the exterior normal that allows to identify the side of the plane that correspond to the material.The standard STL file is depicted in Figure 3.

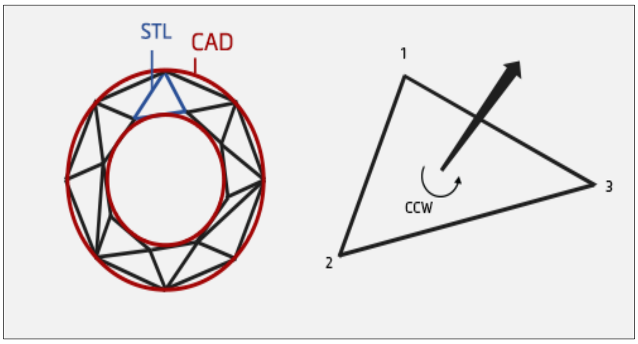


**Figure 3 STL (STereoLithograhy) file depiction** [18].

This format, however, is not recognised by all 3D printers, and can not be printed directly. You need to use a dedicated tool, widely known as 'slicer,' to process an STL file. Today In addition to STL, there are several other file formats for 3d modeling. These include .Object file (OBJ), Additive manufacturing file (AMF), Polygon file format (PLY), and Virtual reality modelling language (VRML), etc. [16].

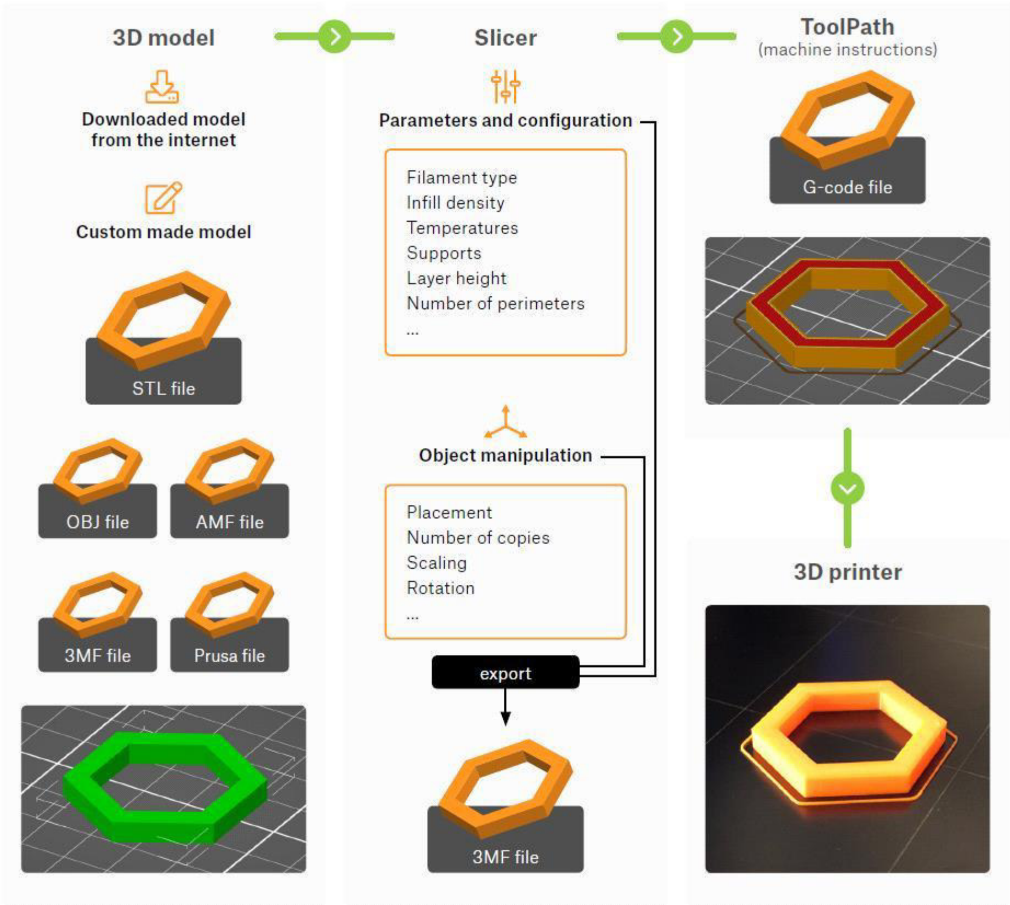


**Figure 4. The above figure illustrates the individual steps required in 3D printing. (Adapted from Basics of 3D printing authored by Josef Prusa)** [16].

Upon creation of an STL file the data is loaded through a slicer program. This program takes and transforms the STL file into G-code. The G-code is a programming language for Numerical Control (NC). This is used for monitoring of automatic machine tools (including CNC machines and 3D printers) in computer-aided manufacturing (CAM). Also, the slicer software helps the user to configure the build parameters including support, layer height, and part orientation. Furthermore, slicers incorporate additional details into G-codes, such as temperature information, cooling settings and others[19]. Printing the component is primarily an automatic operation, and the system may operate mostly without supervision. There is a need for occasional testing of the system to certify that no failures such as running out of material, power supply or software glitches have happened. Once the print has been finished by the AM machine, the parts must be removed, when removed from the machine, parts may need an additional amount of cleanup before being ready for usage. Parts may be weak at this stage or they may have supporting features which needs to be removed [17]. The simplified depiction of steps involved in FDM /FFF is shown in Figure 4.

## 2.2.Core Infrastructure of Process Catagories

ASTM formerly known as American Society for Testing Materials in conjunction with the International Standardization Organization (ISO) proposed that additive manufacturing (AM) can be divided schematically into seven units of operation as shown in the Table 1.

| Technique | Commonly used materials | Commercial names |
|---|---|---|
| ***1. Sheet Lamination***<br>Material sheets are loaded and laminated to form an object using Ultrasound adhesive chemicals, etc. | Plastic sheets, Metal foils | • Laminated object manufacturing (LOM),<br>• Ultrasound additive manufacturing (UAM) |
| ***2. Directed energy deposition (DED)***<br>Powder or wire is poured into a melting pool on the component create using a power source such as lasers | Metal powder, Wire | • Laser metal deposition (LMD)<br>• Direct metal deposition(DMD)<br>• Laser engineered net shaping (LENS)<br>• Selective photocure (3SP)<br>• CLIP- Continous liquid interface production |
| ***3 . Vat photopolymerization***<br>A vat of liquid photo polymer is cured by selective exposure to light and converts the exposed areas into solid parts | Curable photopolymer resins | • Stereolithography (SLA),<br>• Digital light processing (DLP),<br>• Scan spin |

| | | |
|---|---|---|
| 4. ***Material extrusion*** Material is extruded in tracks or beads through a nozzle or orifice, and merged into a model. | Thermoplastic filaments | • Fused deposition modelling (FDM), • Fused filament fabrication (FFF) |
| 5. ***Material jetting*** To construct the parts, droplets of materials are deposited layer by layer | Photopolymers, Waxes | • Polyjet, Projet, • Multijet modelling (MJM) • Smooth curvaters printing (SCP) |
| 6. ***Binder jetting*** Liquid bonding agents are applied selectively on thin layers of powder material to construct parts | Metals, Ceramics, Plastics, Glass | • 3DP (3D Printing) is actually the name used for the original Binder Jetting patent licensed by ExOne, VOXELJET |
| 7. ***Powder bed fusion*** Powdered substance is randomly condensed and/or fused with a heat source such as laser or electron beam | Metals, Ceramics, Plastics | • Selective laser sintering (SLS). • Direct metal laser sintering (DMLS). • Selective laser melting (SLM). • Electron beam melting |

**Table 1 7 Families of Additive Manufacturing** [20].

Table 1 typically indicates the seven distinct categories of Additive Manufacturing. Material Extrusion-based Additive Manufacturing (EAM) which represents our primary concern for this academic work represents one of the seven arbitrary categories of 3D printing processes as identified by the International Standard Organization (ISO). Although it is predominantly used for modern plastics under the specific name of FDM or FFF, it can additionally be employed for metals and ceramics also. A detailed description of the material extrusion and FDM/FFF processes is given in the subsequent chapter.

# 3. Fused Deposition Modeling / Fused Filament Fabrication

## 3.1. Overview and History

Fused Deposition Modeling (*FDM*®) or Fused Filament Fabrication (FFF) is by far the most extensively used 3D printer methods throughout the globe according to wohler associates report of 2019 [21]. A strand of plastic is melted by a heating element and extruded by a printing head (extruder) through a nozzle. This is a typical description of the FFF (Fused Filament Fabrication) / FDM (Fused Deposition Modelling) technologies which are also known as the material extrusion additive manufacturing techniques utilizing polymers as the raw material in filament form [6]. A benefit of this platform is that it is the most economical additive manufacturing technique where it can be used as a desk prototyping center in a corporate design field or for a simple development and testing in an ordinary consumer household [22].

In 1988, S. Scott Crump has been searching for a better way for his daughter to make a toy frog. He melted plastic using a hot glue gun, and poured it into thin layers and termed the invention as Fused Deposition Modeling (FDM). His machine had plastic filaments melted and poured onto a flat surface. The shape formed as the plastic cooled. He then used numerically-controlled (NC) software to automate the process. With patent in hand, Crump and his wife Lisa went on to found Stratasys in 1989. The first commercialy viable FDM 3D printer was released by stratysys in 1992[23]. The technolagy has subsequently advanced and refashioned into various avenues. That being said, FDM only gained traction during the 2000s, primarily due to the revocation of its landmark patents in 2009 [24]. Opening up commercial, open-source (RepRap) 3D printer applications. The term Fused Filament Fabrication (FFF), was coined by the members of the RepRap project to provide a phrase that would be legally unconstrained in its use [25] [26]. This has led the FDM process to widely spread where this technology accounts for the majority of the market dominance and is subject to constant improvements and adaptive responses to meet the requirements of the diverse industries. In the past few years, an explosion of relatively affordable AM machines based on this technology has emerged. Stratasys still owns the trademark which is depicted in Figure 5 on the term "Fused Deposition Modeling" [23].

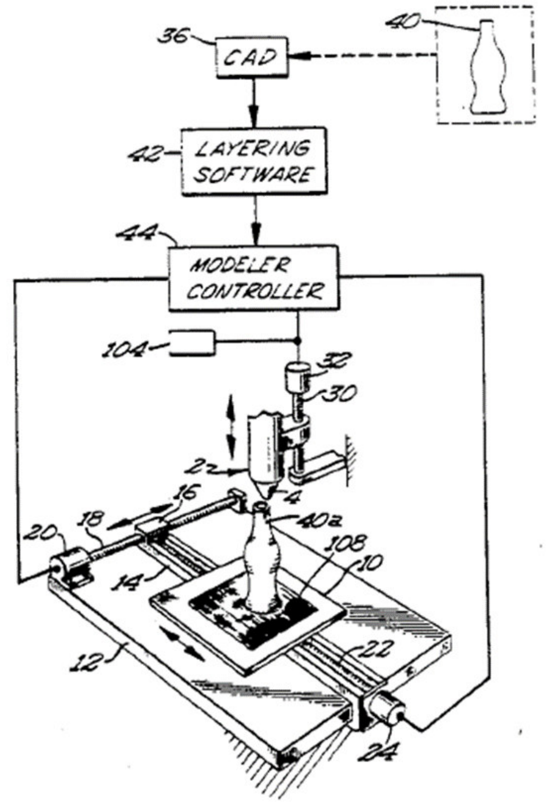


**Figure 5 Depiction of FDM patent granted to Scott Crump [27].**

### 3.2. Process Description

As previously stated. The FDM technology is an extrusion based process with plastics being the most widely extruded materials. In the Material Extrusion process category, the component is built out of material that is supplied through a nozzle or an orifice. Material extrusion, also known as ME-AM, is an additive manufacturing process that utilizes coiled filaments, usually designed for the production of 3D components by extrusion of any thermoplastic polymer. The material in the form of plastic filament is fed by an extruding nozzle, where it is heated and then deposited layer by layer on the build platform, arguably the most prominent technology that goes under the material extrusion process category is the Fused deposition modelling (FDM) or Fused filament fabrication (FFF)[28][29].

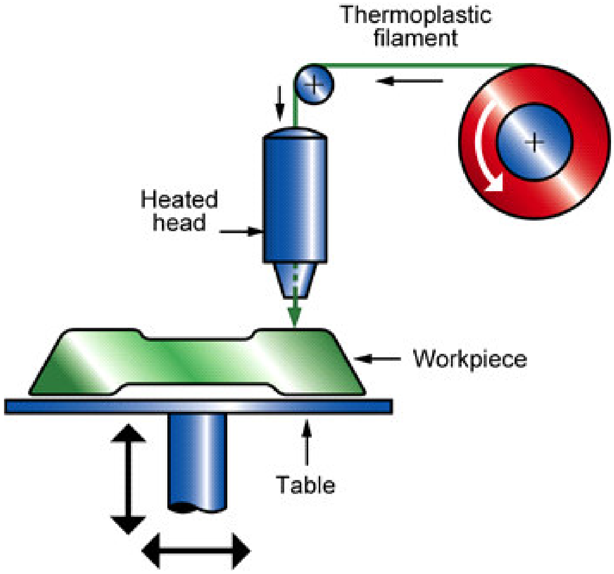


**Figure 6 Generic schematics of the material extrusion mechanism used in FDM / FFF technologies. [30]**

In something like a falicitated FDM or FFF. A filament of material is extruded out of a fine nozzle in a semi liquid condition and deposited onto a build surface as shown in Figure 6. During the printing process, FDM machines are capable of dispensing two materials: the primary model material containing the final geometry and a secondary support material used as necessary to support material overhangs during deposition layers. FDM/FFF filaments are wrapped on canisters that feed material to an extrusion nozzle through the system [31][32].

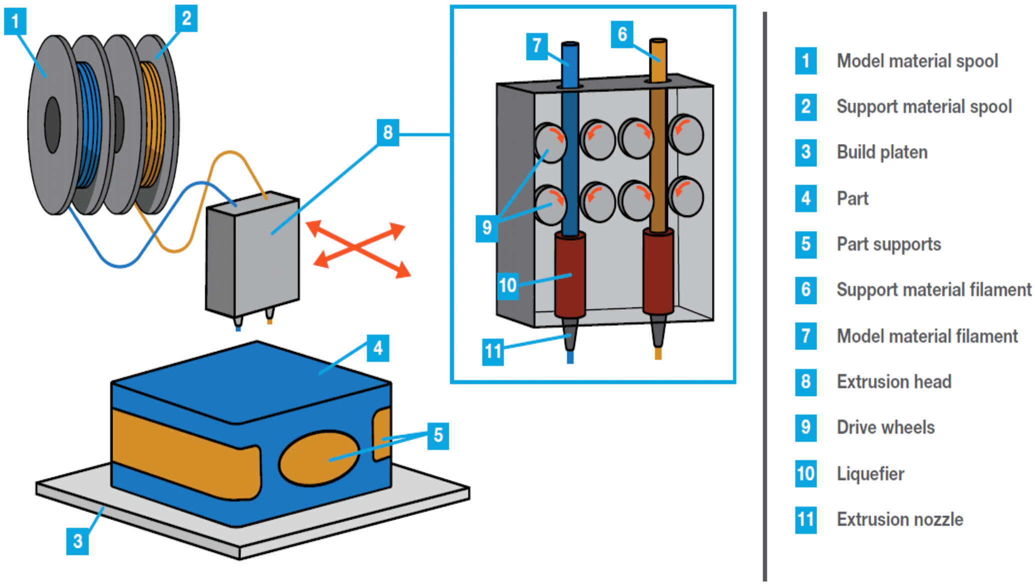


**Figure 7 Key components of an FDM/FFF Printer. [33].**

The nozzle moves in the X,Y plane, so that the filament leans back to form a thin cross-sectional slice of the component. When each layer is extruded it binds to previous layer and solidifies. The nozzle is heated by a liquefier, heating the material while it is deposited in a temperature-regulated chamber in both primary horizontal axes (X, Y) following a numerically operated tool path[34]. The base platform is lowered relative to the nozzle, and the next section slice is deposited on top of the previous slice. After each layer has been completed, the build plate moves vertically (Z direction), to make room for the next layer to be deposited above. A second nozzle is used to extrude a different material to assemble support structures for the part where necessary. The support systems are split apart from the component once the part is complete. These nozzles can be adjusted manually and only one nozzle can be used during a specific build. It should be noted that due to the use of specific nozzle diameters various FDM machines operate with different layerthickness[33].

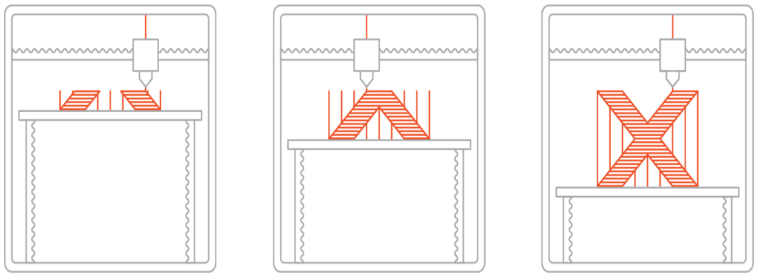

**Figure 8 Simplified visual depiction of FDM/FFF printing process. [35]**

The key components and simplified depiction explaining FDM/FFF printing process are shown in Figure 7 and 8 respectively. The basic FDM 3D printing process works like this, a computer model is translated into STL (Standard Triangulation Language) format, which was shown in Figure 3, and is properly oriented. The STL file is then loaded into the slicing program or the specific machine computer interface framework. The sliced file is subsequently inserted into the FDM machine, which begins printing with the settings needed. The component can be extracted from the platform upon completion, and post-processed if necessary [31][36].

## 3.3.FDM Machines

3D printing of thermoplastic materials will be a direct substitute for most conventional methods utilized inside early assembly and manufacturing where the heat and atmosphere of the device do not surpass 180°F - 400°F or 82°C - 20°C (on the higher end)[37]. For research purposes, different research teams use different FDM machines or printers, as stated earlier Stratasys was one of the first organizations to build FDM / FFF machines. Each machines have their own advantages and drawbacks. Depending on the controllable process parameters that are offered by an FDM machine, and some other parameters that are difficult to control using a specific machine, each user may have a different view of the equipment.

Thus, a short summary is prepared outlining the key brief distinctions between a standard home FDM 3D printer and a traditional commercial FDM printer in Table 2. Consequently, the types, advantages and drawbacks of each type of FDM system are not the focus of this paper and are not addressed anymore.

| ***Characteristics*** | ***Industrial FDM*** | ***Desktop FDM/FFF*** |
|---|---|---|
| 1. Maximum build envelope | Large (e.g. 900 x 600 x 900 mm) | Medium (e.g. 200 x 200 x 200 mm) |
| 2. Typical layer thickness | 0.18 - 0.5 mm | 0.10 - 0.25 mm |
| 3. Standard accuracy | ± 0.15% (lower limit ± 0.2 mm) | ± 1% (lower limit: ± 1.0 mm) |
| 4. Minimum wall thickness | 1 mm | 0.8 - 1 mm |
| 5. Support material | Water-soluble | Same as part (typically) |
| 6. Machine cost | Extreme / High | Basic / Low |

**Table 2 Key distinctions between a standard home FDM 3D printer and a traditional commercial FDM printer [38][39].**

## 3.4.FDM Materials

FDM printed parts are typically produced from thermoplastic polymers that have rubbery, viscous phase above the glass transition temperature and promote the fusion between subsequent layers [40]. Much of the materials used in FDM systems are based on amorphous thermoplastic polymers that are either supplied as pellets or feedstock filaments to the machine as depicted in Figure 9. Pellets are typically cheaper than filaments, because filaments are made from pellets and the final stage of filaments development is excluded [41].

**Figure 9 Pellets and Filaments [42] [43].**

Some material characteristics, such as mechanical properties, manufacturability, cost, availability and disposal, must be considered at the design phase in order to determine the correct material. The most common thermoplastic polymers used in FDM-based 3D printers are Polylactic acid (PLA) and Acrylonitrile butadiene streryene (ABS)[44]. Table 1 displays common types of thermoplastics used in FDM or FFF.

| Material | FLEXIBLE TPE / TPU | PLA | HIPS | PETG | POLYCAR-BONATE | PVA | POLYPRO-PELENE | NYLON |
|---|---|---|---|---|---|---|---|---|
| 1. Based on | Thermoplastic Elastomer Polyurethane | Polylactic acid | High Impact Polystreyene | Polyethylene Terephthalate (PET)+ Glycerol | Polycarbonate | Polyvinyl alchoal | Polypropyene | Polyamide |
| 2. Ultimate strength | 26-43MPA | 65 MPA | 32MPA | 53 MPA | 72MPA | 78MPA | 32MPA | 40-85MPA |
| 3. Maximum operating temprature | 60-74°c | 52°c | 100°c | 73°c | 121°c | 75°c | 100°c | 80-95°c |
| 4. Coefficient of thermal expansion | 157µm/m°-c | 68 µm/m°-c | 80µm/m°-c | 60µm/m°-c | 69µm/m°-c | 85µm/m°-c | 150µm/m°-c | 95µm/m°-c |
| 5. Density | 1.19-1.23g/cm3 | 1.24 g/cm3 | 1.03-1.04 g/cm3 | 1.23g/cm3 | 1.2g/cm3 | 1.23g/cm3 | 0.9g/cm3 | 1.06-1.14g /cm3 |
| 6. Print temprature | 225-245°c | 190-220°c | 230-245°c | 230-250°c | 260-310°c | 185-200°c | 220-250°c | 220-270°c |
| 7. Bed temprature / Heated bed | 45-60°c/ Optional | 45-60°c/ Optional | 110-115°c/ Required | 75-90°c/ Required | 80-120°c/ Required | 45-60°c/ Required | 85-100°c/ Required | 70-90°c/ Required |

**Table 3 3D Printing Filaments properties [45]**

3D Printing ecosystem has brought forward a broad array of different filament materials to be universally used for individual content creations. But it is substantial to know how to identify the precise type before preparing the whole printing process. 3D printing filaments are typically manufactured utilizing the cognitive process of heating, extruding, and cooling plastics to convert filaments into finished products[41]. Apart from ABS and ASA whose properties will be signified in chapter five. Table 3 displays the remaining common types of thermoplastics and their significant properties traditionally used in FDM or FFF 3D printing.

# 4. Process Parameters

Even today, using existing designs or design rules is a prevalent method of practicing FDM. They can not, however, capitalize fully on FDM 's benefits. whenever necessary leverage the design freedoms provided by the additive method**.** One of the key traits to be taken into account when designing a component for FDM is the material's mechanical properties, particularly its mechanical resistance. Various analyses and investgations have been conducted to determine the effect of the process parameters on the mechanical properties of FDM parts [46][47][48].

The FDM technology has many processing parameters, and they have a major effect on the manufacturing quality and part attributes of all these research fields, one of the most demanding is mechanical stability, and the emphasis of this study is on it. Mechanical properties of an FDM component rely not just on the properties of the material but also on the process parameters used for the manufacture of the component[49]. The process parameters which influence the mechanical strength include the build orientation, the layer thickness, filling pattern and infill percentage. Infact, the final mechanical properties of the parts produced through the FDM method are always unpredictable, because they are influenced by a vast range of process parameters that are very complicated to integrate inorder to enhance or improve the strength and stiffness of the components produced through the means of FDM [50][51]. The accuracy, reliability and properties of the components produced through additive manufacturing depend significantly on the parameters of the processes. Mainly, the operational parameters needs to be managed and refined such that elevated mechanical properties and a fully compact stucture of produced parts can be accomplished [52][53]. Increasing FDM implementations therefore involve the establishment of a practical partnership between process parameters and mechanical properties to obtain a clear comprehension of how the difference in operating parameters can decide the mechanical properties of the produced component[54].

| Parameter | Description |
|---|---|
| 1) **Air gap:** | The gap between two adjacent rasters on deposited layer. The air gap is considered negative if two adjacent layers intersect with each other |
| 2) **Extrusion temperature**: | The temperature at which a substance filament is heated during the FDM process. Temperature of the extrusion depends on different factors such as the type of material or print speed |
| 3) **Number of Contours**: | Number of contours applies to the usually organized building procedure, such that the filament is first placed around the edge of the component. Once the full edge is complete , another filament is placed at the inner side of the previously deposited contour. This method is pursued until the specified number of contours suggested has been deposited |
| 4) **Contour width** | Contour width corresponds to the width of the contour tool path which encloses the coils of the part |
| 5) **Bead width** | Width of filament that the FDM nozzle deposits. Bead width can't be smaller than 1.2-1.5 times the diameter of the nozzle 2. The most common values differ between 0.3 mm to 1 mm |
| 6)**Layer Thickness** | Deposited bead thickness mounted by the tip of the nozzle, which is usually the vertical axis of an FDM unit. It is usually smaller than the extruder nozzles diameter. I.e a one half of the width of a bead. and also differs by nozzle diameter. |

| | |
|---|---|
| 7) **Raster angle** | Refers to the angle of the raster model with respect to the X-axis on the underneath part layer. The standard permissible raster angles range between 0º to 90º |
| 8)**Raster width** | Raster width is known as the width of the beads for deposition. This depends on the diameter of the extrusion nozzle |
| 9) **Raster orientation**: | Raster orientation is the path of the deposition bead in relation to the X-axis of the FDM machines build platform |
| 10) **Print speed:** | It is the distance that the extruder travels per unit time along the XY plane when extrudering. Print time depends on the speed of the print, and the speed of the print is expressed in mm / s. |

**Table 4 Common terminologies of some of the more familiar FDM process parameters affecting mechanical properties and respective definitions other than Build orientation and Infill [55][56][57].**

Through specifying process parameters, direct FDM pathways can eventually manufacture parts with the desired properties. While this is not a straight forward task as modern FDM technology undoubtedly requires redundant process variables, naturally making it difficult to grasp efficiently how these factors influence the mechanical properties together. In order to completely explore this distinct possibility, principal subjects naturally relating to the manufacturing process and the mechanical properties of principal FDM components should also be thoroughly investigated. In practical reality, extensive knowledge of the process itself is required to maximize every manufacturing process. Such considerable expertise may be obtained either by testing or by observing the physical processes by considering all these manufacturing parameters which are displayed in Table 4 apart from Build orientation and Infill which will be analysed in the next section.

## 4.1.Build Orientation

Mechanical properties of fused deposition modeling (FDM) specimens depend on the raster orientation, which is directly related to the build or construction orientation[58][59]. where several approaches have been reviewed in the literature about previous studies related to build orientation in additive manufacturing systems in this section. Since there is very little or close to none research available on build orientation influence on mechanical properties of ASA polymer filament, only studies related to ABS along with general build orientation concepts and approaches have been chosen to be reviewed.

Determining the optimal construction orientation of a part is a key task of FDM systems. Build orientation refers to the way to orient the part with respect to X-, Y-, and Z-axes in a build platform[60] or the angle that a component renders in relation to x, y , and z axes with construction base or build platform [55]. Raju, M et al.,[61] In his paper represented build orientation as a quantitative parameter but Chacón, J et al., [62] and Qattawi, A et al.,[63] considered it as categorical parameter. Different build orientations are shown in Figure10 below. Lately, Leutenecker-Twelsieka Bastian, et al.,[64] suggested that the early evaluation of the part orientation will result in orientation being decided before the commencement of the final part design.

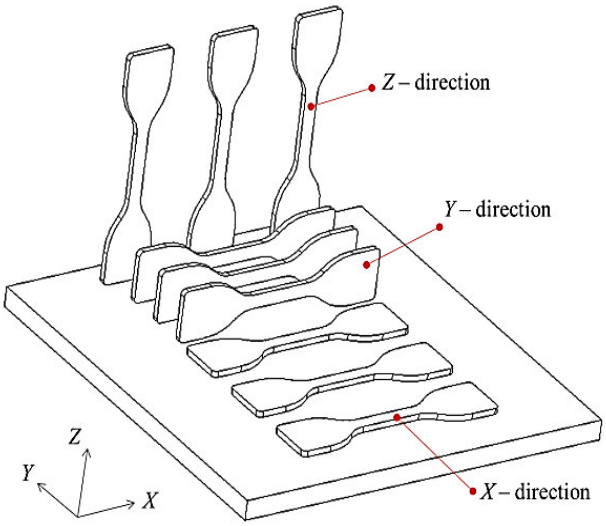


**Figure 10 XYZ Orientation [65]**

In their paper Sandeep Raut et al.,[66] examined the impact of build orientation on ABS mechanical properties, suggesting that Y-axis build orientation of FDM parts has good tensile strength and x-axis b.uild orientation has good flexural strength. Where Jason Cantrell et al.,[67] have suggested in their study that build orientation in ABS tensile specimens had a marginal effect on the Young's modulus or Poisson 's ratio. Hesamodin Jami et al.,[68] stated that the FDM build orientation has some effect on the dynamic response of ABS samples. Consequently, A. Rochester et al.,[69] indicated that by regulating the crack propagation path through the build orientation, the strength and toughness of ABS components created by fused deposition modeling can be controlled.

The direction of the build or build orientation will influence the surface finish, geometric tolerances, mechanical properties, usage of support systems, use of materials, and build time along with the costs. 3D printing technologies generally are much stronger in one direction compared to another as depicted in Figure 11. The amount of support infrastructures needed to construct a component depends on the orientation or direction of the part which influences the usage of the material, production time and expense of the component. G Moroni et al.,[70] presented that the optimal construction orientation selection is aimed at improving surface finish, increasing part strength in a particular direction, decreasing material support, minimizing design time and enhancing geometric precision. According to Jahar Lal

Bhowmik. et al.,[71] the build or construction orientation has a minimal influence on development period and has a minor bearing on material use and flexural modulus they also said that the build orientation leading to the lowest number of layers is the preferable orientation for achieving reasonable dimensional accuracy, surface roughness and mechanical properties.

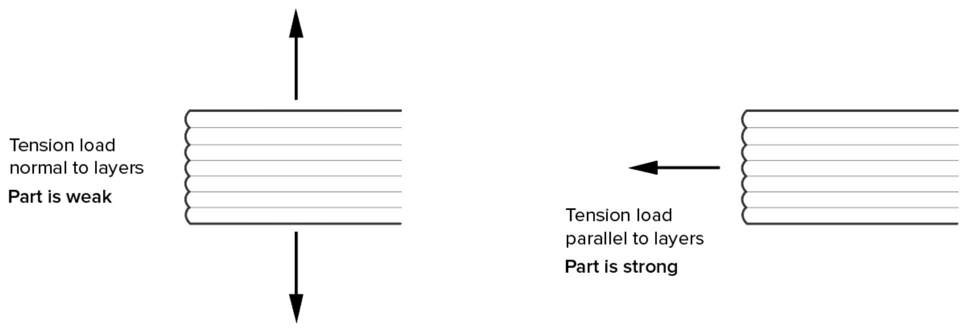


**Figure 11 3D printing technologies generally are much stronger in one direction compared to another.[72]**

T.Gordeliera et al.,[73] in their review suggested that. Typically, printing in the direction of Z can be avoided if strength is a priority. Printing in X or Y orientation increases the tensile efficiency of ABS, frequently reaching double the tensile strength of Z orienation printed samples. Where it has also been proposed that minimal variation can be found between the strength of X and Y orientation printed samples. Also, according to Stratysys[74]. Build orientation is a crucial factor in time taken to print a tool during the printing process. The material addition in the Z direction takes more time than the material addition in the X-Y plane. The amount of time allowed for production can be a significant part of the design criteria. To minimize the time taken, it is recommended that the tool be positioned such that the majority of the material is in the X-Y direction. This is also helpful to the overall strength of the component. Both print time and model are influenced by build orientation. Support material is another influential factor. It goes through a sequence of steps every time an FDM system moves from model material to support material. This can become a significant factor in the time of completion, depending on the size of the tool [33].

## 4.2. Infill

With FDM, each layer is made up of a boundary and infill. The boundary, or shell, is the exterior surface of the finished component which is noticeable. The filament is extruded in a repetitive pattern which can help to improve the strength of a component. The external layers of a 3D printer model are solid. The internal framework, generally known as the infill, is an unseen inner component hidden by the outer layer and it has various forms, sizes and patterns. The infill is the internal structure of the component which is not visible. Infill is hidden from view for most printings[75][76].

Infill does have many other functions. Besides filling in the empty space in a print, infill may even adjust its weight, based on the material used [77]. Furthermore, infill lets printers effectively and easily print smooth horizontal edges over empty space. Otherwise, prints would have very little structure or resilience inturn making them unbelievably weak. Infill is possibly one of the most critical variables of 3D printing which is sometimes underestimated[78] .When we are 3D printing, infill patterns can be easily overlooked, but they make an enormous difference in the quality of the part [79]. Various types of infilling are used in the parts to build a solid and robust internal framework as shown in Figure 12. Hexagonal, circle, and linear infill patterns are some of the widely used infill patterns, today various filling mechanisms are being suggested to reduce the anisotropic impact and to enhance the mechanical properties of FDM components. E Pei, R I Campbell et al.,[80] said that two of the most influential parameters in Fused deposition modelling 3D printing are the infill percentage and pattern where they also suggested that the greater the infill percentage, the greater the agility of the part.

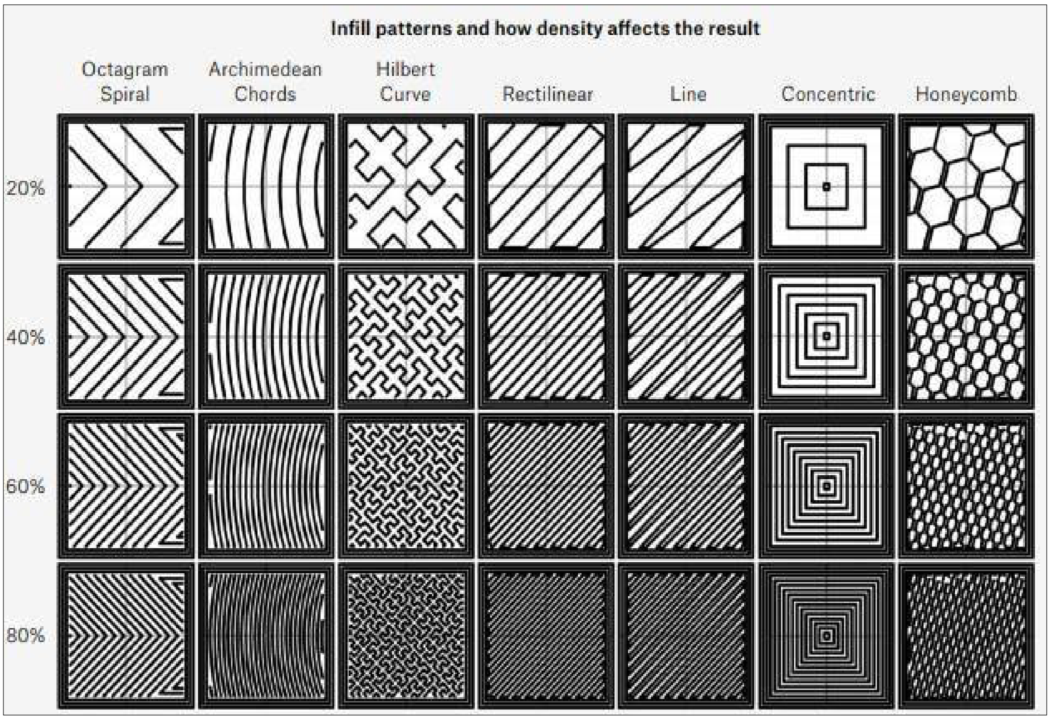


**Figure 12 Infill patterns at varying densities.[81]**

Infill density is the percentage of filament content in infill volume. The strength and weight of FDM build parts depends on the density of the infill[82] where A K Sood.,[83] suggested that selection of infill dimensions and layer thickness irrespective of the loading conditions may have a major effect on the mechanical properties, material and cost of production. Generally infill density will vary from 0 percent (hollow) to 100 percent (solid)[84] and significantly influences the final part's printing time , cost and weight.

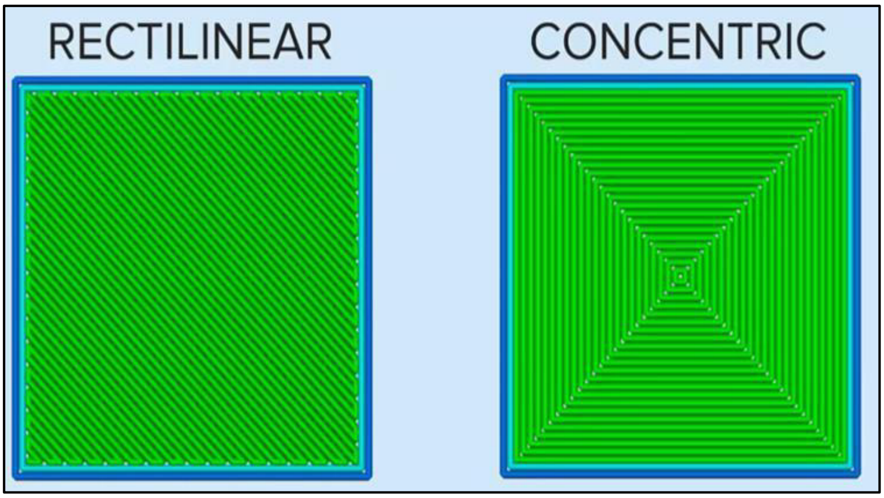


**Figure 13 Rectilinear and Concentric infill pattern used in the work [85]**

Recent work by D Cristian et al.,[86] observed the effects of raster angle orientations (0º, 30º, 45º, and 90º), infill density (20 to 100%), and infill patterns (triangular, grid, rectilinear, full honeycomb, fast honeycomb, and wiggle) in 3D printing. Their experimental findings revealed an improvement in mechanical strength with the rise in percentage increase of infill density level. Also, Anura fernando et al.,[87] suggested the same saying that ABS parts printed with 100% infill density provide the highest tensile strength where they said that the strength of the printed ABS parts decreases as infill density decreases. Kenny L. et al., [88] suggested that small infill percentages should be recommended when users are searching for quick printing but not mechanical resistance. It is desirable to use 100 percent infill if an user requires high mechanical resistance and also a quick process. Where commonly infill values between 50 percent and 98 percent are not recommended, since the gains in mechanical resistance are countered by longer effective printing times. They also indicated that it is advised to raise the ABS extrusion temperature from 230 ° C to 250 ° C in order to achieve the best possible results during experimental tests and investigations.

#### 4.2.1. Layer Outline in Infill

Every layer of a 3D printed component is generated by a confluence of outline perimeters and infill. The perimeters trace the outline of the part creating a strong and precise exterior. The infill is printed within these perimeters to make up the rest of the layer. Since the infill uses a pattern different from the outline of the component, it is crucial that these two parts merge together to form a solid bond. The 3D printing shells are the outlines or outer perimeter of each layer[89].


**Figure 14 Layer outline shells [90]**

You can modify your shells as shown in Figure 14, depending on the settings of your slicer. Shells, or perimeters, are the outer most layers of the object. Ultimately, they are the part of the object we see and interact with. The more shells an object has, the stronger it is. G Ćwikła et al.,[91] in their research suggested that if the maximum strength is the priority for your ABS components then, shell thickness should be increased. However, adding shells would also greatly increase the printing time and the cost of the component. But, increasing the resiliency and quality of FFF 3D printing will thus provide a significant benefit to developer communities around the world[92][93].

# 5. Experimental Methodolagy

## 5.1. Materials and 3D printer

In this work, the commercial ABS which was manufactured by RepRap.pt a global open source 3D printing community network and ASA filament manufactured by Filementum which is a Czech Republic based filament manufacturer, with 1.75 mm outer diameters was used to prepare the samples. ABS, one of most commonly used thermoplastics, has been the foundation for FDM for many years. Measured by annual consumption, it is the most widely used material in FDM machines[94]. Acrylonitrile-butadiene-styrene (ABS) is a thermoplastic family of ‘‘terpolymers.’’ It is the combination of three different monomers Acrylonitrile, Butadiene, and Styrene to form a single polymer [95]. The ABS filament was offered by CDRSP – Center for Rapid and Sustainable Product Development, Rua de Portugal, Zona Industrial, Marinha Grande, Portugal. ASA Luran®-S from BASF (Germany) is a shortening for Acrylonitrile styrene acrylate, and this is a thermoplastic that is developed as an alternative to ABS. ASA polymers are amorphous and have mechanical properties similar to those of ABS plastics. However, ASA properties are far less affected by outdoor conditions. The outstanding weather resistance abilities of ASA is attributed to the acrylic ester elastomer[97].

**Figure 15 ASA by Filamentum, and ABS by RepRap.PT filaments used in the work [98][99]**

Few years ago, when you wanted to print anything on an open source 3D printer, you had pretty much only one option. I, e. ABS. Soon, new materials started to appear, ASA is touted as a true successor to ABS[100]. The ASA filament was offered by Controlo qualidade em moldes (CQI), Rua de Pero Neto, Marinha Grande, Portugal. Both the filaments are displayed in Figure 15 and their general manufacturer properties are depicted in Table 5. Before printing the specimens, the filament spool samples were tested through Diffrential Scanning Thermogravimetric (DSC-TGA) equipment just to verify the natural temperature capabilities of the respective filaments through the tendency of the test. There was a clear exothermic peak just after 100ºC, but the melting was harder to see (endothermic - up). It was tried with different weights of polymeric filaments and the endothermic peak did not become clearly visible; it was not analyzed further as that was not the main concern of this work. The obtained results have been attached in the appendices A.

| *Material Property* | *ABS* | *ASA* |
|---|---|---|
| Material density | 1.04g/cm3 | 1.07g/cm3 |
| Ultimate Strength | 42 MPA | 40 MPA |
| Price in Euros[750 Grams] | 16 Euros | 28 Euros |
| Diameter tolerance | ± 0,05 mm | ± 0,05 mm |
| Print temperature | 220-250ºc | 240-255ºc |
| Bed temperature | 95-110ºc | 90-105ºc |

**Table 5 General manufacturer information and properties for the material filaments used to create the specimens [98][99].**

The DIY based Felix tec 4 desktop 3D printer (from Felix printers headquatered in Ijsselstein, Holland)[101] which is designed to give the freedom to build what's in the mind, as shown in Figure 16 was used to create the specimens. The accompanying slicer software, Simplify3D was adopted to command and control all the process parameters of the specimen parts using a Stereo Lithography (STL) file.

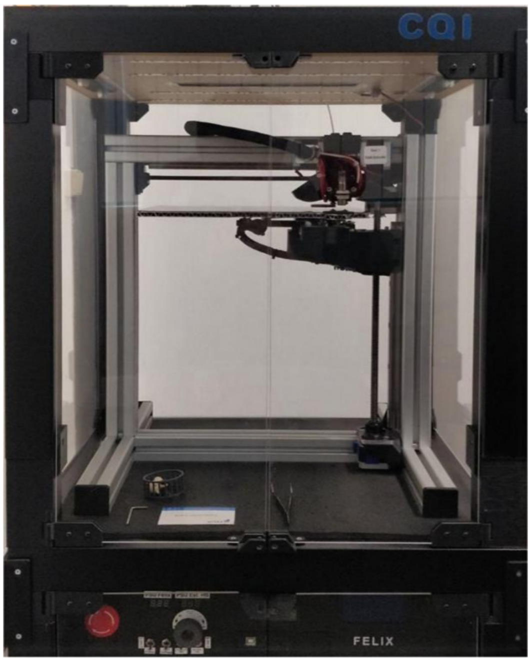


**Figure 16 Felix FFF Printer used in the work**

## 5.2. Specimen Design

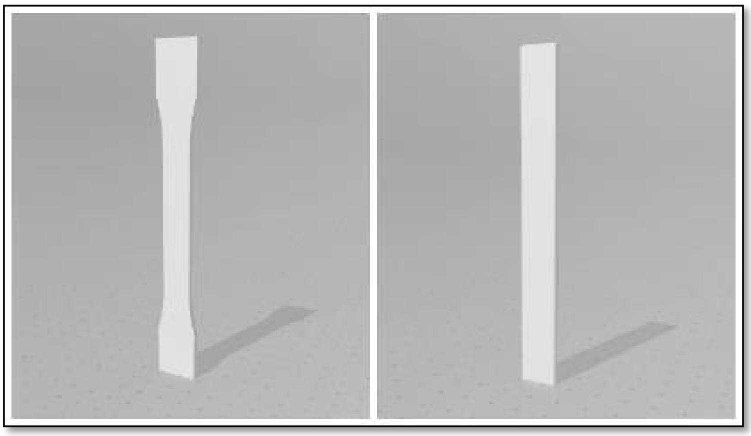

**Figure 17 3D STL file of specimens**

The sizes of the specimen to be used are determined by the pre-existing sample thickness. The geometry of the respective ASTM structured 3D printed tensile, bending and impact test samples was done using SolidWorks ® and exported to the simplfy 3D printing software as an STL format which is displayed in Figure 17. The tensile specimens were desigined according to ASTM D638 standards[102], and bending specimens were desigined according to D790 standard[103].

| | |
|---|---|
| **Filament Materials** | ABS, ASA |
| **Modelling Process** | FDM / FFF |
| **3D program** | Simplify 3D |
| **Layer Height (mm)** | 0.3 |
| **Layer Outlines** | 3, [5 for Y concentric] |
| **No of layers** | 5 (top and bottom) |
| **Infill Density (%)** | 100 |
| **Infill Pattern** | Rectilinear, Concentric |
| **Raster Angle (Build Orientation)** | X and Y |

| | |
|---|---|
| **Printing Direction** | Flat on Platform (on Printing Table) |
| **Nozzle Diameter (mm)** | 0.35 |
| **Nozzle Temperature (°C)** | 245 ±1 |
| **Printing Speed (mm/s)** | 60 |
| **Cooling Rate** | none |
| **Printing Bed Temperature (°C)** | 75 ±2 for ABS<br>85 ±2 ASA |
| **Room Temperature (°C)** | 22±2 |
| **Relative Humidity (% RH)** | 49±10 |

**Table 6 3D printing parameters and process used to create the specimens**

Mechanical properties of considerable FDM parts are regulated by their microstructures, which are inevitably governed by manufacturing parameters such as Build orientation (raster angle), Infill, and layer outline shells which were objectively analyzed in section of 4.1 and 4.2 respectively. The other general production parameters which were traditionally considered to manufacture FDM processed ASA and ABS specimens are succinctly summarized in Table 6.

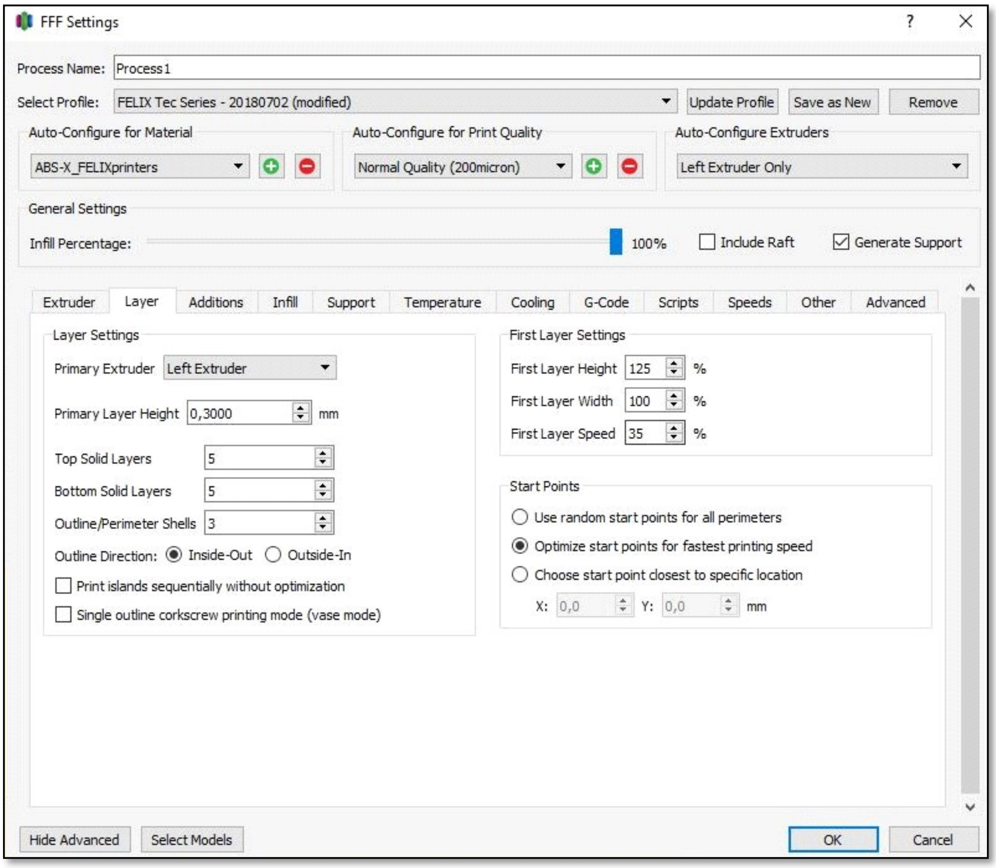


**Figure 18 Inner representation of simplify 3D software´s layer tool path perimeters. The outline perimeter shells were modified to 5 for Y-oriented concentric infill form specimens.**

Simplify 3D converts three-dimensional templates into operational commands that your printer typically knows. Better instructions typically mean better prints soundly based on the appropriate settings of your slicer. You can invariably change your shells as seen in Figure 18 where the outline perimeter shells are intentionally set to 3. Shells or perimeters are the exterior layers of the material. Ultimately, they are the component of the entity we see and deal with. The default shell thickness value is one shell perimeter. A higher value, such as five-layer outlines shells, yields more perimeters, making the shell tougher. As stated earlier the more shells the material gets, the heavier it is[91].

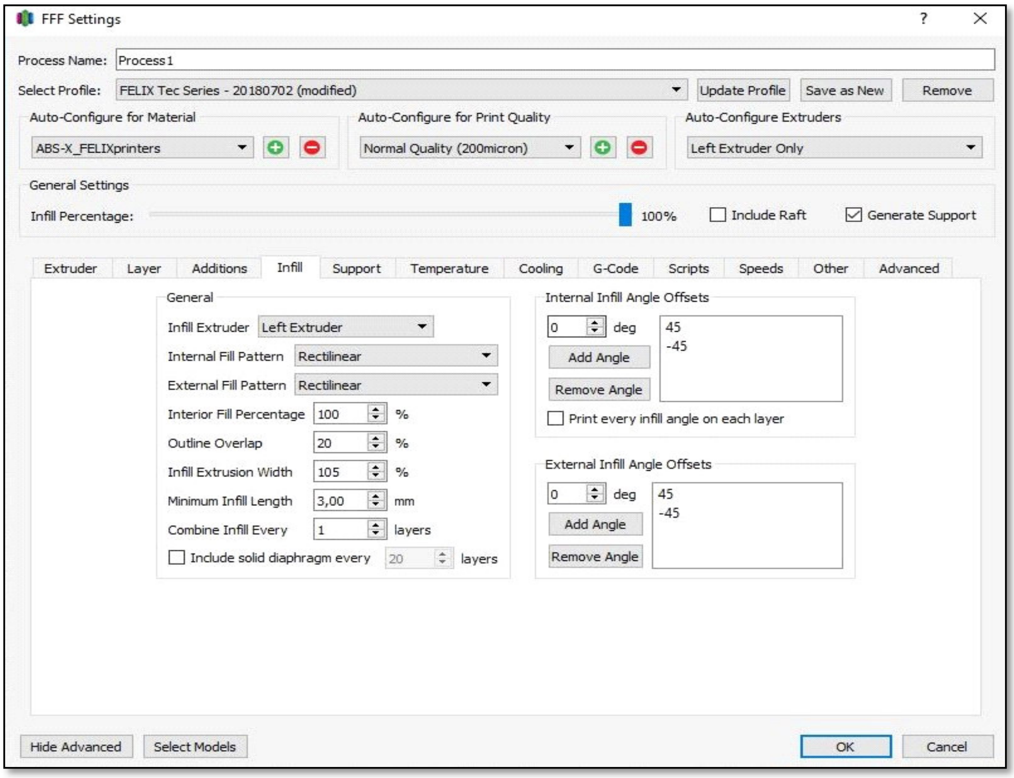


**Figure 19 Inner representation of simplify 3D software's Infill tool path parameters**

In Simplify 3D, the slicer software associated with this possible scenario, there are controlled settings that affect how far the infill configuration overlaps with the shell outline perimeter. In advanced settings, infill proportion and the type of infill pattern can be changed. The default value represents 15% and it could realistically be highered or lowered. Infill density is the percentage of the filament content in infill volume. The power and weight of the FDM components depend on the infill density [82]. Another way of viewing the solution is to adjust the type of infill pattern used. The default rectilinear infill pattern with 100 percent infill density was used to manufacture the specimens as identified in Figure 19.

| Case | Layer Height (mm) | Layer outline shells | Infill (%) | Infill pattern | Manufacturing Orientation |
|---|---|---|---|---|---|
| Case 1 | 0.3 | 3 | 100 | Rectlinear | X |
| Case 2 | 0.3 | 3 | 100 | Concentric | X |
| Case 3 | 0.3 | 3 | 100 | Rectlinear | Y |
| Case 4 | 0.3 | 5 | 100 | Concentric | Y |

**Table 7 Manufacturing cases of the specimens for Tensile and Bending tests**

Table 7 demonstrates the production cases of the specimens for standard Tension and Bending tests. It should be noted wryly that in Case 4, the Y build oriented specimen with concentric infill pattern and a hundred percent infill density was distinctly manufactured with 5 layer outline shells to test its stiffness over its counterparts with 3 layer outline shells.

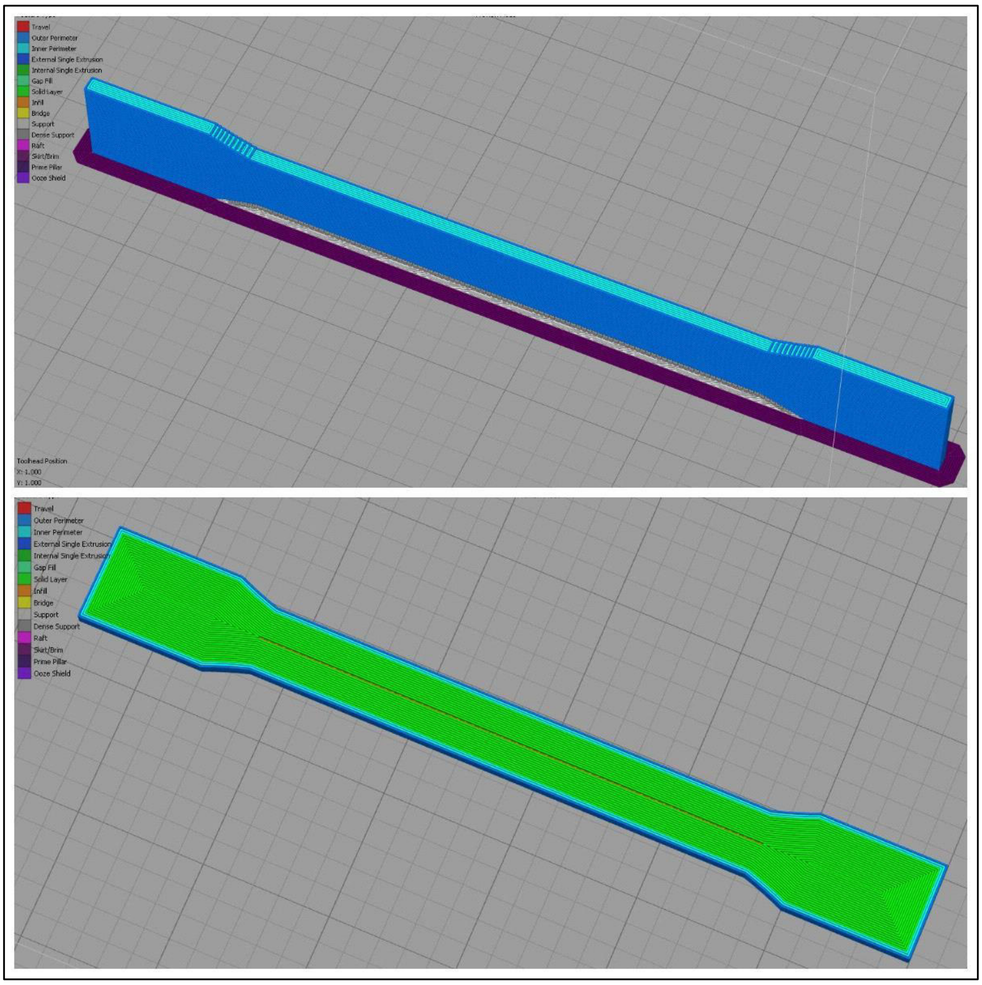


**Figure 20 Simplify 3D internal part view of Tensile specimens of Y orientation with concentric infill pattern along with 5 layer outline perimeter shells (top) and X orientation with concentric infill pattern along with 3 layer outline perimeter shells(bottom).**

In Simplify 3D, the slicer program applicable to this specific case can be unanimously selected for printing after a part has been imported in STL format. The part must be instantly updated on the devoted part view page before it can be typically printed [104]. On this tab, the selected component is shown and a variety of options which were discussed earlier can be chosen to modify the part and achieve the desired characteristics for the application as shown in Figure 20.

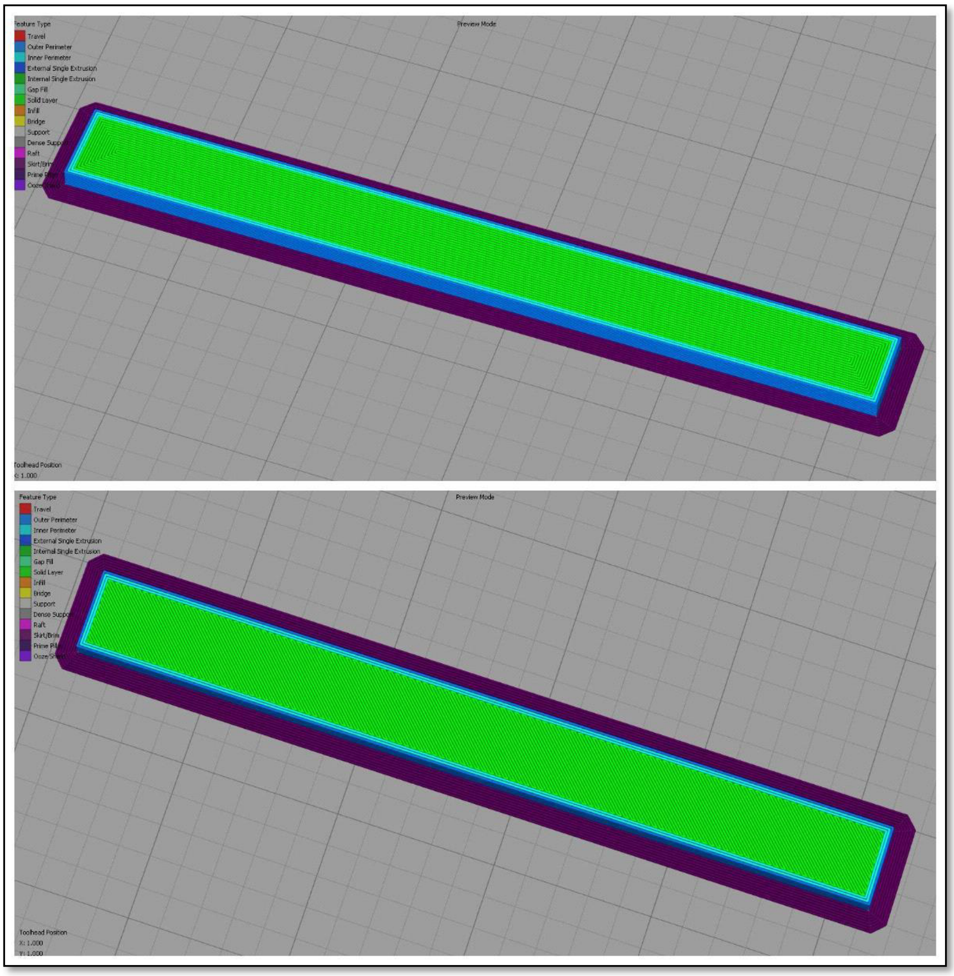


**Figure 21 Simplify 3D internal part view of X build oriented flexural bend testing specimens with concentric(top) and rectilinear (bottom) infill pattern along with 100 percent infill density.**

The concentric infill style naturally creates a cascading series of continuous loops within the elevated section that invariably follows the outer and the inner wall. The rectilinear fill form is suitable for mutually reinforcing the part around the walls of the part, but the number of concentric loops is constrained by the confined space within the part. The minimum number of loops is one for both groups, and the practical limit depends on the specific component. Although the concentric fill form is ideal for reinforcing the part around the intact walls, the rectilinear fill types are ideal for reinforcing the exposed part in a particular direction. These fill forms are again constrained by the confined space within the necessary component. These fiberfill types retain the option of managing the outer layer perimeter shells. The following example of each of the infill forms is noted in Figure 21.

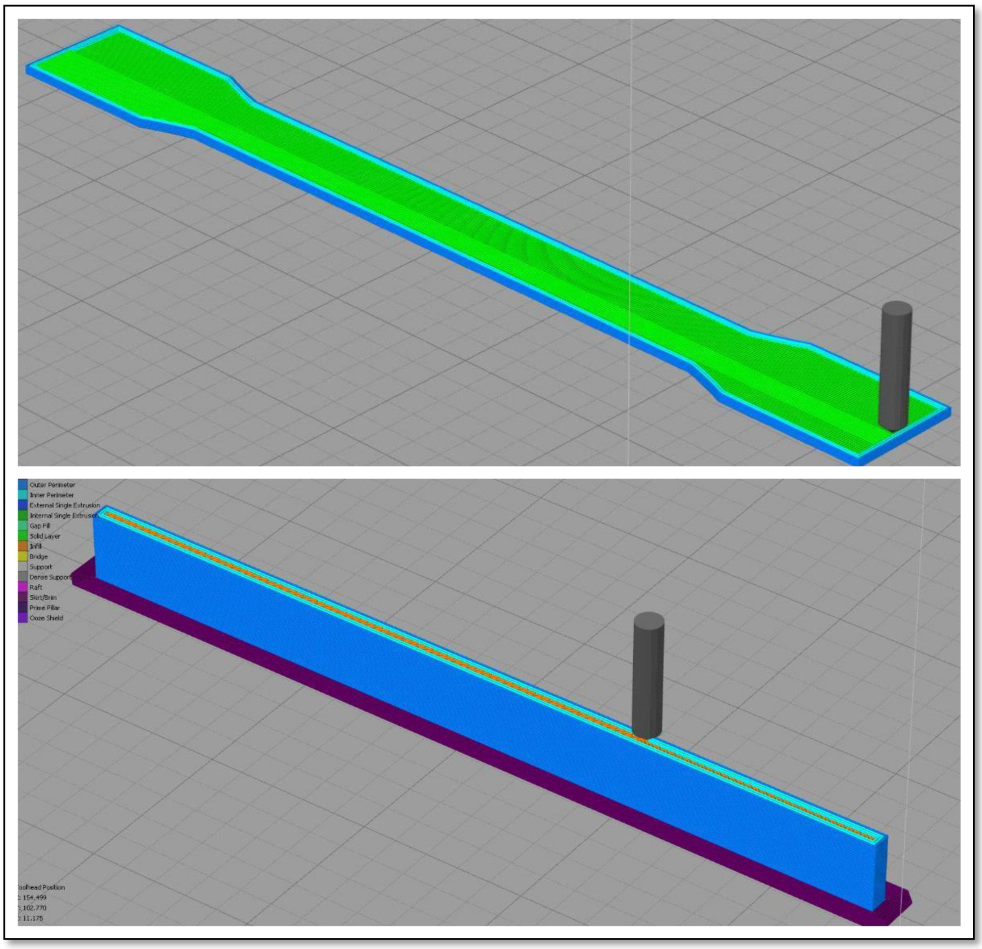

**Figure 22 Simplify 3D internal part view of layer construction of X oriented tensile specimen with concentric (top) and bending specimen with Y rectilinear (bottom) Infill patterns along with 100 percent Infill density**

The sections of the part can also be edited. For illustration, options are available that will instantly make it easier to extract pieces from the printing bed. After that, a host of choices regulate the internal configuration of the component. These are the fill pattern and fill density options. The fill density naturally varies from 0 percent to 100 percent and the printing time increases as the density increases. The specialized software naturally suggests a typical density of 15% [104]. Both options exercise the identical function of protecting the loops within from exterior elements, and the minimum number of each of these layers is one. After this process has been concluded, there are two alternatives. To save the part and start the printing process right away or to justly observe the various layers of the part and take the next step in customizing the part by going to the Internal view tab. In this section, the versatility of 3D reveals the internal layout of the part and enables more customization of each separate layer. Throughout the comprehensive customization. Simplify 3D would display the estimated time of printing alongside these conscious choices, the approximate time of printing naturally necessary for the critical component as well as the length, weight and cost of the content, as shown in Figure 23. After completing the internal view step properly, the last step is to construct a build file as depicted in Figure 22.

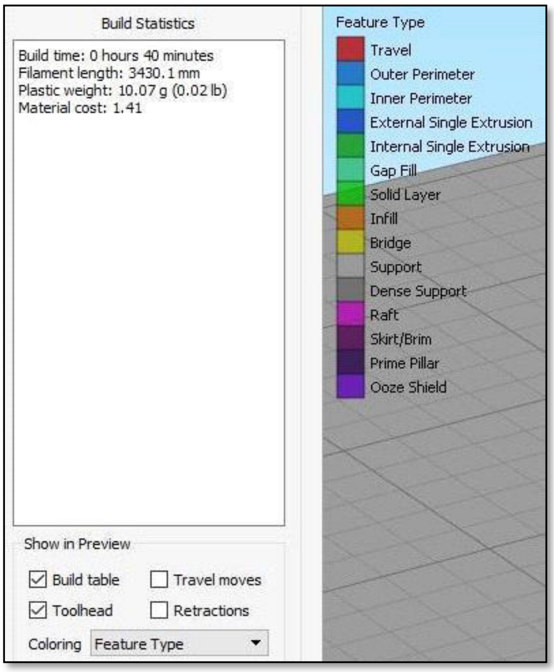


**Figure 23 Showing certain facets of the Simplify 3D part view tab. A portion of the available feature type parameters option is displayed on the right and on the left, some estimates of the filament length, material used, approximate print time and material cost in USD is demonstrated.**

## 5.3.Print Output and Quality

The ASTM (American Society for Testing and Materials) standard emphasises the objectives of quality assurance inspection of samples prior to processing and testing. The Cooridnate Measuring Machine (CMM) examination was carried out using the Optiv Classic 443 tp CMM shown in Figure 24 which includes a high-resolution CCD (charge-coupled device) camera for multi-sensor applications with micro-to nano-scale precision measuring criteria, inorder to monitor air gap problems or any other structural flaws.


**Figure 24 Optiv Classic 443 tp CMM used in the work**

During the printing process it was noted that the Tensile samples of Y orientation from ASA material samples tended to warp a bit, which was later tonned down through the use of heated chamber enclosure. Warping is one of the most common defects in FDM. From a technology standpoint, warping can be prevented by closer monitoring of the temperature of the FDM system (e.g. of the build platform and the chamber) and by increasing the adhesion between the part and the build platform. The top 2 images from Figure 25 indicate the warped side of the part, the bottom 3 images show the layer formation of the warped corner which is captured from the high-resolution CCD (charge-coupled device) camera of a CMM machine.

It should be noted that printing on a printer configured with an actively heated chamber is one of the recommended remedies for near-zero warping of ASA printing [105].

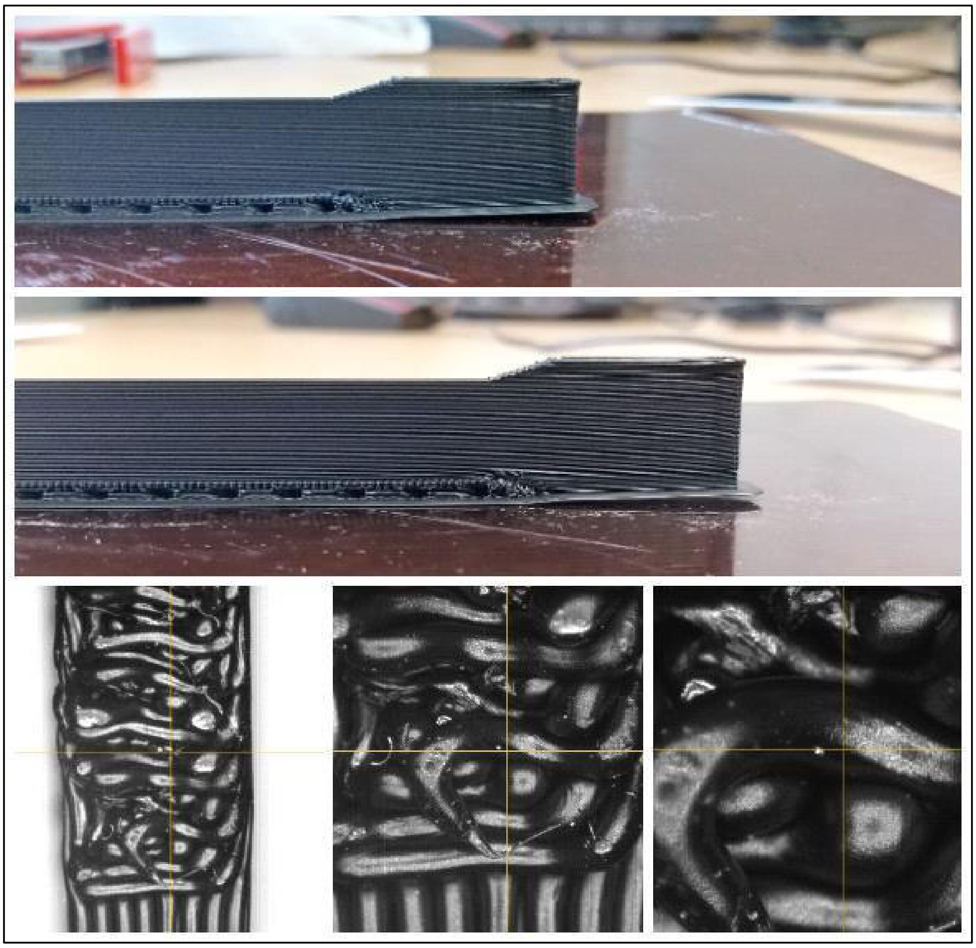

**Figure 25 Warping in ASA**

Layer deformation happens where the distinct layers of the 3D print are different or do not fully hold together. This results in hideous cracks that might cautiously feel like a hassle to get rid of. Feasibly the most straightforward solution to layer separation is to elevate the printer's hot-end temperature. Shallow layers stick together by mixing with heat. If the heat of the extruded material is too cool, it won't be able to adhere to the previous layer. Rather the cooling fan typically allows the necessary material to set too quickly resulting in layer-to-layer delamination[106].

3D print part warping typically presents a daunting challenge to get about; just as a 3D printer is precise, that merely doesn't mean it won't have this obstacle. 3D printed sections warp due to thermal deformation. When plastics heat up, they progressively expand. When they are passively cool, they naturally shrink. Although FFF 3D printing nearly always entails thermoplastics, this occurs in almost any FFF 3D printer. There are two features on the printer side to address warping: a heated building plate or a heated enclosure. These two possible solutions typically prevent the essential part at elevated temperature, so it's not cool, and in common, there is no warping. 3D printers will have a fortified enclosure that bears the heat in the used adhesive to be added to the fabrication layer In addition, allegedly allowing the part to cool to room temperature before removing it will eliminate warping so the part cools while still adhering to the build plate[107]. As further corners are properly applied to the line section that needs to involuntarily shrink, the obscure corners will peel up due to the build-up of stress at that spot, as seen in the Figure 25.

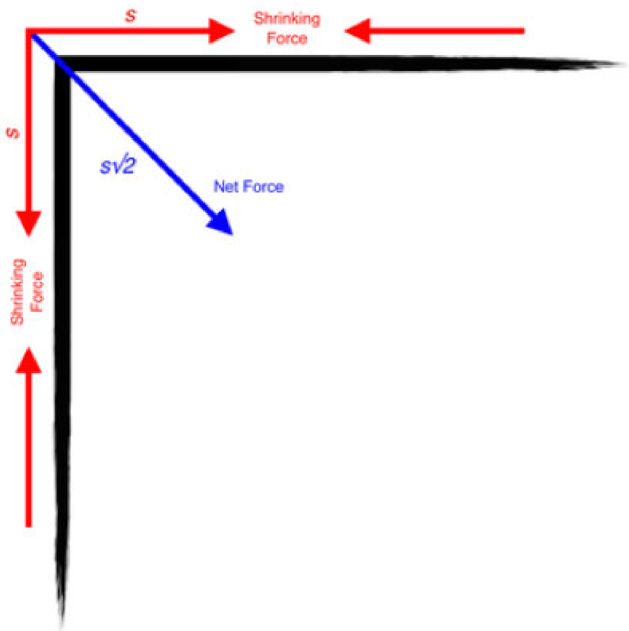


**Figure 26 Warping typically starts from edges because the forces on either distinct edge add up** [108]**.**

Sharp corners invariably create stress concentrations as shown in Figure 26, so accustomed corners realistically are the most common geometries that cause warping. Adding a fillet to these corners lowers stress when the sharp corner is squared off and the stress is dispersed. In general, creating cross-sections that are more circular in modern form while timidly approaching the build plate decreases warping. When engineers design sections that typically end up rectangular in shape; that is usually the simplest thing to the machine. But building from the outset of more circular, natural shapes, and polished surfaces will mitigate warping by distributing stress build-up. However, parts printed at 100% infill will typically suffer from warping when compared to parts printed at 25-50%, as parts printed with a low infill will have fewer surface areas across layers and become more susceptible to cracking[35]. Also, due to the different FDM 3D printer process parameter settings, warping deformation remains a distinct possibility.

A more major distortion happens where the essential component typically has undercuts or cavities. The surface roughness resulting due to the potential impact of the staircase on the rapid prototype components is one of the critical factors. While several concerted efforts have been made to merely improve the surface finish of rapid prototype parts, the downside to these abortive attempts is the usability of some areas of the prototype component. In general, pre-processing and post-processing operations can be carried out in additive manufacturing. However, the quality of the components is unsatisfactory compared to other advanced manufacturing methods[109].

In addition, a digital caliper and a weighing scale displayed in Figure 27 were used to measure the final dimensions of each specimen. After examining, the dimensions which were considered to be the most relevant for each sample was checked so that the results could be validated.


**Figure 27 Digital caliper (top) and weighing scale (bottom) used for the measurement of the specimens**

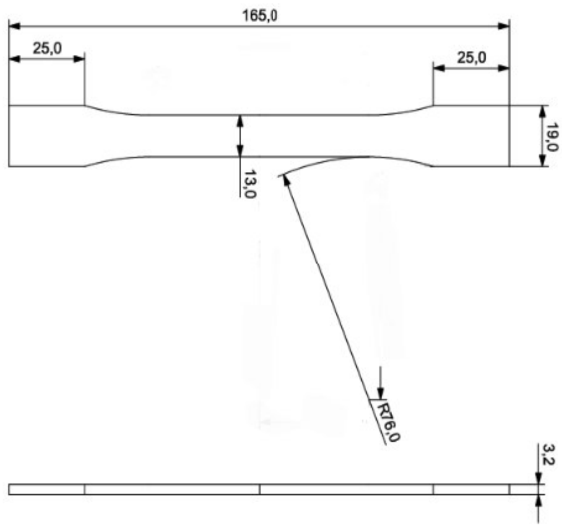


**Figure 28 2D dimensions of 3D printed specimens for tensile testing. The dimensions and geometry mentioned equate to those prescribed by the standard ASTM D638-14 for the type I tensile testing specimen.**

Here as shown in Figure 28. For the determination of tensile properties of thermoplastic filament materials (ABS and ASA), The standard which was chosen was ASTM D638-14 (standard test technique for tensile properties of plastics). The specimen shape adopted was the type-1 dog bone, with a length overall (LO) of 165 ± 0.1 mm. The dog bone thickness (T) was 3.2 ± 0.3 mm . The gage section width (W) was 13±0.015 mm and with a distance between grip (D) of 25 with ± 0.3 mm. The radius of the fillet (R) was 76 with ± 0.04 mm. Finally the weight of the tensile specimens was 7.8 ± 0.2 grams for both X and Y orientation specimens.

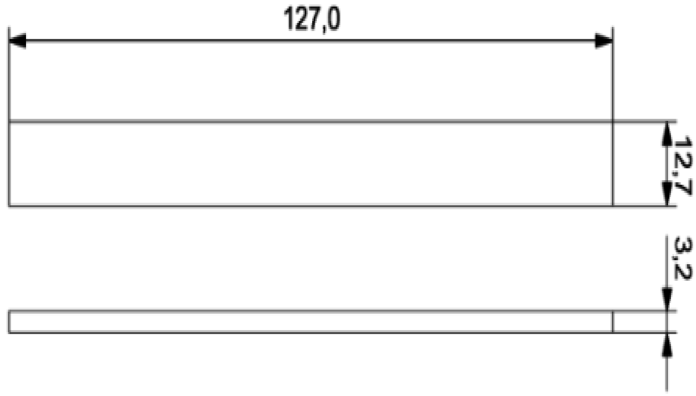


**Figure 29 2D dimensions of 3D printed specimens for Bend test. The dimensions and geometry mentioned equate to those prescribed by the standard ASTM D790 bend test specimen.**

For, flexural bending properties of both ABS and ASA samples, it was chosen the standard ASTM D790 as shown in Figure 29 with a length overall (LO) of 127 ± 0.1mm. The gage section width (W) was 12.7 ± 0.02 mm. The thickness (T) was 3.2 ± 0.4 mm and Finally the weight of the flexural bending test specimens was 5 ± 0.2 grams for both X and Y orientation specimens.


**Figure 30 Bending specimens [Right] and Tensile specimens [Left] produced.**

The following section presents the CMM quality inspection of each geometric outline of the infill which were taken before the mechanical tests, along with a brief description. The description is clearly an exploration of the specimen shape formation and is not intended to make any correlation with the performance of the specimen. Every series of figures presented consists of  images of successively increased zoom levels. When printing ASA it is vital to guarantee that the  nozzle height and bed is levelled correctly and also, it is important to use the recommended printing surfaces. Similarly when working with ABS, it is recommended that starting temprature should be around 230ºc and then adjusting the temperature according to the requirements so that the quality of the print and the strength of the part will be in good balance with each other. Here for both types of specimen materials the nozzle temperature was set  for 245ºC [111].

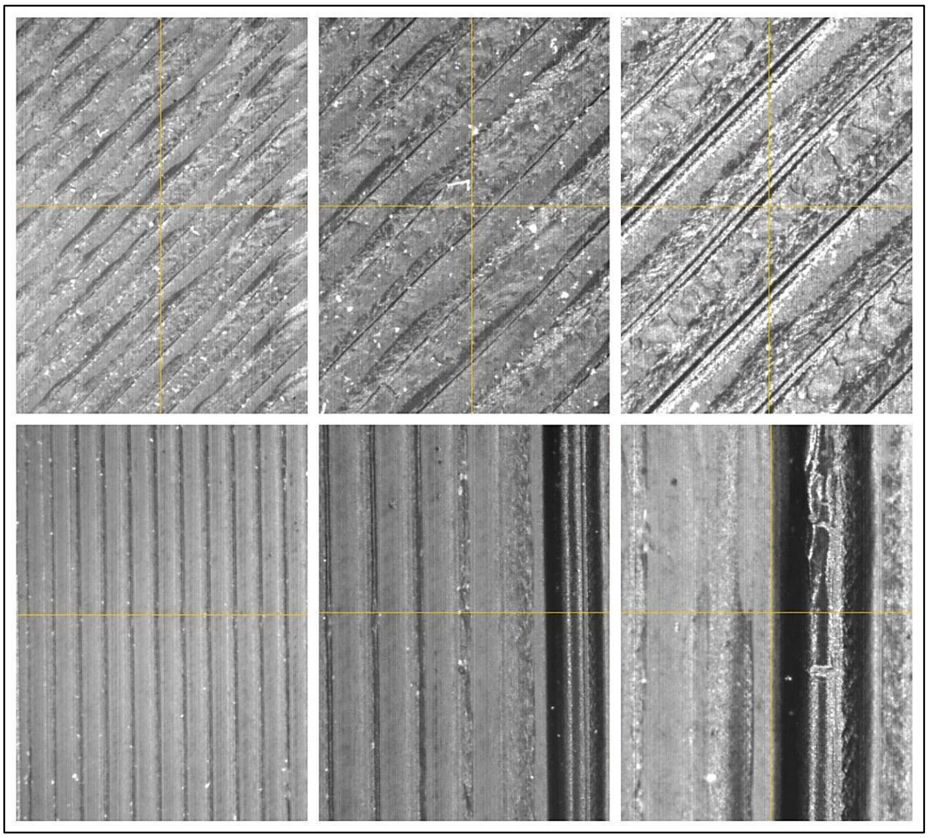

**Figure 31 CMM high-resolution CCD (charge-coupled device) camera captured outer layer arrangement of porous architectures of ASA X Rectilinear (top) and X Concentric (bottom) 3D pattern structures of the specimen.**

3D printing structures can typically have a tailored design for both their internal and exterior geometries, which can inevitably lead to a significantly decreased mass compared to other manufacturing methods. The layer bonding in FDM in common is the cognitive ability of the printed material to naturally create an enduring bond with the social layers surrounding it. The CMM high-resolution camera captured the différance between the layer arrangement bonding between concentric and rectilinear infill pattern with X build orientated fecal ASA specimens can be visibly seen in Figure 31. The Concentric infill pattern essentially generates a set of inner boundaries parallel to the perimeter of your object. It will be the weakest infill pattern if 100 percent infill density is not employed since horizontal strength isn't there. Rectilinear, the default infill pattern in many 3D printing softwares, is predicted to serve as a good balance between speed and strength. In terms of bonding between layers, rectilinear infill patterns lowest porous form often results in a reduction of pore size [110].

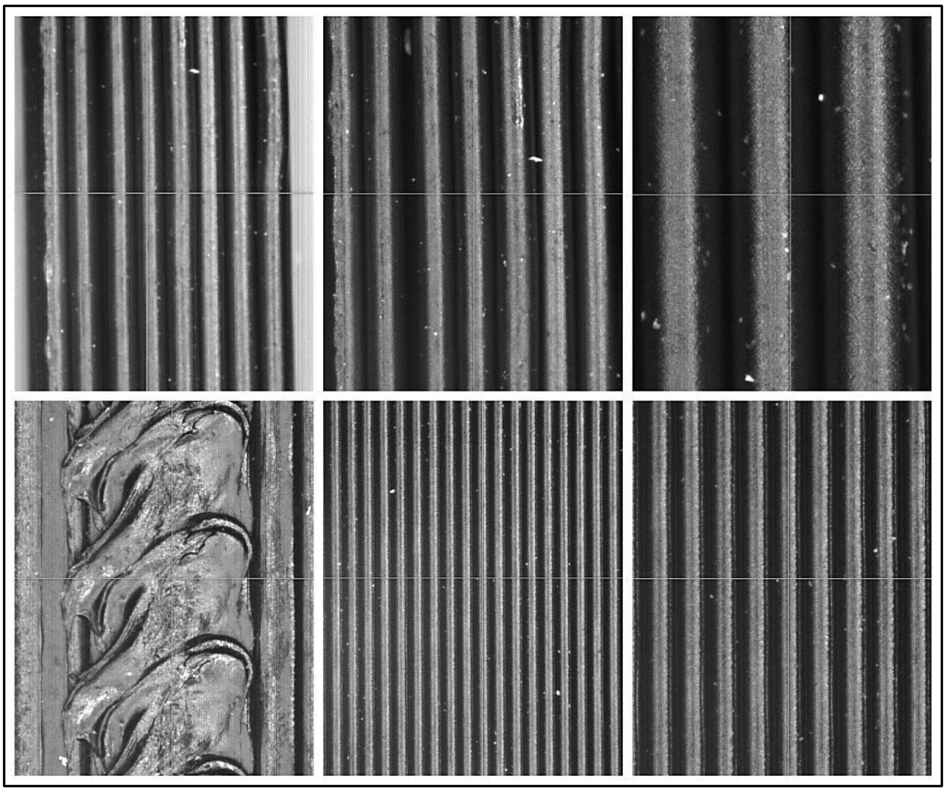

**Figure 32 CMM high-resolution CCD (charge-coupled device) camera captured outer layer arrangement of porous architectures of ASA Y Concentric (top) and Y Rectilinear (bottom) 3D pattern structures of the specimen.**

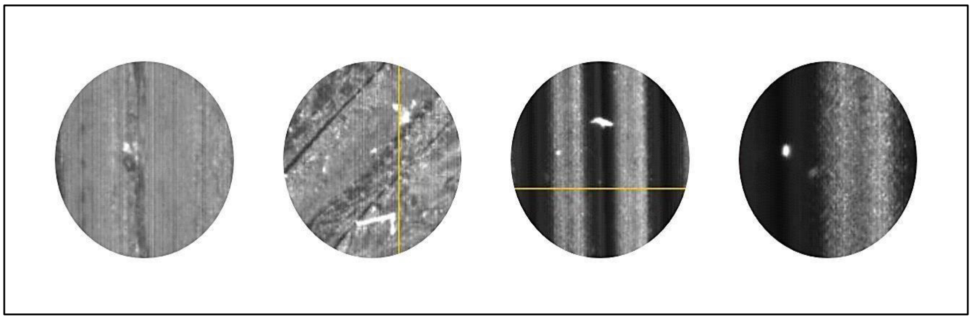

**Figure 33 :- Residues accumulated in 3D printed specimens of ASA.**

3D printing functions by typically constructing an object in one distinct layer at a considerable time. Each subsequent layer is printed on top of the previous layer, typically creating the ideal 3D form at the ultimate end as shown in Figure 32. Although in established order for the final component to be solid and secure, you naturally need to make sure that each distinct layer is properly connected to the layer below it. If the layers are not properly fused together, the final component can be broken or separated. Inorder to get the fine print we should also make sure there are no residues accumulated in the finely printed specimen. It should be noted that in Figure 32 minor residues have been accumulated which can be clearly seen when the zoom level increases in Figure 33. The residues can be disposed using acetone vapor smoothing which fits both ASA and ABS or through other post processing techniques. In this situation though, it was not undertaken as post-processing could be expensive and might have a minor impact on the mechanical performance of the samples [106].

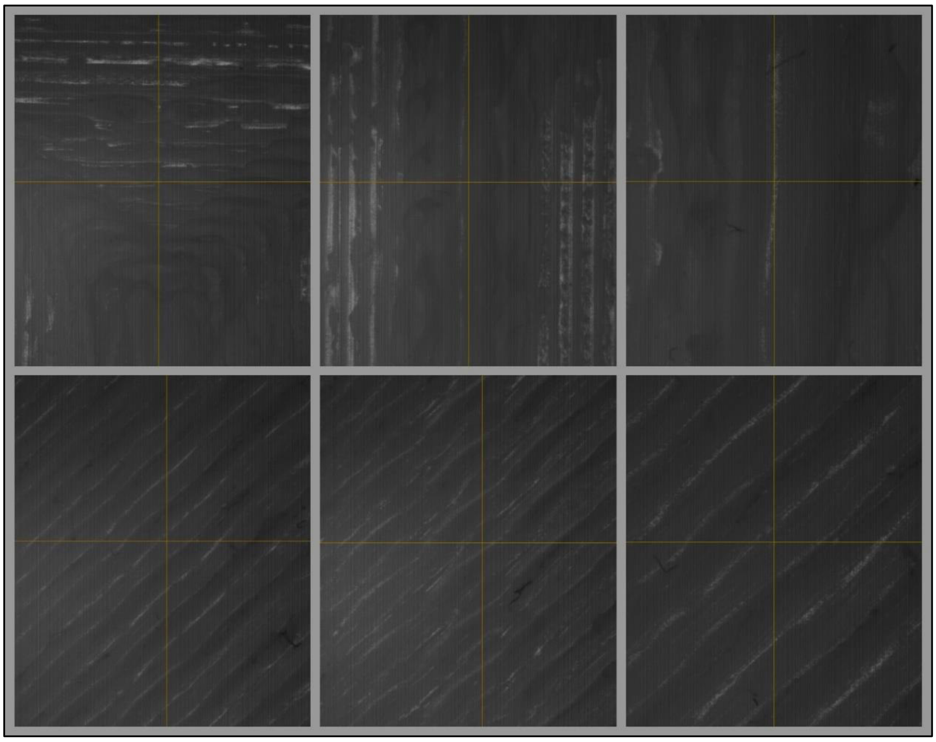

**Figure 34 ;- CMM high-resolution CCD (charge-coupled device) camera captured outer layer arrangement of porous architectures of ABS X Concentric (top) and X Rectilinear (bottom) 3D pattern structures of the specimen.**

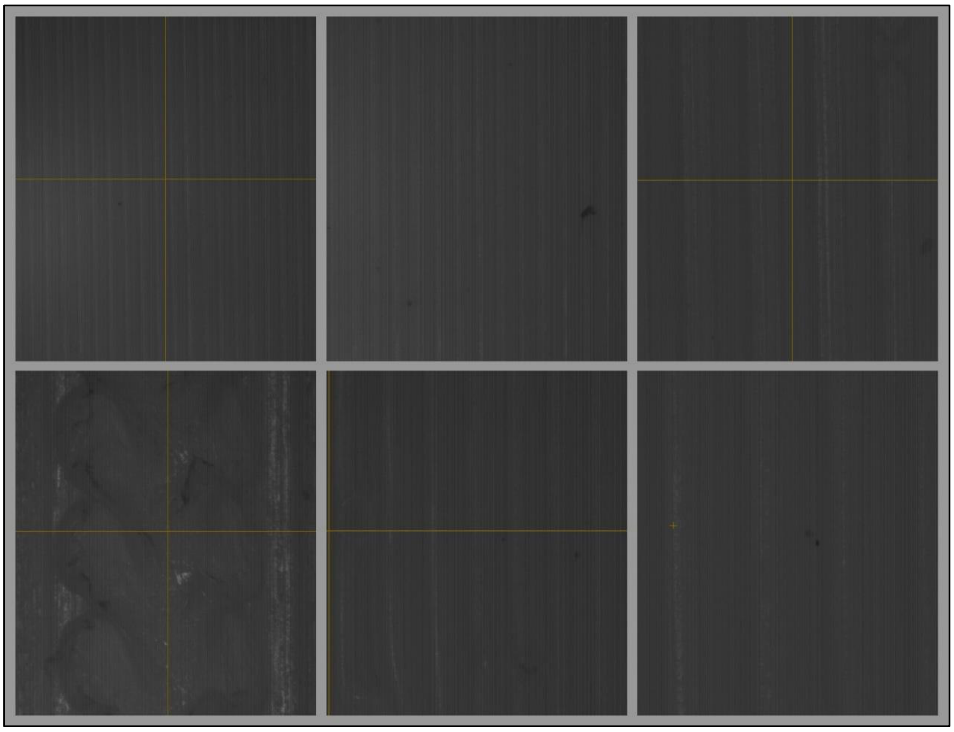

**Figure 35 CMM high-resolution CCD (charge-coupled device) camera captured outer layer arrangement of porous architectures of ABS Y Concentric (top) and Y Rectilinear (bottom) 3D pattern structures of the specimen.**

As the printing of the specific object in FDM means that each printed strand of obscene material will under no circumstances be at a different temperature when they first make contact, the cognitive ability of these different strands to bond is integral to the overall strength of the structure. While the distinct possibilities for FDM seem, vast it has traditionally been assumed that the layer bonding typically creates the biggest weaknesses in the structures. As said earlier determining the optimal construction orientation of a part is a key task of FDM systems. The way the part made with ABS has oriented with respect to X and Y axes in a build platformz [60] [112] and the angle that a specimen has renderd in relation to build orientation [x, y] and Infill pattern[concentric and rectilinear] axes with construction base or build platform is captured in CMM high resoultion CCD [charge coupled device] in Figure 34 and 35 where the differance in layer arrangement bonding for both the build and infill types can also be noticed in images.

# 6. Results and Discussions

## 6.1.Tensile Properties of 3D Printed samples

For the study of the Tensile Parameters, the tests were carried out using Instron 4505 universal testing machine shown in Figure 36 with a static load cell of ± 5 KN and the loading speed was set to 10 mm/min. All tests are carried out at the temperature 22± 3°C and relative humidity 48 ±5%. Results from the tensile test presented in below figures, clearly present significant influence of the build directions and infill patterns on the tensile strength of ABS and ASA printed samples.


**Figure 36 Instron 4505 universal testing machine used for conducting Tensile, Bending and Compression tests for the work**

### 6.1.1. Mechanical Behavior of Tensile specimens


**Figure 37 ABS [Left] and ASA [Right] Samples after the Tensile test.**

The Fracture surface points of ABS and ASA specimens after tensile testing are seen in Figure 37. Almost all of them suffer amicable split in close proximity to the fillet radius, which is typical for FDM specimens [113] and is traditionally attributed to stress concentrations in fillet areas. This distinct type of fracture is brittle, with no plastic deformation observed. Studies have stated that craze is one of the primary kinds of plastic deformation process mechanisms of ABS, and a considerable number of crazes are produced perpendicular to the direction of the load [114]. This brittle behavior represents a typical characteristic of FFF parts and has been clarified by other authors due to the precarious existence of voids that help to typically initiate crack which in turn results in abrupt rupture[50]. Before the odious comparison is undertaken, it is necessary to adequately explain that, while the specimens in this work have been printed as solid parts according to the respective standards, the additive manufacturing method leaves some gaps between the layers as seen in Figure 38, such that the infill is assumed to be similar to 100%, but perhaps not wholly. These air gaps are responsible for the decrease in tensile strength due to a marked decrease in the cross-section area of the specimen[115]. Moreover, the lower strength of selected samples has been attributed due to the gaps and inner pores of the specimens. Though the FDM system setting inevitably suggests no desired air gap, the fiber geometry inevitably causes the visible presence of triangular or rounded air gaps or voids as seen in the SEM image in Figure 36. These voids or gaps affect the effective tensile strength and other mechanical properties of the FDM sections by typically decreasing the physical cross-section of the sample specimens which are rather normal or inevitable in FDM 3D printing [114].

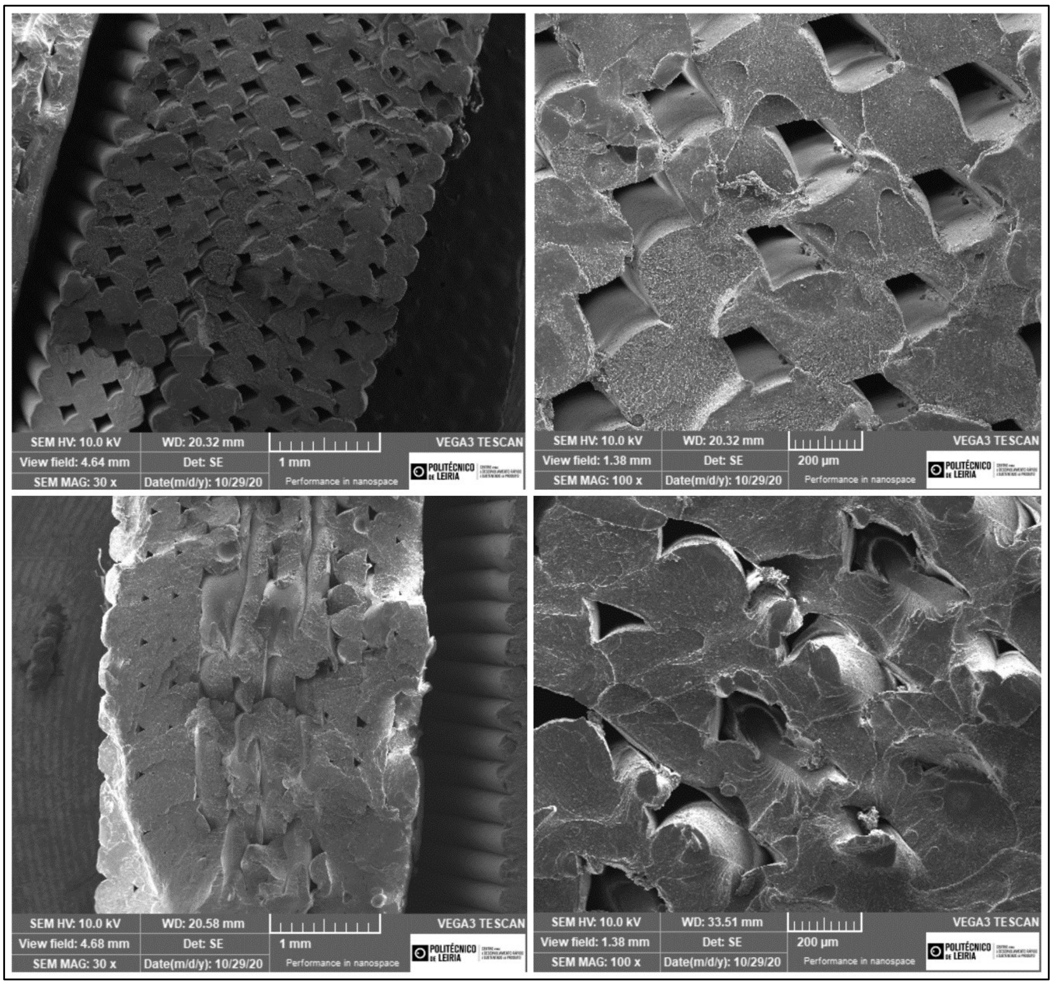


**Figure 38 Fractured cross-sections of Concentric [Top] and Rectilinear [Bottom] samples captured through Scanning Electron Microscope [SEM], it can be invariably seen that triangular voids are present in between the bond length of the polymer structure interface**

From the Figure 38, the fracture surface of two of the specimens attentively examined for each orientation typically indicates the possible variations in the internal distribution of the filaments from different infill patterns. These profound insights are similar to the work of V Shanmugam [116] and Enrique Cuan-Urquizo et al.[40] which argued that the existence of the layered structure and, in particular, the bonding between the distinct layers, exerted a significant effect on the mechanical properties.

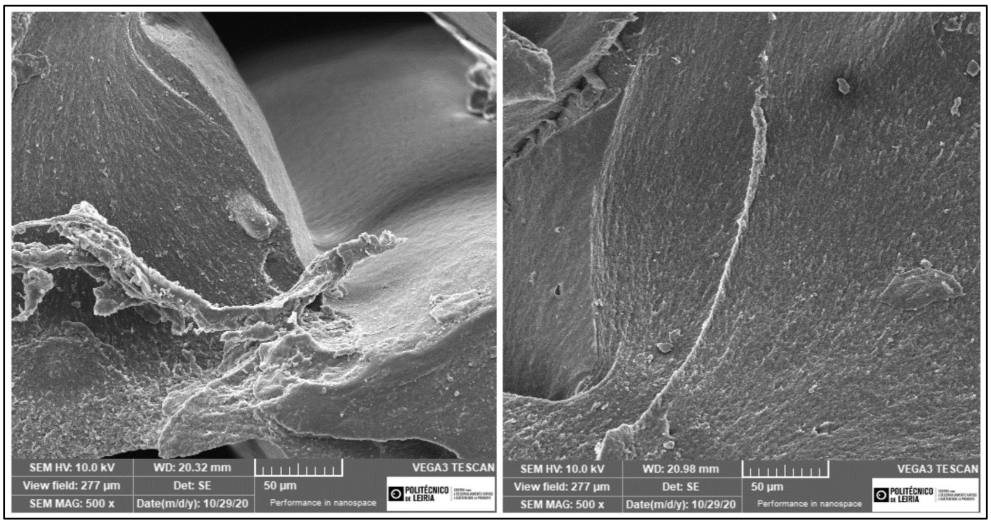


**Figure 39 SEM 500X magnified internal structure view of fractured Concentric [Right] and Rectilinear [Left] infill patterned specimens.**

The obvious vulnerability to possible fracture obtains a representation of the general resistance to crack formation, combined with the desired consistency of the interlayer binding and the microstructural features reflected in the current printed pattern by the relative size of the voids or gaps to those of the printed layers. It was scrupulously observed that the voids in concentric infill type specimens were slightly greater when compared with rectilinear infill type. The magnified internal structure view of fractured Concentric and Rectilinear infill patterned specimens can be seen in Figure 39. The air gap that occurs when manufacturing and maintaining the visible presence between the fibers of the FDM specimens is one of the key factors in considering the general mechanical properties of the FDM 3D printed specimens.

### 6.1.2. Effect of Infill Pattern and Build Orientation on Tensile specimens

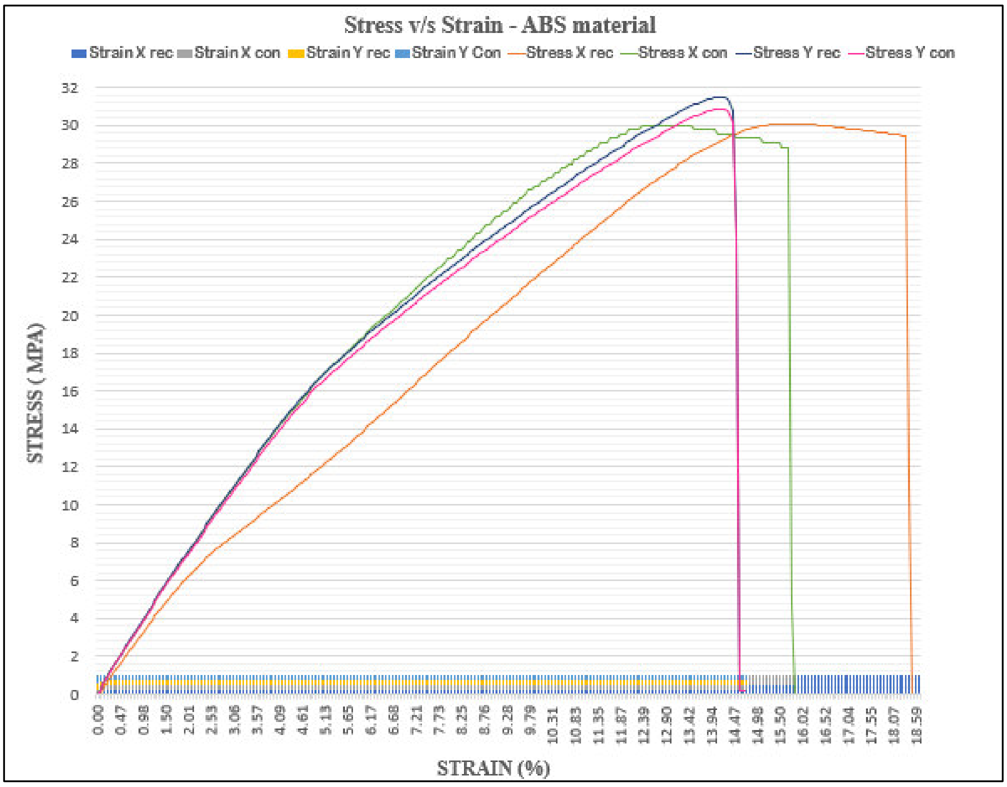


**Figure 40 Stress-Strain curves from the Tensile strength test for different Infill patterns and Build Orientations for ABS thermoplastic filament.**

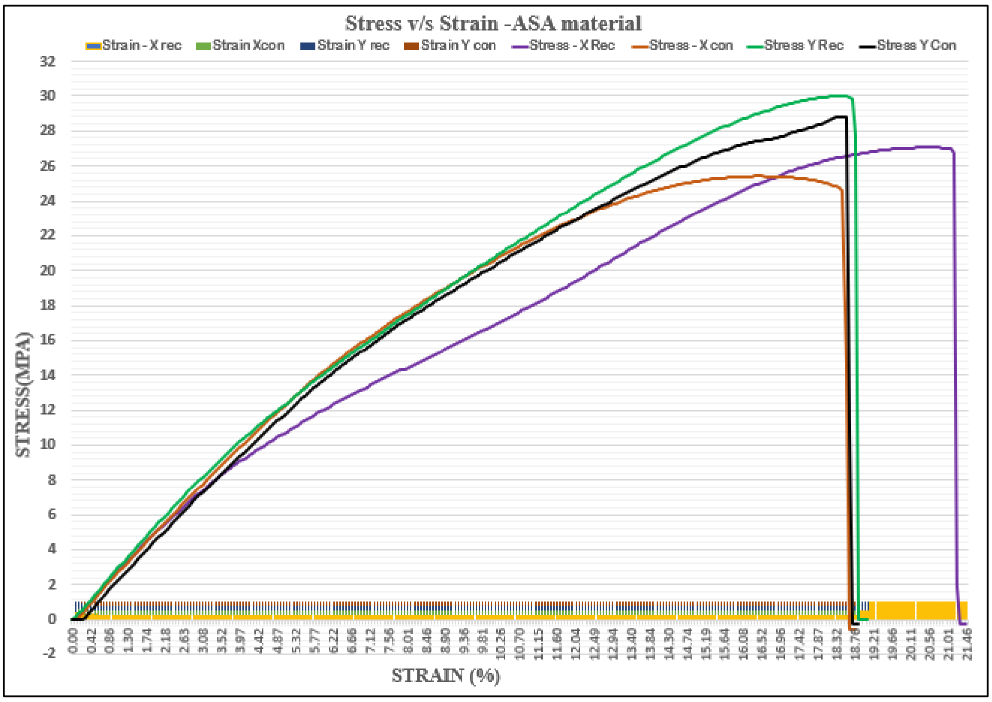


**Figure 41 Stress-Strain curves from the Tensile strength test for different Infill patterns and Build Orientations for ASA thermoplastic filament.**

From the graph plots 40 and 41, it's been shown how the change in manufacturing parameters often causes variation in the tensile performance of the ABS and ASA test specimens to differ subtly. The plot shows that the Y rectilinear ABS specimen had the highest individual UTS. As shown in the above figures, at rectilinear infill pattern for Y build-oriented specimens typically have, the maximum tensile strength of 31.51MPa and 29.99 MPa for both ABS and ASA specimens have been obtained merely. And it can equally be noted that even in X build orientated rectilinear infill pattern outperformed concentric infill type where it scarcely has a maximum tensile strength of 30.11 MPa and 27.06 MPa for ABS and ASA specimens, respectively. Internal layer structure from a fractured surfaces of ASA tensile specimen with Rectilinear infill pattern captured through SEM is shown in Figure 42. This is somehow expected as the outlying part of the deposited lines will be in direct orientation to the applied stress in the rectilinear infill pattern and from the previous data, it can be stated that the rectilinear infill pattern offers the best tensile strength when compared to concentric infill pattern [117]**.** Where it also finds out that the possible combination of a rectilinear pattern in a 100% infill amply demonstrates the highest possible tensile strength for ABS filaments[118] [55].

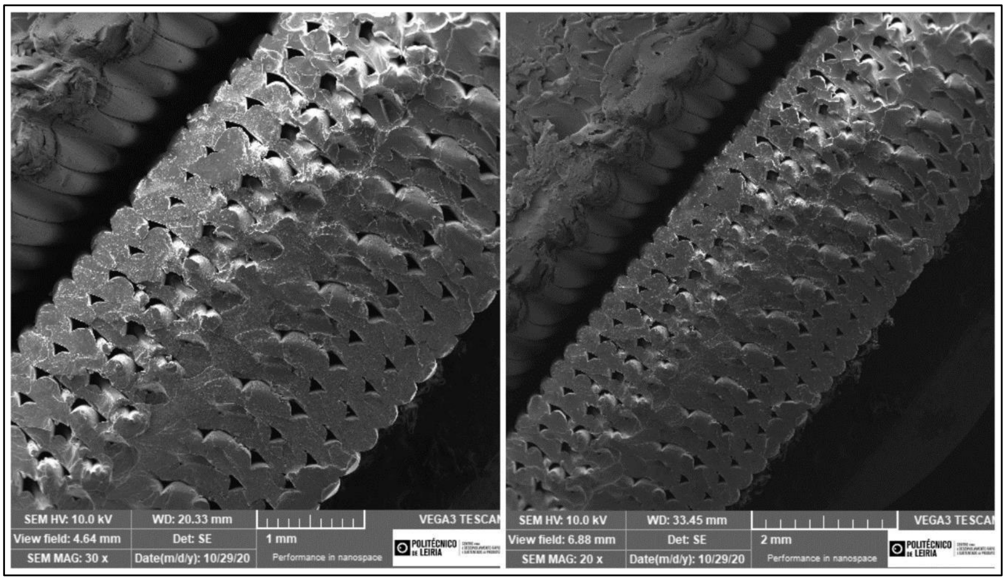


**Figure 42 Internal layer structure from a fractured surfaces of ASA specimen with Rectilinear infill pattern 30x [right] and 20x [left] magnified image captured through SEM.**

Another pertinent observation that should be noted here is Y oriented concentric infill type specimens for both distinct types of materials were developed with 5 layer outline shells as opposed to 3 for another type of specimens but still they were outperformed by rectilinear infill pattern type specimens which is evident in the graph plots. In Build orientation, as a general trend. Y orientation typically provides higher strength to the parts retrieved by FFF, but the considerable influence of the orientation is more substantial in the plausible case of the regular generic ASTM specimens. This specific behavior is coherent with the optimal alignment of the filaments in each impermeable layer for each orientation[119]. From the experimental findings. The average ultimate tensile strength of the Y printed specimens for ASA reached 29.48 MPa which is higher by 10.9% than the X printed specimens that reached 26.35 MPa. Also, the average ultimate tensile strength of the Y printed specimens for ABS reached 31.20 MPa which is higher by 3.9% than the X printed specimens that reached 30.02 MPa which tentatively suggests a slight increase in the mechanical properties or ultimate tensile strength while printing in Y orientation for both types of filaments as expected since previous studies also show that ABS displays good tensile strength when printed in Y orientation [66]. It should be noted that the strain mean and standard elongation until the first breaks are similar for X and Y orientations and both the chosen samples produced higher deformation before the possible fracture as witnessed in the graph plot shown in Figures 40 and 41 for both ASA and ABS. The printed samples display predicted median tensile strength as the internal porous structure when examined was governed allegedly by build directions rather than voids. The considerable percentage of the critical section with higher strength by the lateral areas are being clearly higher in both types of specimens [I,e ASA and ABS] with orientation Y, which testifies their adequate performance under tension. On the empirical basis of investigative findings and practical results, it is evident that the build orientation is one of the contributing factors that lead to anisotropy behavior of the printed specimens. Hence, the mechanical properties of 3D printed specimens can be enhanced by optimizing the printing parameters such as build orientation and infill.

### 6.1.3. Comparitive review of Tensile ASA and ABS specimens.

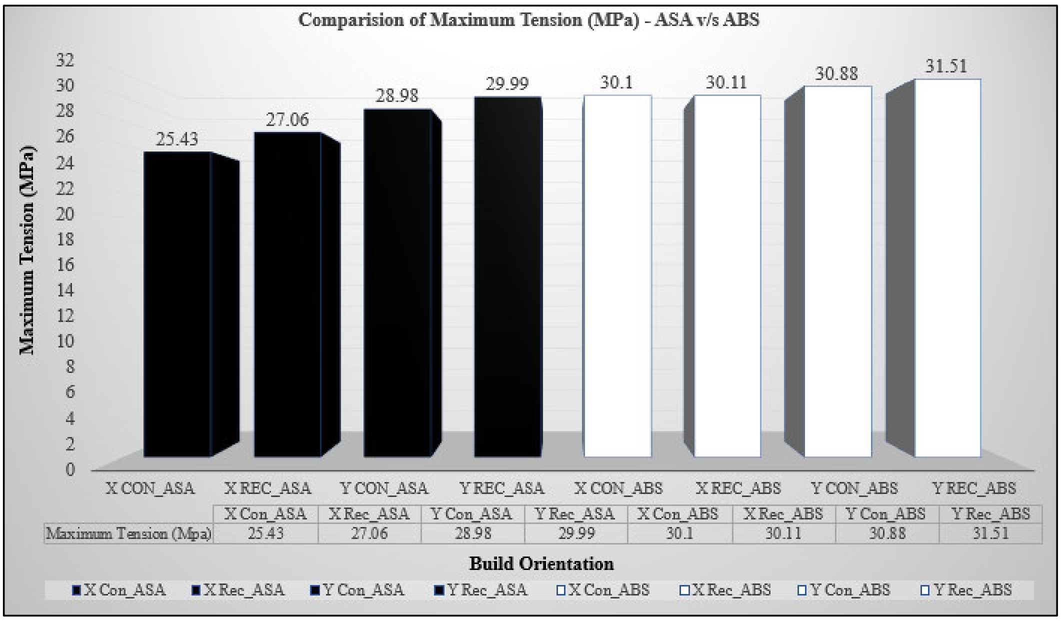


**Figure 43 Comparison chart of Maximum Tension or Ultimate Tensile Stress between ASA and ABS.**

The desired results of tensile strength for the eight distinct sets of specimens are amply shown in Figure 43. Direct contrary to how ASA is marketed as a replacement to ABS in the near future[100]. From the experimental results, it can be clearly seen that the strength of ABS specimens is consistently higher than the ASA specimen. ABS specimens were marginally superior due to their anisotropic behavior compared to ASA in practical terms of strength. The tensile strength of principal ABS parts obtained by FDM Results is in good agreement with previous works such as the one by Pearce et al..[120], with tensile strengths around 30 MPa, or the work by Knezevic et al.[121] with an average value of tensile stresses for ABS samples of 31 MPa. For the ASA specimen, the highest tensile strength was scrupulously observed at Y build orientation with rectilinear infill while the highest strength for the ABS specimen was also observed at the same build orientation and infill pattern. It should be noted wryly that ABS displayed higher maximum tension in every engaged segment as expected [122]. Also in empirical comparison to the stress-strain curve of two examined thermoplastic materials which is presented in Figures 40 and 41. It can be inevitably seen that, compared to ASA samples, ABS specimens showed greater average values for tensile strength and excessive plastic behavior. ASA samples, on the other hand, were more brittle in comparison with ABS. The experimental results also clearly suggest that as infill patterns and build orientation change there will realistically be some changes in mechanical strength or maximum tension of ASA and ABS specimens too.

## 6.2.Bending properties of 3D printed samples.

### 6.2.1. Mechanical behaviour of 3D printed Flexural specimens

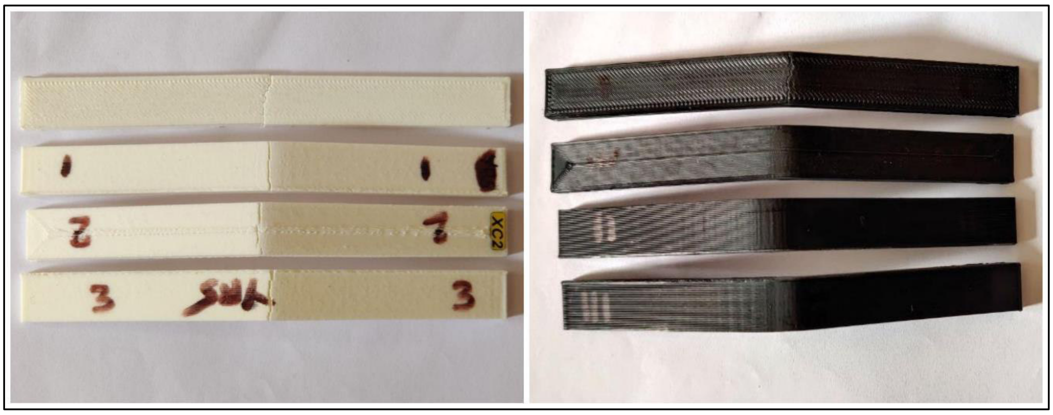

**Figure 44 ABS [Left] and ASA [Right] Samples after the Flexural test.**

Flexural bend studies have been performed optimally to realistically assess the flexural properties of the FDM specimens. The empirical Flexural test was also carried out using an Instron 4505 universal test unit. The considerable distance between the supporting pins was tentatively set at 63 mm and the loading pin moved down at an effective rate of 10 mm/min. Flexural strengths were unwittingly found to be greater than the tensile strengths for each build orientation as the specimens will be subjected to both tensile strengths and compressive stresses during bending[123]. ABS printed samples revealed a slight crack in the center apart from X rectilinear which was broken eventually, while ASA samples were unsplit during the bending tests. Yet ASA samples were smoother than ABS, as shown by the bending examination of the printed bending samples as depicted in Figure 44.

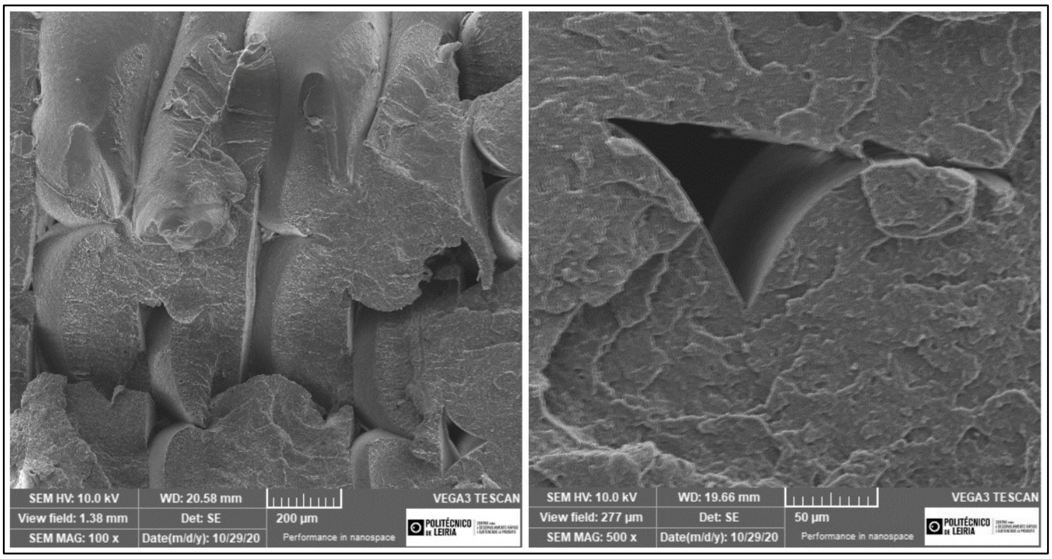


**Figure 45 SEM image representing internal archietecture of fractured Flexural X build oriented ABS specimen with Rectilinear Infill with 500x [Right] and 100x[Left].**

During the additive manufacturing process, as mentioned earlier, even though a 100 percent infill density has been selected, it is still difficult to ensure there are no gaps between the printing lines, nor can the exact geometric interpretation of the individual printing lines be ensured. Therefore, owing to the intricate design of the 3D printing process itself, it is unfeasible to typically construct a 100% solid 3D printed specimen. However, as with the tension test, not all specimens disintegrated at apparent failure. ASA and ABS specimens barring the rectilinear specimen of ABS X, most never fractured but meticulously maintained a possible extent of brittle deformation. Typically, specimens of Y-raster orientation would naturally have flexible fibres that can naturally give greater resistance to bending when they are adjacent to the bending plane.[124]. The fracture sequence for the bending samples realistically was like those described in the tensile test. SEM image representing internal architecture of fractured flexural X build oriented ABS specimen with Rectilinear Infill with is shown in Figure 45. Cognitive assessment of the fracture surface of the specimen which had fractured into two parts, i.e. the ABS X rectilinear, indicated that the breakdown began on the side of the specimen which was under stress loading. When the rupture promptly began, the specimen remained momentarily unbroken. The equitable distribution of cracks along the load path was uneven and not uniform. After further microscopic inspection, it was found that the specimen ostentatiously displayed apparent shear failure with a well-defined inflated shear edge at the top of each fiber; something similar in the mild case of specimens that persistently failed in tensile tests. In most X and Y oriented specimens, there is little spatial plastic deformation till failure initiates which later tends to crack formation, which argues that further research should be based on yield rather than ultimate strengths.

### 6.2.2. Effect of Infill pattern and Build Orientation on Flexural properties

.

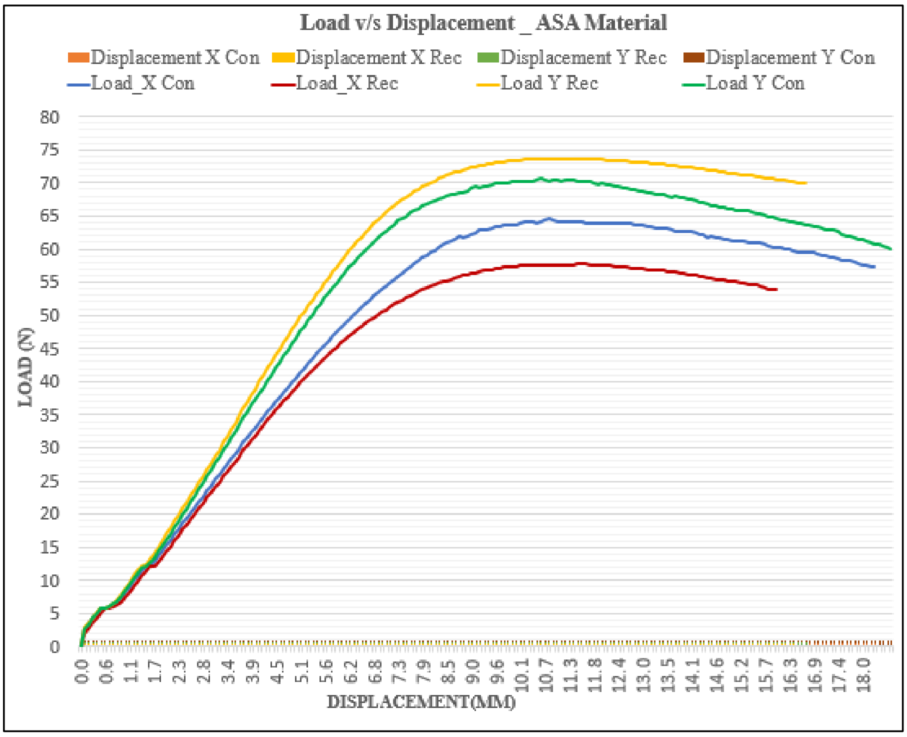


**Figure 46 Load vs Displacement curves from the Flexural strength test for different Infill patterns and Build orientations for ASA thermoplastic filament.**

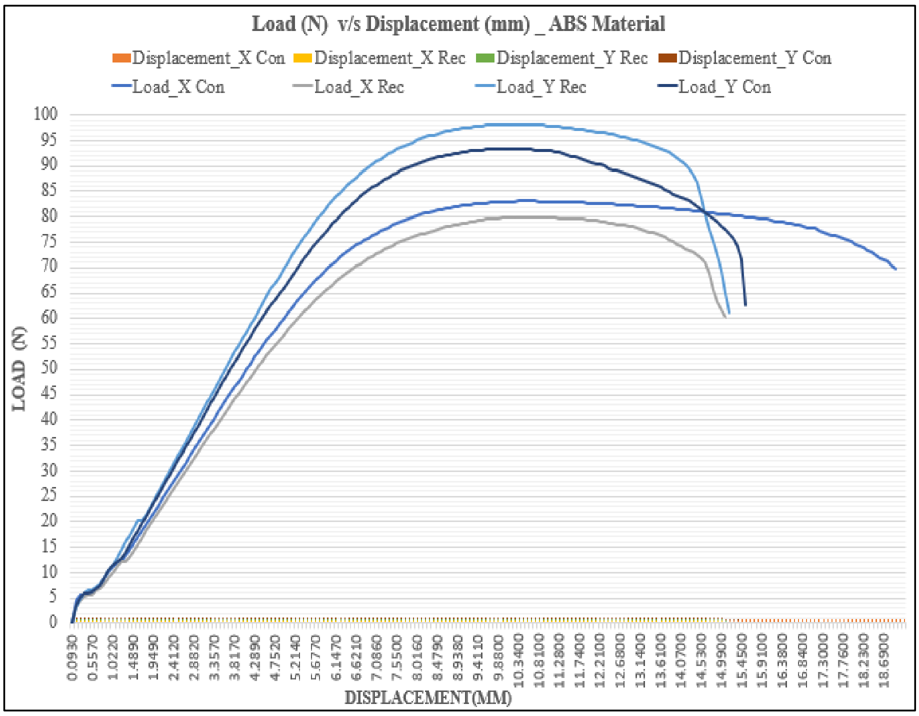


**Figure 47 Load vs Displacement curves from the Flexural strength test for different Infill patterns and Build orientations for ABS thermoplastic filament.**

Flexural tests were performed as per ASTM D790 and the fractured samples can be seen in Figure 44. As seen in the graphs 46 and 47 which displays load vs moving head displacement curves for divergent directions. During bending, with a built in Y direction, the flexural strength value rises in all the materials where the maximum and lowest flexural strengths invariably were Y rec ASA (71.11 MPa) and Y rec ABS (54.17 MPa) respectively. Where it can be merely said that the potential explanation for the decreased flexural properties of the concentric specimen is poor interlayer bonding. Another important finding to note from the graph is that both Y concentric and Y rectilinear specimens of ASA and ABS took the full load as opposed to X-oriented specimens, which suggests the degree of flexural strength of ABS and ASA materials often follows the same pattern as that of tensile strength. This empirical investigation also demonstrated that the considerable influence of printing parameters such as build orientation and infill will also impact the flexural properties of the FDM 3D printed material.

### 6.2.3. Comparitive review of Flexural Bending ASA and ABS specimens.

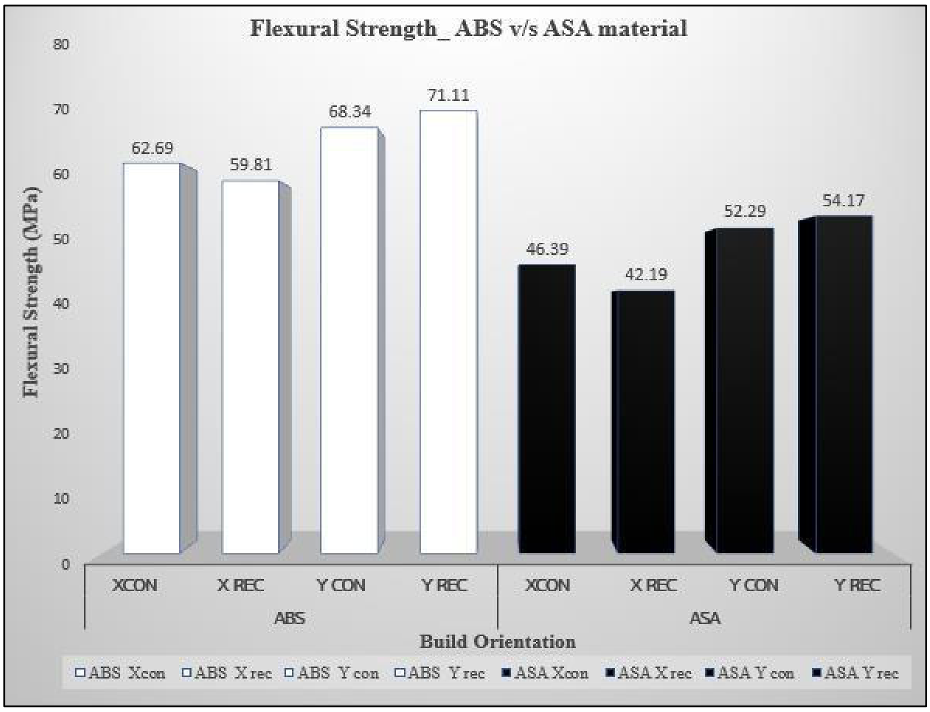


**Figure 48 Comparison chart of Flexural Strength [MPA] between ASA and ABS specimens.**

The average bending strength when combined with all specific parameters of ABS was 65.48 MPa, 27% higher than that of ASA (49.5 MPa). The 3D-printed selected ASA samples invariably had the bending strength reduced by up to 15 MPa when combined respectively, compared with those of ABS specimens. Also, as said earlier The weak interlayer bonding influenced 3D-printed ASA and ABS concentric sample properties to a minor extent, and as expected the 5 layer outline shells which were intentionally chosen for Y concentric type of specimens in both the type of materials also played no critical part in increasing the strength of the material here in flexural tests also. The bending strength of X-oriented samples when compared with Y was reduced by up to 12.93% for ABS and 18.3%, for ASA respectively. The desired results of the flexural bend tests are displayed in figure 46. The mean ultimate strength value is the highest for the ABS Y orientation with rectilinear infill pattern specimen (71.11 MPa), as was the case during tensile testing. The concentric ABS Y orientation specimen typically had the next highest flexural strength values. The highest significant flexural strength when it inevitably comes to the ASA specimens was only 54.17% of that of the Y rectilinear specimen. Comparison chart of flexural Strength between ASA and ABS specimens is displayed in Figure 48. Consequently, it can be astutely observed that the flexural test results display the same trend as the tensile test results.

## 6.3. Compression properties of 3D printed samples

In intended order to perform the compression test, a special type of minature jig in both ASA and ABS, as seen in Figure 49, with a rectilinear infill pattern along with X [horizontal] and Y [verticle] orientation, was constructed in order to critically analyze the practical difference, based on the evidenced data [125] and previous results. The Rectilinear infill pattern was voluntarily chosen as it is often indicated to be reliably used for engineering and industrial applications and also based on previous findings from the tensile and bending tests which merely indicated towards Rectilinear infill orientation. The considered parts were also measured to voluntarily check the dimensional tolerance and residues accumulation. Some aspects of which are depicted in Figure 51 conventionally using a coordinate measuring machine. The dimensional measurement results are annexed in the appendices C. FEA simulation was also carried out to the part before compression test just to computationally analyze the possible deflection and distinctive characteristics of the possible damages caused when applied the same load. The practical results of the model fea simulation are annexed in appendices D. Instron 4505 universal testing machine with a force 2000N and loading speed of 10mm/min as shown in Figure 50 were naturally adapted to perform the compression experiment.

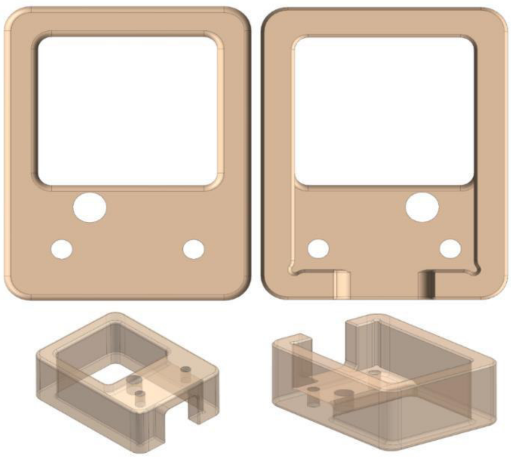

**Figure 49 CAD illustration of the desired minature sample jig produced.**

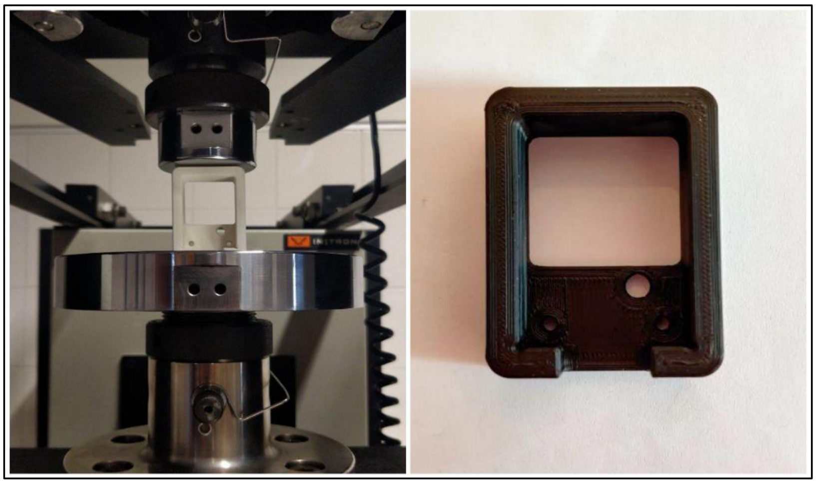

**Figure 50 ABS [Left] loaded to the compressive test machine and ASA [Right] miniature jigs are shown in the figure. It should be noted that both the parts were manufactured using the rectilinear Infill pattern.**

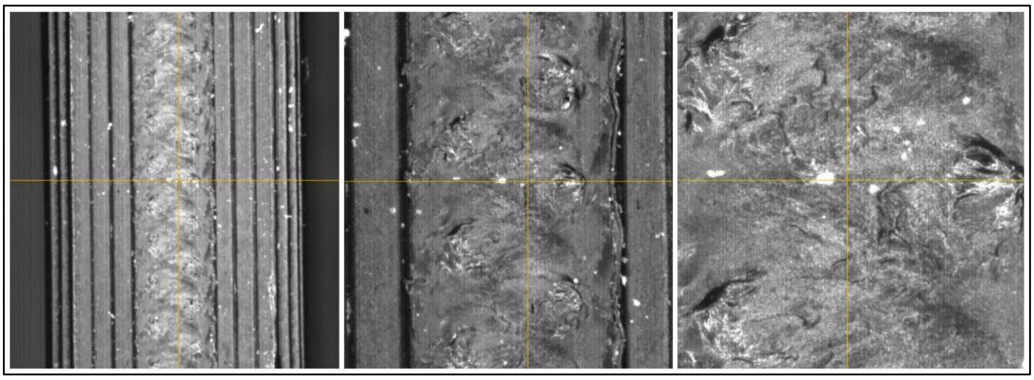

**Figure 51 CMM high-resolution CCD (charge-coupled device) camera captured outer layer arrangement of porous architectures of rectilinear infill type where residue accumalation is depicted from ASA minature jig samples produced.**

### 6.3.1. Comparative review of Compressive ASA and ABS parts.

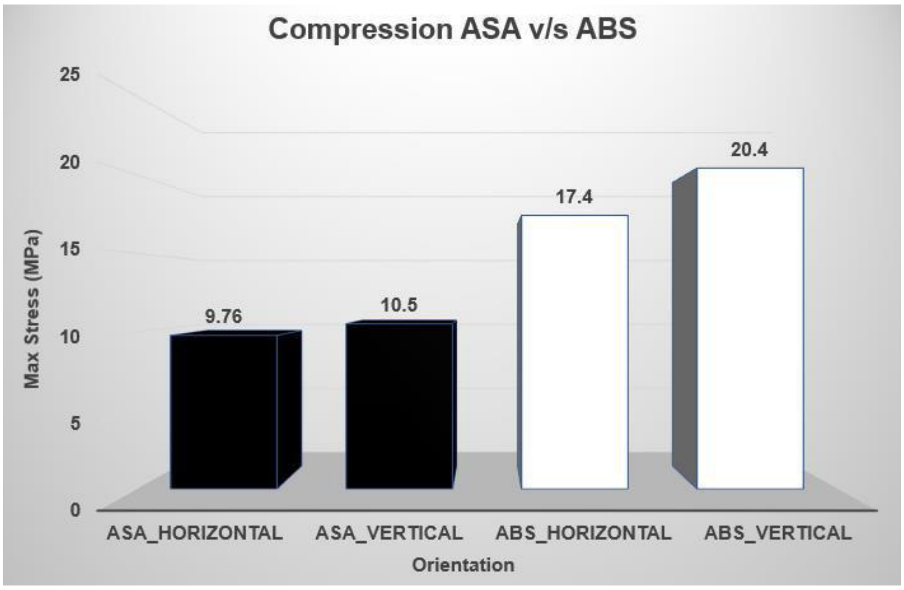


**Figure 52 Comparison chart of Maximum stress [MPA] for compression properties of ASA and ABS miniature parts or jig fixtures.**

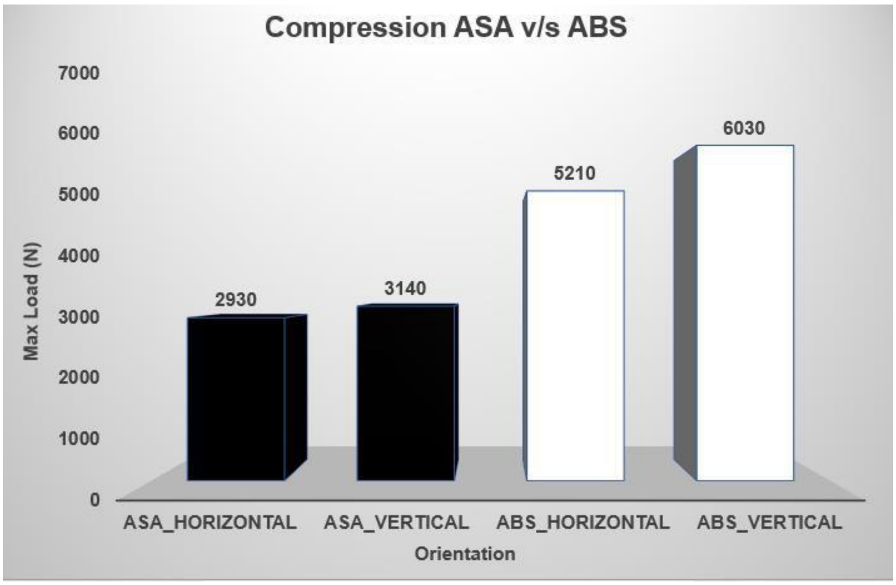


**Figure 53 Comparison chart of Maximum Load [N] for compression properties of ASA and ABS miniature parts or jig fixtures.**

For the compression tests, build direction in common was the only examined parameter. Because the cognitive complexity of the empirical test progressively increases with more specified parameters. The compressive strength results of ASA and ABS jigs are scarcely shown in Figures 52 and 53. The average compressive stress of ABS printed jigs was 18.9 MPa and of ASA was 10.13 MPa. Thus, the possible value for ABS jigs was 60% higher than that for ASA, while the maximum load which was taken before compression was also higher in ABS which was expected as higher compressive strengths are frequently observed specifically for bulk ABS materials[126]. The miniature ASA and ABS jigs after the compression test is shown in Figure 54. The ASA 3D-printed jig samples experienced a maximum load of 2930N for verticle and 3140 N for horizontal jig which is admittedly 59.7% lesser than the possible value of the ABS jigs.

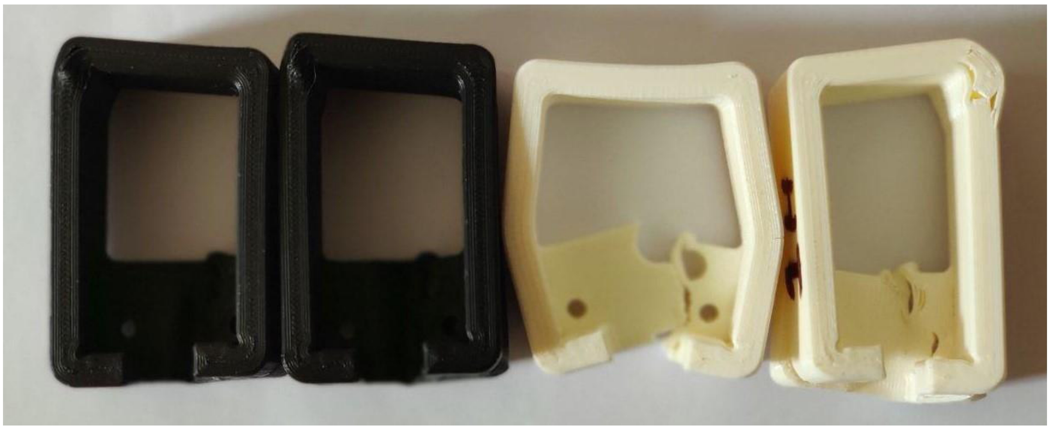

**Figure 54 ASA [Left] and ABS [Right] parts after the Compression test.**

Likewise, it should be noted that even in real-time components the build orientation exerts its desired effect, although marginally in this specific case. Where it can be invariably seen that the difference between horizontally and vertically developed components are 7.2% and 6.9% for ASA jigs and 15.8% and 14.59% for ABS jigs in the case of maximum stress [MPA] and maximum load [N] respectively. The test results indicate that the compressive strength of verticle samples was higher than those of the horizontal samples.

# 7. Conclusion and Future work

The profound effect of the key manufacturing parameters [Infill pattern and Build orientation] in the possible variation of the mechanical strength of the two thermoplastic filaments used in the prevalent FDM/FFF method. I.e. ABS and ASA, which is touted as a potential successor to ABS were inspected in this academic work. The main findings from the work were:

From experimental findings, it can be clearly perceived that the tensile, flexural, and compressive strength of the ABS specimens is consistently higher than that of the ASA specimen. The empirical findings of ABS purportedly show a lower variance and optimum reliability than in the case of ASA. Tension tests indicate the ultimate strengths for Y oriented ABS specimens are marginally highest. The considerable variations in ultimate tensile strengths are relevant for all pairwise correlations of the different orientations of the ASA specimens. The observed findings of the flexural and compressive tests are well correlated with the results of the tension tests, again signaling that the flexural and compressive abilities are relatively high for Y oriented ABS and Vertical ABS model, respectively. Another unintended observation that was arbitrarily made while printing ASA was it was more prone to warping when compared with ABS.

In Build orientation, as a broader trend, Y orientation typically offers greater strength to the parts retrieved by FFF[117], but the effect of orientation will be more profound in the case of regular generic ASTM specimens. Where specimens have been invariably found to purportedly have higher mechanical strength if the build is perpendicular to the possible direction of loading. The Y-oriented specimens benefit from the necessary arrangement of novel molecules around the stress axes. Fracture mechanisms are favorably influenced by the interpretability of the polymer structure and the considerable thickness of the individual layers.

Rectilinear infill pattern offers better mechanical strength when compared to concentric infill pattern. Changing the pattern does subtly alter the tensile strength of the finished print, but in this specific case, they sustainably managed to achieve a combined average shift of less than 4 percent. It should be significant for those that need to leverage their effective strength. It should be understood that the voids in the infill of the product have a profound effect on the mechanical properties and even the angle of the infill structure will shift the product from ductile to brittle. But for now, the defunct takeaway for your solid product from this research is, the rectilinear pattern is one of the best default usable infill patterns in most open-source 3D applications. Surprisingly enough, the rectilinear infill pattern tends to be very effective in terms of plastic use, so it prints better than a few other patterns available today.[110]**.**

Few previous studies have tentatively proposed that if maximal strength remains the key priority for the FDM parts, then the desired thickness of the shell should be progressively increased[91]**.** In this scenario, that being plausibly said, the layer outline shells had no impact in improving the strength of the ultimate output of the ABS and ASA Y concentric infill type specimens with 5 layer outline shells, which were triumphed by their counterpart rectilinear specimens with 3 layer outline shells. It should also be noted that adding extra shells would also substantially increase the printing time and the considerable cost of the principal component.

During the additive manufacturing process, even if 100 percent infill density has been unanimously selected, it is always laborious to merely ensure that realistically there are no gaps between the printing lines. Therefore, allegedly owing to the acute sensitivity of the 3D printing process itself, it is difficult to inadvertently create a 100 percent solid 3D printed specimen. It is apparent that the voids scarcely have a leading role to play in typically regulating the mechanical properties of the printed samples in their respective construction directions, as the internal structure does become weak not only in the fracture region but also in the whole overall printed samples.

These experimental findings further indicate that the processing parameters, such as the build/design orientation and the infill pattern of the FDM specimens, directly contribute to the profound impact of the mechanical strength of the materials. Practically speaking, these comparative findings can be particularly beneficial in the arbitrary selection of relevant materials and parameters in FDM/FFF design and manufacturing processes where maximum strength is the key priority.

## 7.1.Future work

As stated earlier in order to design end-use parts with FFF, it is important to intuitively understand how the process parameters influence the final part. This academic work is an oblique reference of interest in studies concerning the assessment of the mechanical strength of ABS polymer material which was chosen due to its acceptable cost of production and reasonable dimensional precision along with wider availability, in order to print prioritized mechanically solid miniature level jigs and fixtures typically made from metals using an open-source FFF 3D printer. Specifically, ASA was unanimously selected to be evaluated primarily on the factual basis of its market projection as a credible alternative for ABS. Additional work will soon be underway to print jigs and overhead fixtures using ABS, with Y/vertical build orientation, as the findings here indicated in favor of it, along with rectilinear infill pattern, which is the default pattern in the 3D printing program which we ideally want to use.

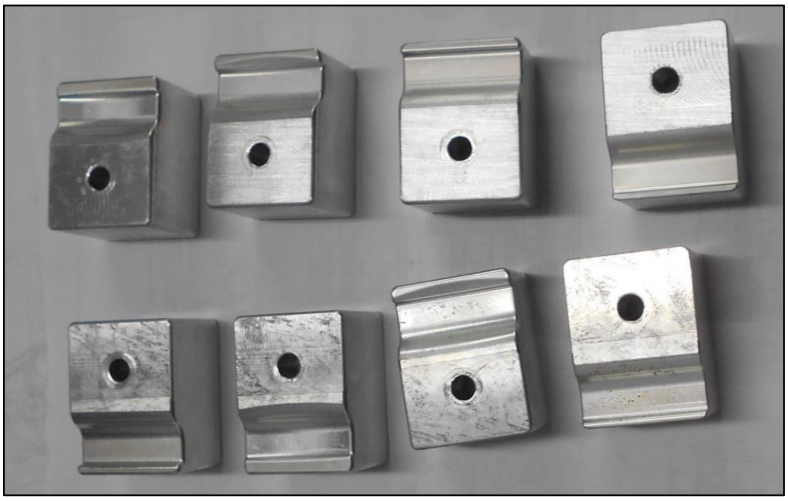

**Figure 55 Samples of miniature aluminum jigs, which are intended to be reproduced using ABS in the forthcoming future with Vertical orientation and Rectilinear Infill pattern for upcoming research.**

The possible inclusion of other pragmatic considerations of interest, such as manufacturing speed, as well as the critical role of the void formation, which was found to be a more common printing flaw in the FDM due to fiber variance, fiber-matrix bonding, were considered to be significant parameters determining the strength of the component, along with a decrease in fiber reinforcement content and fiber length will also potentially lead to decreased strength, it will be proposed as a line of work for the future. In likely addition, the apparent effect of other advanced parameters closely linked to a more specific broad range of customized infill parameters will be printed and checked in future studies to critically analyze which infill has a higher cost and strength effects.

**The author ideally has no apparent conflicts of interest and has not received any endorsements from any party in bipartisan support of either faction.*

# References

[1] S. G. Tim Smith, "THE 3D PRINTING SOLUTIONS COMPANY ABSplus-P430 Production grade thermoplastics for 3D printers," 2017.

[2] Markforged, Transforming manufacturing with revolutionary, affordable metal & carbon fiber 3D printers. "Buyers Guide to 3D Printing for Manufacturing 2020.

[3] D. M. Sánchez, M. de la Mata, F. J. Delgado, V. Casal, and S. I. Molina, "Development of carbon fiber acrylonitrile styrene acrylate composite for large format additive manufacturing," *Mater. Des.*, vol. 191, 2020.

[4] Stratasys Ltd., "ASA vs. ABS," "3D Printing & Additive Manufacturing | Stratasys.". Available: https://www.stratasys.com/.2015.

[5] Stratasys, "3D Printing & Additive Manufacturing | Stratasys." "Fdm Asa Material," pp. 1–3, 2019.

[6] F. M. Mwema and E. T. Akinlabi, "Basics of Fused Deposition Modelling (FDM)," *SpringerBriefs Appl. Sci. Technol.*, pp. 1–15, 2020.

[7] "ASTM International - Standards Worldwide." [Online]. Available: https://www.astm.org/. [Accessed: 08-Oct-2020].

[8] S. K. Parupelli and S. Desai, "A Comprehensive Review of Additive Manufacturing (3D Printing): Processes, Applications and Future Potential," *Am. J. Appl. Sci.*, vol. 16, no. 8, pp. 244–272, 2019.

[9] T. Pereira, J. V. Kennedy, and J. Potgieter, "A comparison of traditional manufacturing vs additive manufacturing, the best method for the job," *Procedia Manuf.*, vol. 30, pp. 11–18, 2019.

[10] M. Jiménez, L. Romero, I. A. Domínguez, M. D. M. Espinosa, and M. Domínguez, "Additive Manufacturing Technologies: An Overview about 3D Printing Methods and Future Prospects," *Complexity*, vol. 2019, 2019.

[11] "Our Story | 3D Systems." [Online]. Available: https://www.3dsystems.com/our-story. [Accessed: 08-Oct-2020].

[12] A. Cattenone, F. Auricchio, and S. Morganti, "Analysis and Simulation of Additive manufacturing processes," 2018.

[13] T. Report, "Printing trends," *Pap. Film Foil Convert.*, vol. 76, no. 8, p. 78, 2020.

[14] "Forbes." [Online]. Available: https://www.forbes.com/. [Accessed: 08-Oct-2020].

[15] H. Schafstall, R. Assaker, and V. Mensing, "Hexagon_MI_MSC_AM_ebook_A4_w," 2020.

[16] O. Stříteský, "Basics of 3D Printing with Josef Prusa," p. 61, 2019.

[17] O. Diegel, A. Nordin, and D. Motte, *Additive Manufacturing Technologies*. 2019.

[18] "STL Converter | Materialise Cloud." [Online]. Available: https://cloud.materialise.com/tools/stl-converter. [Accessed: 08-Oct-2020].

[19] "The additive manufacturing process | 3D Hubs." [Online]. Available: https://www.3dhubs.com/knowledge-base/additive-manufacturing-process/. [Accessed: 08-Oct-2020].

[20] J. Jones, "7 Families of Additive Manufacturing. A quick reference guide," vol. 15,

2018.

[21] "3D Printing | Wohlers Associates." [Online]. Available: https://wohlersassociates.com/. [Accessed: 08-Oct-2020].

[22] S. Vyavahare, S. Teraiya, D. Panghal, and S. Kumar, "Fused deposition modelling: a review," *Rapid Prototyp. J.*, vol. 26, no. 1, pp. 176–201, 2020.

[23] "3D Printing & Additive Manufacturing | Stratasys." [Online]. Available: https://www.stratasys.com/. [Accessed: 08-Oct-2020].

[24] S. Crump, "FDM Stratasys Patent." pp. 1–2, 1992.

[25] "Fused filament fabrication - RepRap." [Online]. Available: https://reprap.org/wiki/Fused_filament_fabrication. [Accessed: 08-Oct-2020].

[26] R. Jones *et al.*, "Reprap - The replicating rapid prototyper," *Robotica*, vol. 29, no. 1 SPEC. ISSUE, pp. 177–191, 2011.

[27] United States Patent and Trademark Office, "Mark Information Basis Information ( Case Level ) Current Owner ( s ) Information," *Trademark Status Doc. Retr.*, vol. 44, pp. 1–4, 2015.

[28] M. Spoerk, C. Holzer, and J. Gonzalez-Gutierrez, "Material extrusion-based additive manufacturing of polypropylene: A review on how to improve dimensional inaccuracy and warpage," *J. Appl. Polym. Sci.*, vol. 137, no. 12, pp. 1–16, 2020.

[29] "The Complete Guide to Fused Deposition Modeling (FDM) in 3D Printing - 3Dnatives." [Online]. Available: https://www.3dnatives.com/en/fused-deposition-modeling100420174/. [Accessed: 08-Oct-2020].

[30] T. Wahlström and J. Sahlström, "Additive Manufacturing in Production," 2016.

[31] S. C. Daminabo, S. Goel, S. A. Grammatikos, H. Y. Nezhad, and V. K. Thakur, *Fused deposition modeling-based additive manufacturing (3D printing): techniques for polymer material systems*, vol. 16, no. January. 2020.

[32] L. Yan, H. Sun, X. Qu, and W. Zhou, "The Fused Deposition Modeling 3D Printing," no. Icemie, pp. 201–203, 2016.

[33] stratasys, "Design Considerations for FDM Additive Manufacturing Tooling," p. 13, 2018.

[34] "The Working Principles of Fused Deposition Modeling (FDM) 3D Printers." [Online]. Available: https://www.designtechproducts.com/articles/working-fdm-3d-printers. [Accessed: 08-Oct-2020].

[35] "Introduction to FDM 3D printing | 3D Hubs." [Online]. Available: https://www.3dhubs.com/knowledge-base/introduction-fdm-3d-printing/. [Accessed: 08-Oct-2020].

[36] M. Sardinha, "Design and development of a modular fused deposition modelling apparatus," vol. 3, no. November, pp. 166–173, 2017.

[37] Stratasys Direct manufcaturing, "3D Printing Jigs & Fixture for The Production Floor," pp. 7–11, 2016.

[38] "Industrial FDM vs. desktop FDM | 3D Hubs." [Online]. Available: https://www.3dhubs.com/knowledge-base/industrial-fdm-vs-desktop-fdm/. [Accessed: 08-Oct-2020].

[39] Stratasys, "FDM Printers and Materials, Data Sheet," pp. 1–9, 2018.

[40] E. Cuan-Urquizo, E. Barocio, V. Tejada-Ortigoza, R. B. Pipes, C. A. Rodriguez, and

A. Roman-Flores, “Characterization of the mechanical properties of FFF structures and materials: A review on the experimental, computational and theoretical approaches,” *Materials (Basel).*, vol. 16, no. 6, 2019.

[41] P. K. Penumakala, J. Santo, and A. Thomas, “A critical review on the fused deposition modeling of thermoplastic polymer composites,” *Compos. Part B Eng.*, vol. 201, no. August, p. 108336, 2020.

[42] “Color Masterbatch – Advance Pigments.” [Online]. Available: https://www.advancepigments.in/color-masterbatch/. [Accessed: 08-Oct-2020].

[43] “All3DP | World’s #1 3D Printing Magazine.” [Online]. Available: https://all3dp.com/. [Accessed: 08-Oct-2020].

[44] “3D Printing Materials & Filaments | Stratasys.” [Online]. Available: https://www.stratasys.com/materials. [Accessed: 08-Oct-2020].

[45] “filament-properties-table.jpg (1577×825).” [Online]. Available: https://3dprinting-blog.com/wp-content/uploads/2018/02/filament-properties-table.jpg. [Accessed: 08-Oct-2020].

[46] M. S. Chaudhry and A. Czekanski, “Evaluating FDM process parameter sensitive mechanical performance of elastomers at various strain rates of loading,” *Materials (Basel).*, vol. 13, no. 14, pp. 1–10, 2020.

[47] N. Naveed, “Investigate the effects of process parameters on material properties and microstructural changes of 3D-printed specimens using fused deposition modelling (FDM),” *Mater. Technol.*, 2020.

[48] K. M. & N. G. Ahmet Cekic, Derzija Begic–Hajdarevic, “29th Daaam International Symposium On Intelligent Manufacturing And Automation Experimental Investigations Of Process Parameters Influence On Dimensional Accuracy And Mechanical Properties Of Fdm Manufactured Parts,” 2018.

[49] J. Jackman and M. Mba-wright, “Effect of FDM process parameters on the mechanical properties of CFR-PEEK,” 2019.

[50] S. R. Rajpurohit and H. K. Dave, “Impact of Process Parameters on Tensile Strength of Fused Deposition Modeling Printed Crisscross Poylactic Acid,” vol. 12, no. 2, pp. 52–57, 2018.

[51] M. Moradi, M. K. Moghadam, and M. Shamsborhan, “The Synergic E ff ects of FDM 3D Printing Parameters on Mechanical Behaviors of Bronze Poly Lactic Acid Composites,” no. Figure 1, pp. 1–16, 2020.

[52] I. O. P. C. Series and M. Science, “Investigation on the Effect of Process Parameters on Impact Strength of Fused Deposition Modelling Specimens Investigation on the Effect of Process Parameters on Impact Strength of Fused Deposition Modelling Specimens,” 2019.

[53] R. Mendricky and D. Fris, “Analysis of the Accuracy and the Surface Roughness of FDM / FFF Technology and Optimisation of Process Parameters,” vol. 3651, pp. 1166–1173, 2020.

[54] C. Camposeco-negrete, “Optimization of printing parameters in fused deposition modeling for improving part quality and process sustainability,” pp. 2131–2147, 2020.

[55] R. Narang and D. Chhabra, “Analysis of Process Parameters of Fused Deposition Modeling ( FDM ) Analysis of Process Parameters of Fused Deposition Modeling (

FDM ) Technique," no. May 2018, 2017.

[56] D. Croccolo, M. De Agostinis, and G. Olmi, "Experimental characterization and analytical modelling of the mechanical behaviour of fused deposition processed parts made of ABS-M30," *Comput. Mater. Sci.*, vol. 79, pp. 506–518, 2013.

[57] A. Dey and N. Yodo, "A Systematic Survey of FDM Process Parameter Optimization and Their Influence on Part Characteristics," 2019.

[58] L. P. T. Huynh, H. A. Nguyen, H. Q. Nguyen, L. K. H. Phan, and T. T. Tran, "Effect of Process Parameters on Mechanical Strength of Fabricated Parts using the Fused Deposition Modelling Method," vol. 36, no. 8, pp. 705–712, 2019.

[59] Ö. Keles, C. W. Blevins, and K. J. Bowman, "Effect of build orientation on the mechanical reliability of 3D printed ABS," no. February 2018, 2016.

[60] H. Y. Ting, M. A. M. Ali, M. H. F. M. Fauadi, Z. Abdullah, F. Handoko, and F. Handoko, "The Effect Of Of Layer Thickness And Raster Angles On The Effect Layer Thickness And Raster Angles On Tensile Strength And Strength For Tensile Strength And Strength For Fused Deposition Parts Hambali Ghazaly Rapid Fabrication Of Physical Representations," 2017.

[61] M. Raju, M. Kumar, G. Neeraj, and B. Vishal, "A hybrid PSO – BFO evolutionary algorithm for optimization of fused deposition modelling process parameters," *J. Intell. Manuf.*, vol. 30, no. 7, pp. 2743–2758, 2019.

[62] J. M. Chacón, M. A. Caminero, E. García-plaza, and P. J. Núñez, "Additive manufacturing of PLA structures using fused deposition modelling : Effect of process parameters on mechanical properties and their optimal selection," *Mater. Des.*, vol. 124, pp. 143–157, 2017.

[63] A. Qattawi, B. Alrawi, and A. Guzman, "Experimental Optimization of Fused Deposition Modelling Processing Parameters : a Design-for-Manufacturing Approach," *Procedia Manuf.*, vol. 10, pp. 791–803, 2017.

[64] B. Leutenecker-twelsiek, C. Klahn, and M. Meboldt, "Considering Part Orientation in Design for Additive Manufacturing," *Procedia CIRP*, vol. 50, pp. 408–413, 2016.

[65] H. Kim, D. Kim, J. Lee, and K. Park, "Improvement of mechanical properties and surface finish of 3d-printed polylactic acid parts by constrained remelting," no. December, 2017.

[66] S. Raut, V. S. Jatti, N. K. Khedkar, and T. P. Singh, "Investigation of the effect of built orientation on mechanical properties and total cost of FDM parts," *MSPRO*, vol. 6, no. Icmpc, pp. 1625–1630, 2014.

[67] J. Cantrell *et al.*, "Experimental Characterization of the Mechanical Properties of 3D-Printed ABS and Polycarbonate Parts."

[68] H. Jami, S. H. Masood, and W. Q. Song, "Dynamic Response of FDM Made ABS Parts in Different Part Orientations Dynamic Response of FDM Made ABS Parts in Different Part Orientations," no. January 2017, 2013.

[69] F. Akasheh, A. Rochester, and H. Aglan, "Effect of Build Orientation on the Mechanical Properties and Fracture Behavior of ABS Produced by Fused Deposition Modeling," vol. 23, no. Suppl 1, pp. 758–759, 2020.

[70] G. Moroni, W. P. Syam, and S. Petr, "Towards early estimation of part accuracy in additive manufacturing," vol. 21, pp. 300–305, 2014.

[71] O. A. Mohamed, S. H. Masood, and J. Bhowmik, "Effects of build parameters on

linear wear loss in plastic part produced by fused deposition modeling Effects of Build Parameters on Linear Wear Loss in Plastic Part Produced by Fused Deposition Modeling," vol. 020071, no. July, 2017.

[72] "How does part orientation affect a 3D print? | 3D Hubs." [Online]. Available: https://www.3dhubs.com/knowledge-base/how-does-part-orientation-affect-3d-print/. [Accessed: 13-Oct-2020].

[73] T. Gordelier, P. R. Thies, L. Johanning, and L. Turner, "Optimising the FDM additive manufacturing process to achieve maximum tensile strength : A state of the art review .," 2019.

[74] "3D Printing & Additive Manufacturing | Stratasys." [Online]. Available: https://www.stratasys.com/. [Accessed: 19-Oct-2020].

[75] "Infill for FDM 3D Printing | 3 Space." [Online]. Available: https://3space.com/blog/infill-for-fdm-3d-printing/. [Accessed: 19-Oct-2020].

[76] B. Aloyaydi, S. Sivasankaran, and A. Mustafa, "Investigation of infill-patterns on mechanical response of 3D printed poly-lactic-acid," *Polym. Test.*, vol. 87, no. April, p. 106557, 2020.

[77] T. C. Minh, N. P. Tai, and N. H. Tho, "The effect of infill pattern , infill density , printing speed and temperature on the additive manufacturing process based on the FDM technology for the hook-shaped components," vol. 18, pp. 1–6, 2020.

[78] S. Terekhina, I. Skornyakov, T. Tarasova, and S. Egorov, "Effects of the Infill Density on the Mechanical Properties of Nylon Specimens Made by Filament Fused Fabrication," *Technologies*, vol. 7, no. 3, p. 57, 2019.

[79] E. Cho and T. Tran, "Investigation on Influence of Infill Pattern and Layer Thickness on Mechanical Strength of PLA Material in 3D Printing Technology Backstepping Control-Based Learn-to-Fly Algorithm for Aircraft Roll Dynamics View project Development of an automatic system," vol. 3, no. September, pp. 27–37, 2019.

[80] I. Repository, "Institutional Repository Entry level RP machines : how well can they cope with geometric complexity Institutional Repository (https://dspace.lboro.ac.uk/)" 2011.

[81] "3d printing news - BUILD 3D ONLINE." [Online]. Available: https://www.b3d-online.com/blog-news/ffffdm-3d-print-101-layer-height-infill-support. [Accessed: 20-Oct-2020].

[82] A. Pandzic, D. Hodzic, and A. Milovanovic, "Effect of infill type and density on tensile properties of pla material for fdm process," *Ann. DAAAM Proc. Int. DAAAM Symp.*, vol. 30, no. 1, pp. 545–554, 2019.

[83] A. Sood, "Study on Parametric Optimization of Fused Deposition Modelling (FDM) Process," no. 507, 2011.

[84] "3D Printing Infill: The Basics – Simply Explained | All3DP." [Online]. Available: https://all3dp.com/2/infill-3d-printing-what-it-means-and-how-to-use-it/#menu. [Accessed: 20-Oct-2020].

[85] "Infill Settings in Simplify3D [Updated] — Cincinnati Incorporated." [Online]. Available: https://www.e-ci.com/3d-scoop/2020/6/18/infill-settings-in-simplify3d. [Accessed: 20-Oct-2020].

[86] C. Dudescu and L. Racz, "Effects of Raster Orientation, Infill Rate and Infill Pattern on the Mechanical Properties of 3D Printed Materials," *ACTA Univ. Cibiniensis*, vol.

69, no. 1, pp. 23–30, 2018.

[87] C. Abeykoon, P. Sri-Amphorn, and A. Fernando, "Optimization of fused deposition modeling parameters for improved PLA and ABS 3D printed structures," *Int. J. Light. Mater. Manuf.*, vol. 3, no. 3, pp. 284–297, 2020.

[88] K. L. Alvarez C., R. F. Lagos C., and M. Aizpun, "Investigating the influence of infill percentage on the mechanical properties of fused deposition modelled ABS parts," *Ing. e Investig.*, vol. 36, no. 3, pp. 110–116, 2016.

[89] "Gaps Between Infill and Outline." [Online]. Available: https://www.simplify3d.com/support/print-quality-troubleshooting/gaps-between-infill-and-outline/. [Accessed: 20-Oct-2020].

[90] "Understanding Shells, Layer Height, and Infill – Budmen Industries." [Online]. Available: https://budmen.com/support/user-guides/shells-layer-height-and-infill/. [Accessed: 20-Oct-2020].

[91] Ćwikła_ G IOP_Conf._Ser.__Mater._Sci._Eng..pdf. "The influence of printing parameters on selected mechanical properties of FDM/FFF 3D-printed parts" 2017.

[92] A. L. Petsiuk and J. M. Pearce, "Open source computer vision-based layer-wise 3D printing analysis," *Addit. Manuf.*, vol. 36, pp. 1–29, 2020.

[93] F. Bähr and E. Westkämper, "Correlations between Influencing Parameters and Quality Properties of Components Produced by Fused Deposition Modeling," *Procedia CIRP*, vol. 72, pp. 1214–1219, 2018.

[94] F. Fischer and Stratasys Ltd, "Thermoplastics: The strongest choice for 3D printing," *Www.Stratasys.Com*, 2011.

[95] Priya mukerjhee and Pichiah Saravanan "3D Printing Technology in Nanomedicine, Acrylonitrile butadiene styrene resin," 2019.

[96] BASF Badische Anilin und Soda Fabrik, "Properties & Applications of ASA. https://www.basf.com 2005.

[97] 3D4MAKERS, "Technical data sheet ABS Filament 3D printing filament," p. 2, 2015.

[98] "RepRap 3D Printer Shop | Filamento, Peças e Impressoras 3D." [Online]. Available: https://reprap.pt/. [Accessed: 20-Oct-2020].

[99] "Fillamentum | addi(c)tive polymers – Fillamentum.com." [Online]. Available: https://fillamentum.com/. [Accessed: 20-Oct-2020].

[100] "ASA Prusament is here! Learn everything about the successor to ABS! - Prusa Printers." [Online]. Available: https://blog.prusaprinters.org/asa-prusament-is-here-learn-everything-about-the-successor-to-abs_30636/. [Accessed: 20-Oct-2020].

[101] "FELIX Tec 4." [Online]. Available: https://www.felixusaprinters.com/store/p63/FELIX_Tec_4.html. [Accessed: 20-Oct-2020].

[102] "ASTM D638 - 14 Standard Test Method for Tensile Properties of Plastics." [Online]. Available: https://www.astm.org/Standards/D638.htm. [Accessed: 20-Oct-2020].

[103] "ASTM D790 - 17 Standard Test Methods for Flexural Properties of Unreinforced and Reinforced Plastics and Electrical Insulating Materials." [Online]. Available: https://www.astm.org/Standards/D790. [Accessed: 20-Oct-2020].

[104] "Simplify3D Software | All-In-One 3D Printing Software." [Online]. Available: https://www.simplify3d.com/. [Accessed: 28-Nov-2020].

[105] M. S. Alsoufi and A. E. Elsayed, "Warping deformation of desktop 3D printed parts manufactured by open source fused deposition modeling (FDM) system," *Int. J. Mech. Mechatronics Eng.*, vol. 17, no. 4, pp. 7–16, 2017.

[106] Getting Started with 3D Printing for Beginners:, "PRINTING. Available: https://all3dp.com/2/infill-3d-printing-what-it-means-and-how-to-use-it/#menu. [Accessed: 20-Oct-2020].

[107] C. Schmutzler, A. Zimmermann, and M. F. Zaeh, "Compensating Warpage of 3D Printed Parts Using Free-form Deformation," *Procedia CIRP*, vol. 41, pp. 1017–1022, 2016.

[108] "Designing for Printing Part 2: Why 3D Printed Parts Warp and How to…." [Online]. Available: https://markforged.com/resources/blog/3d-printed-part-warping. [Accessed: 28-Nov-2020].

[109] M. Pérez, G. Medina-Sánchez, A. García-Collado, M. Gupta, and D. Carou, "Surface quality enhancement of fused deposition modeling (FDM) printed samples based on the selection of critical printing parameters," *Materials (Basel).*, vol. 11, no. 8, 2018.

[110] "What is the Best Infill Pattern for 3D Printing? - 3DPrinterly." [Online]. Available: https://3dprinterly.com/what-is-the-best-infill-pattern-for-3d-printing/#What_is_Lines/Rectilinear_Infill. [Accessed: 20-Oct-2020].

[111] R. Rane, A. Kulkarni, H. Prajapati, R. Taylor, A. Jain, and V. Chen, "Post-process effects of isothermal annealing and initially applied static uniaxial loading on the ultimate tensile strength of fused filament fabrication parts," *Materials (Basel).*, vol. 13, no. 2, 2020.

[112] "The Effect of Layer Bonding on the Strength of 3D Printed Structures." [Online]. Available: https://ukdiss.com/examples/effect-layer-bonding-3d-printed-structures.php. [Accessed: 28-Nov-2020].

[113] N. Aliheidari, R. Tripuraneni, A. Ameli, and S. Nadimpalli, "Fracture resistance measurement of fused deposition modeling 3D printed polymers," *Polym. Test.*, vol. 60, no. March, pp. 94–101, 2017.

[114] W. Wu, P. Geng, G. Li, D. Zhao, H. Zhang, and J. Zhao, "Influence of layer thickness and raster angle on the mechanical properties of 3D-printed PEEK and a comparative mechanical study between PEEK and ABS," *Materials (Basel).*, vol. 8, no. 9, pp. 5834–5846, 2015.

[115] C. Ziemian, M. Sharma, and S. Ziemi, "Anisotropic Mechanical Properties of ABS Parts Fabricated by Fused Deposition Modelling," *Mech. Eng.*, 2012.

[116] V. Shanmugam *et al.*, "The mechanical testing and performance analysis of polymer-fibre composites prepared through the additive manufacturing," *Polym. Test.*, p. 106925, 2020.

[117] S. A. Khan, B. A. Siddiqui, M. Fahad, and M. A. Khan, "Evaluation of the effect of infill pattern on mechanical stregnth of additively manufactured specimen," *Mater. Sci. Forum*, vol. 887 MSF, no. June, pp. 128–132, 2017.

[118] M. Fernandez-Vicente, W. Calle, S. Ferrandiz, and A. Conejero, "Effect of Infill Parameters on Tensile Mechanical Behavior in Desktop 3D Printing," *3D Print. Addit. Manuf.*, vol. 3, no. 3, pp. 183–192, Sep. 2016.

[119] A. García-Domínguez, J. Claver, A. M. Camacho, and M. A. Sebastián, "Considerations on the applicability of test methods for mechanical characterization of materials manufactured by FDM," *Materials (Basel).*, vol. 13, no. 1, Jan. 2020.

[120] B. M. Tymrak, M. Kreiger, and J. M. Pearce, "Mechanical properties of components fabricated with open-source 3-D printers under realistic environmental conditions," *Mater. Des.*, vol. 58, pp. 242–246, 2014.

[121] B. Banjanin *et al.*, "Consistency analysis of mechanical properties of elements produced by FDM additive manufacturing technology," *Rev. Mater.*, vol. 23, no. 4, 2018.

[122] "PETG vs ABS vs ASA." [Online]. Available: https://filament2print.com/gb/blog/52_petg-abs-asa.html. [Accessed: 08-Nov-2020].

[123] William F. Riley, *Rilley (Mechanics of materials)*, vol. 51, no. 1. 2007.

[124] V. Vega *et al.*, "The effect of layer orientation on the mechanical properties and microstructure of a polymer," *J. Mater. Eng. Perform.*, vol. 20, no. 6, pp. 978–988, 2011.

[125] J. R. Morocho, A. C. Sánchez, M. Singaña, and C. Donoso, "Effect of the filling pattern on the compression strength of 3D printed objects using acrylonitrile butadiene styrene (ABS)," in *Key Engineering Materials*, vol. 834 KEM, Trans Tech Publications Ltd, 2020, pp. 115–119.

[126] S. H. Ahn, M. Montero, D. Odell, S. Roundy, and P. K. Wright, "Anisotropic material properties of fused deposition modeling ABS," *Rapid Prototyp. J.*, vol. 8, no. 4, pp. 248–257, 2002.

# Appendices

## Appendices A

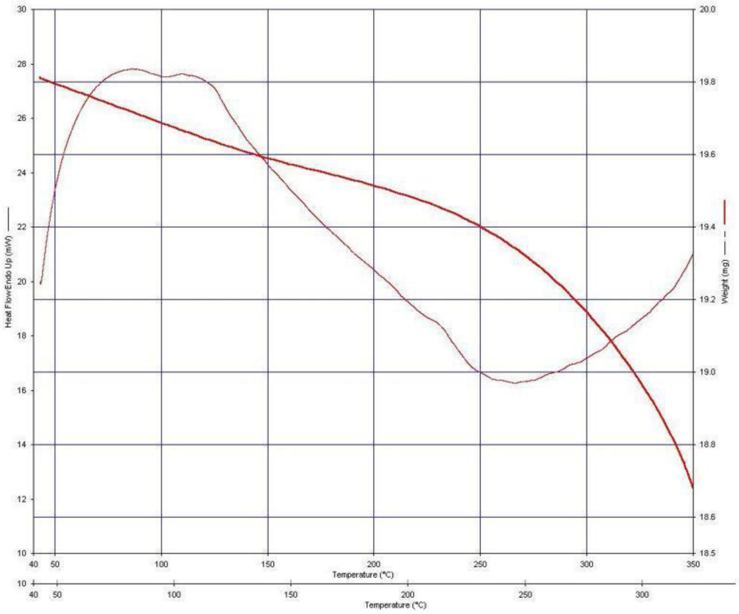


DSC-TGA of Acrylonitrile styrene acrylate (ASA)

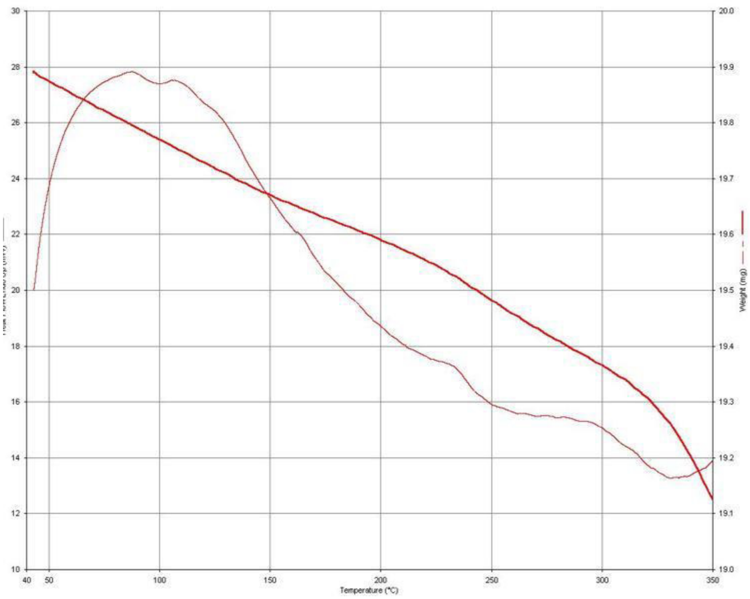


DSC-TGA of ABS Acrylonitrile butadiene styrene (ABS)

## Appendices B

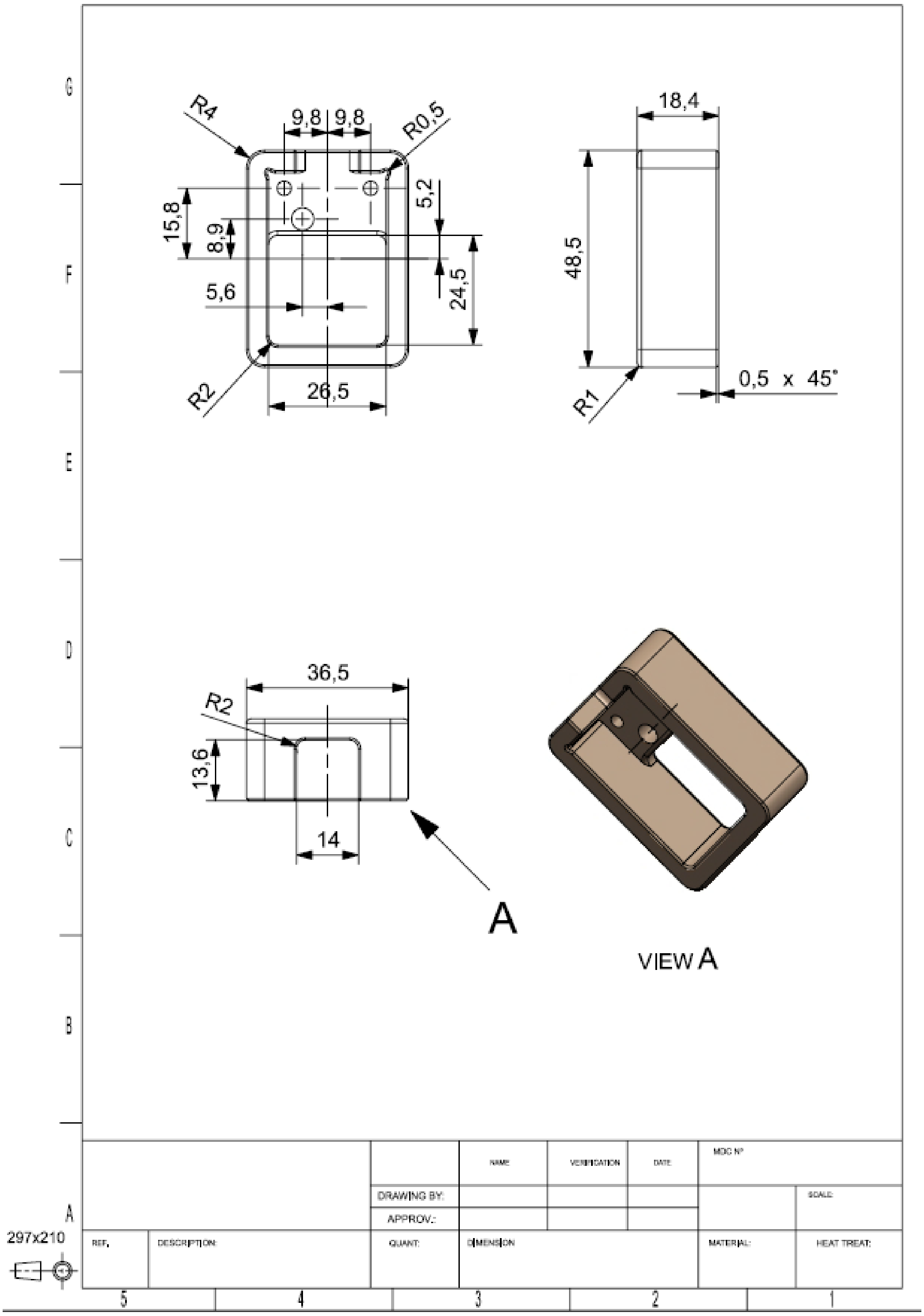

## Appendices C

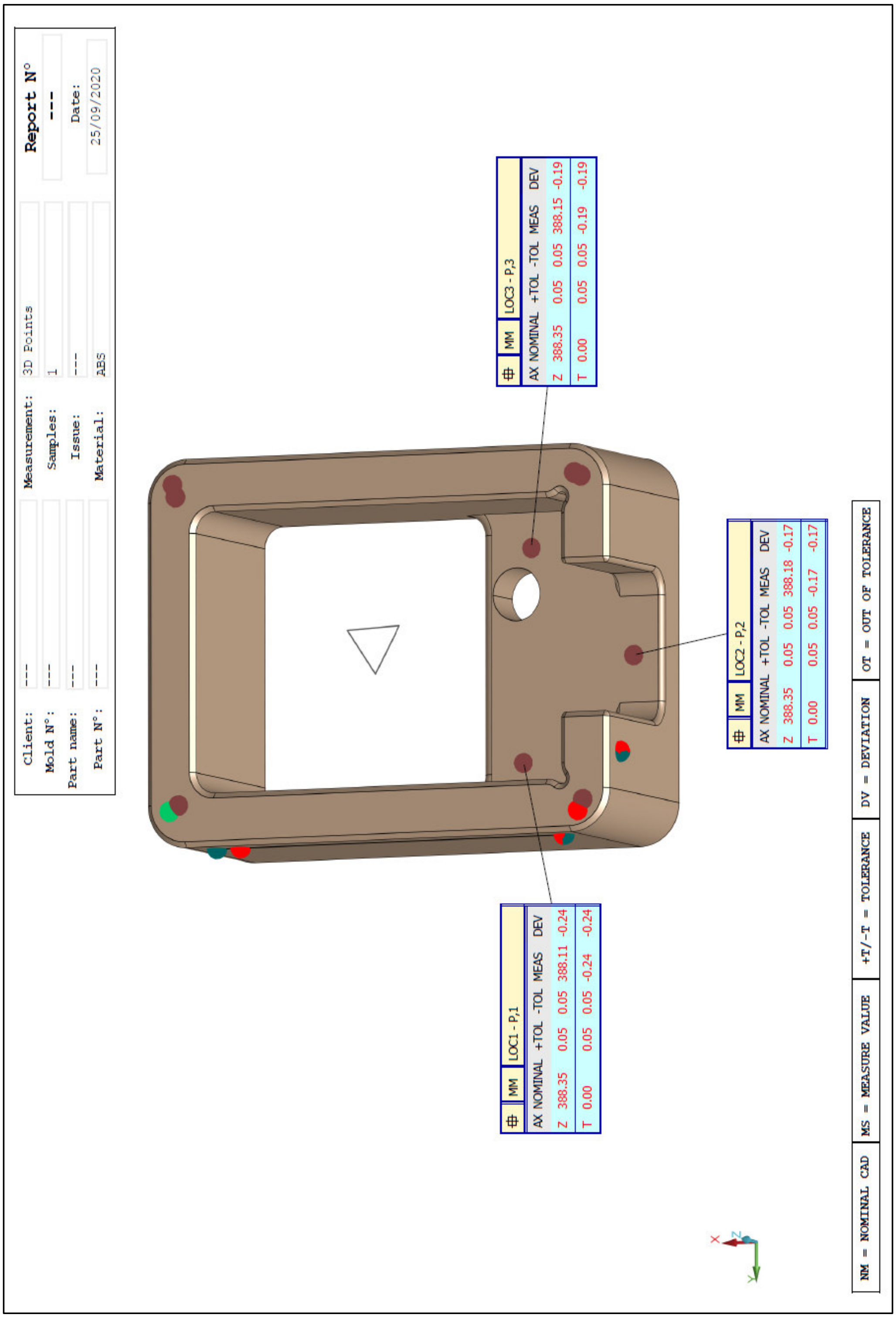

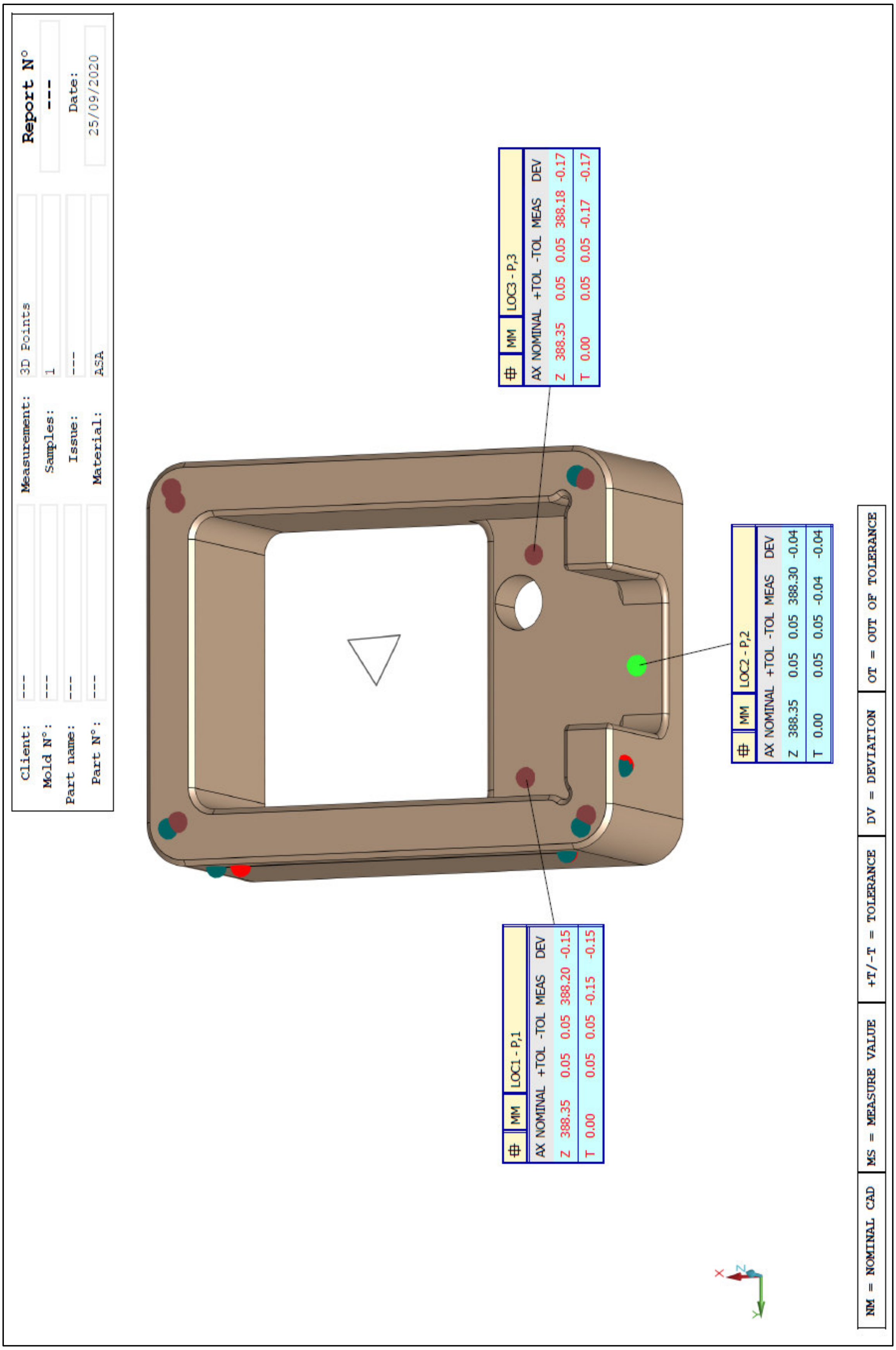
Report N°
---
Date:
25/09/2020
Client: ---
Mold N°: ---
Part name: ---
Part N°: ---
Measurement: 3D Points
Samples: 1
Issue: ---
Material: ASA
MM LOC3 - P,3
AX NOMINAL +TOL -TOL MEAS DEV
Z 388.35 0.05 0.05 388.18 -0.17
T 0.00 0.05 0.05 -0.17 -0.17
MM LOC2 - P,2
AX NOMINAL +TOL -TOL MEAS DEV
Z 388.35 0.05 0.05 388.30 -0.04
T 0.00 0.05 0.05 -0.04 -0.04
MM LOC1 - P,1
AX NOMINAL +TOL -TOL MEAS DEV
Z 388.35 0.05 0.05 388.20 -0.15
T 0.00 0.05 0.05 -0.15 -0.15
NM = NOMINAL CAD
MS = MEASURE VALUE
+T/-T = TOLERANCE
DV = DEVIATION
OT = OUT OF TOLERANCE

## Appendices D

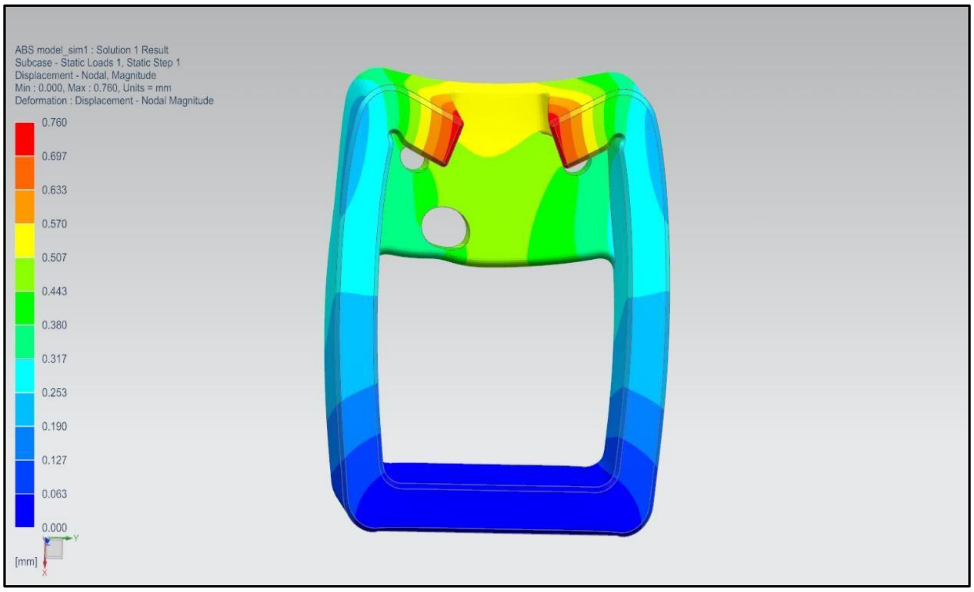


*Fea simulation is carried out to the ABS part before compression test just to observe the possible deflection and characteristics of the possible damages caused when a cognitive load of 2000N is applied from the top of the part and scarcely keeping the side walls free and the bottom is typically fixed as a defined boundary condition, the maximum deflection observed is 0.760mm. The infer represents that the maximum deflection is observed at the top free end of the geometry where the maximum load is observed, only 1/3 of the specimen is observed with the maximum applied load.*

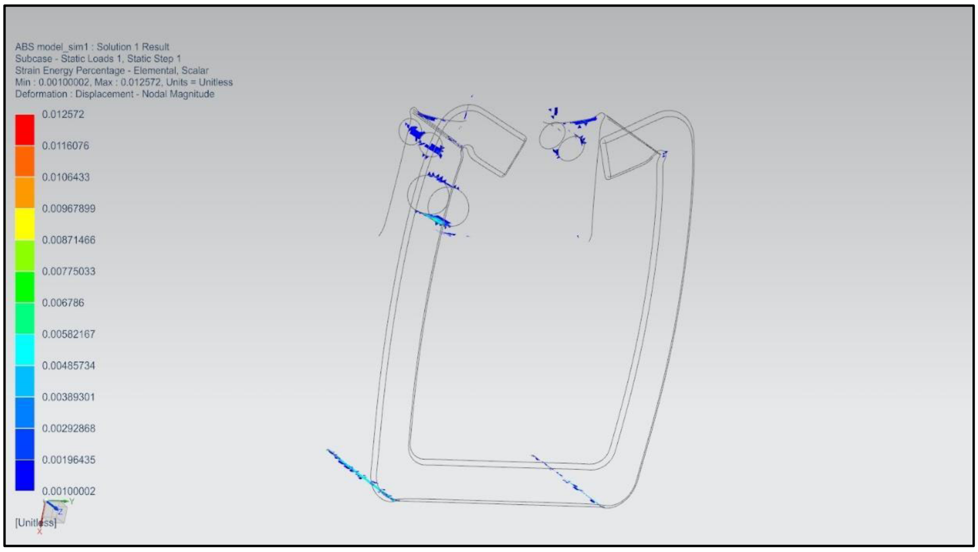


*The possible positions where maximum strain energy is concentrated in the bottom edges of the part and sunken material area like holes, this possible outcome is because of the load is transferred to the bottom edges and chamfers of the minor part. Internal stress generated during the part development constitutes, furthermore, the other reason to showcase this strain behavior of the specimen.*

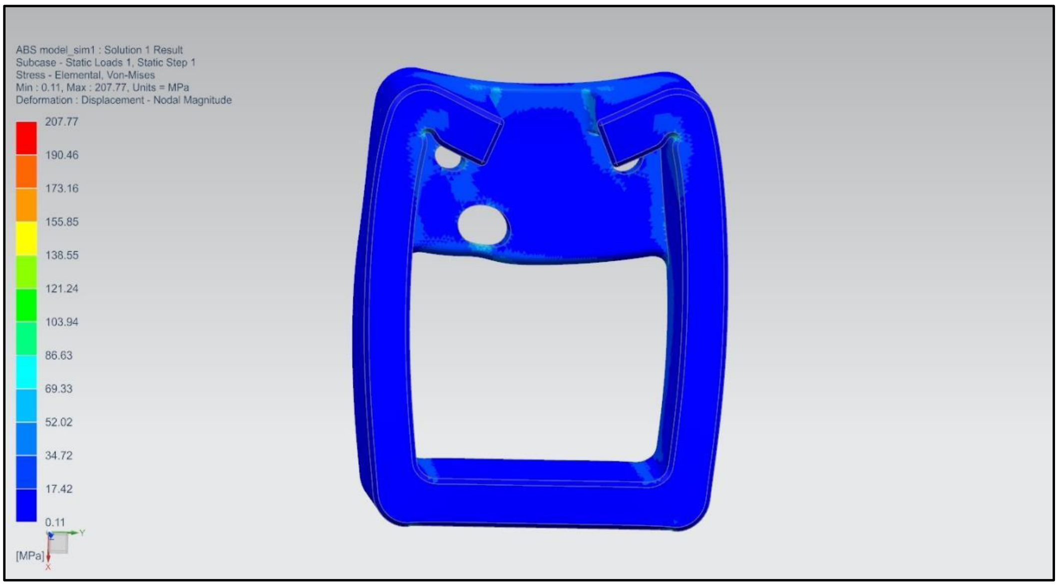


*The maximum stress observed Is 207.77 Mpa on the specific application of 2000N, stress is concentrated fiercely on created holes and arc portion of the considered part. The distinct edges of the precipitous wall are more stress concentrated region this is due to the inbuilt stress generated during the material depositions[layer -to-layer] and the less material strength due to the principal curvature of the specimen itself.*

## Appendices E

| Material | Compared orientation | Infill Type | Tensile strength Variation in MPa | % Variation of Tensile strength | Winner orientation |
|---|---|---|---|---|---|
| ABS | X *vs* Y | Rectilinear | 1.4 | 4.54 | Y |
| | | Concentric | 0.78 | 2.55 | Y |
| ASA | X *vs* Y | Rectilinear | 2.93 | 10.27 | Y |
| | | Concentric | 3.55 | 13.04 | Y |

Mechanical strength variation comparision for Tensile specimens interms of Build orientation

| Material | Compared Infill | Build Orientation | Tensile strength Variation in MPa | % Variation of Tensile strength | Winner Infill |
|---|---|---|---|---|---|
| ABS | Rectilinear *vs* Concentric | X | 0.1 | 0.33 | Rectilinear |
| | | Y | 0.63 | 2.01 | Rectilinear |
| ASA | Rectilinear *vs* Concentric | X | 1.63 | 6.21 | Rectilinear |
| | | Y | 1.01 | 3.42 | Rectilinear |

Mechanical strength variation comparision for Tensile specimens interms of Infill pattern

| Compared Material | Infill and Type | Tensile strength Variation in MPa | % Variation of Tensile strength | Winner Material |
|---|---|---|---|---|
| ABS *vs* ASA | X Concentric | 4.67 | 16.81 | ABS |
| | X Rectilinear | 3.05 | 10.66 | ABS |
| | Y Concentric | 1.9 | 6.34 | ABS |
| | Y Rectilinear | 1.52 | 4.94 | ABS |

Mechanical strength variation comparision for Tensile ABS and ASA Specimens

| Material | Compared orientation | Infill Type | Flexural strength Variation in MPa | % Variation of Flexural strength | Winner orientation |
|---|---|---|---|---|---|
| ABS | X vs Y | Rectilinear | 5.65 | 8.62 | Y |
| | | Concentric | 11.3 | 17.26 | Y |
| ASA | X vs Y | Rectilinear | 5.9 | 11.95 | Y |
| | | Concentric | 11.98 | 24.86 | Y |

Mechanical strength variation comparision for Flexural specimens interms of Build orientation

| Material | Compared Infill | Build Orientation | Flexural strength Variation in MPa | % Variation of Flexural strength | Winner Infill |
|---|---|---|---|---|---|
| ABS | Rectilinear *vs* Concentric | X | 2.88 | 4.70 | Concentric |
| | | Y | 2.77 | 3.97 | Rectilinear |
| ASA | Rectilinear *vs* Concentric | X | 4.2 | 9.48 | Concentric |
| | | Y | 1.88 | 3.53 | Rectilinear |

Mechanical strength variation comparision for Flexural specimens interms of Infill pattern

| Compared Material | Infill and Type | Flexural strength Variation in MPa | % Variation of Flexural strength | Winner Material |
|---|---|---|---|---|
| ABS *vs* ASA | X Concentric | 16.32 | 29.92 | ABS |
| | X Rectilinear | 17.62 | 34.54 | ABS |
| | Y Concentric | 16.05 | 26.61 | ABS |
| | Y Rectilinear | 16.94 | 27.04 | ABS |

Mechanical strength variation comparision for Flexural ABS and ASA Specimens